ABSTRACT

Title of Dissertation: FLOATING WETLANDS AND THEIR POTENTIAL FOR NITROGEN REMOVAL IN ESTUARINE WATERS

Isabel Cristina Butler Viruet, Doctor of Philosophy, 2025

Dissertation Directed By: Dr. Jeremy M. Testa, University of Maryland Center for Environmental Science

Nutrient enrichment of estuarine waters remains a problem globally. New efforts have sought to apply principles of ecological engineering to promote nutrient removal within degraded aquatic systems by constructing habitats that may support enhanced nitrogen removal. Several technologies and approaches are certified as best management practices (BMPs) by the Environmental Protection Agency (EPA). These include the restoration of oyster reefs, stream and estuarine wetlands, and riparian buffers, as well as the implementation of wet retention ponds. Each of these habitats has been suggested to be a “hotspot” for nitrogen removal, but they are also biologically and chemically complex environments. Thus, the quantification of their impact on nutrient removal is difficult due to interactions with other processes that influence nitrogen transformation and loss within tidal estuarine waters. Floating wetlands have traditionally been implemented to increase the nutrient removal efficiency in freshwater retention ponds, where nutrient removal is presumed to be accomplished by plant assimilation and sediment deposition. Similar installations of floating wetlands in tidal waters have recently been implemented to achieve the same ecosystem services as in retention ponds, but little is known about their efficacy. In this dissertation, I quantified floating wetland nitrogen removal and

cycling through a series of mesocosm experiments and numerical modeling. The mesocosm experiments were carried out for 90 days at the Chesapeake Biological Laboratory in both spring and summer periods during the years 2019, 2021, and 2022. My results indicate that denitrification was the major nitrogen removal process, removing ~4 times as much nitrogen as plant uptake. Denitrification rates were comparable between mesocosms with wetland plants and control mesocosm with only the media, suggesting that denitrification was occurring in microzones within the high-surface area media. Thus, a new formulation to incorporate this high surface area media was necessary to reproduce these high denitrification rates in model representations of the experiments. This dissertation research thus clearly demonstrates that floating treatment wetlands can remove nitrogen at rates that are often higher than subtidal sediments, but future work on their durability and efficacy under a wider range of conditions is needed to better assess their potential to become a certified best management practice tool for nutrient management.

FLOATNG WETLADNS AND THEIR POTENTIAL FOR NITROGEN REMOVAL IN ESTUARINE WATERS

by

Isabel Cristina Butler Viruet

Dissertation submitted to the Faculty of the Graduate School of the
University of Maryland, College Park, in partial fulfillment
of the requirements for the degree of
[Doctor of Philosophy]
[2025]

Advisory Committee:
Professor [Dr. Jeremy M. Testa], Chair
[Mr. Gary Shenk]
[Dr. Lora A. Harris]
[Dr. Walter Boynton]
[Dr. Stephanie Lansing]

Dedication

This dissertation is dedicated to my son, my husband, my family and my friends who supported me through this journey. Without you I would not be where I am today. Thank you.

Acknowledgements

I would like to thank:

- Dr. Jeremy Testa
- My committee members
- The CBL Graduate Education Committee
- SEAS Islands Alliance
- Koolhof Earth
- National Aquarium Baltimore
- Lab Manager Casey Hodgkins
- Lab Manager Shelby Cross Johnson
- Testa Lab members: Allison Dreiss and Amir Azarnivand
- Manager for Student Affairs Amy Griffin
- My family and loving friends

Table of Contents

Chapter 1: Introduction

Background and Rationale

Eutrophication and nutrient pollution degrade coastal systems. Nutrients are essential for plants and animals to grow in pristine environments, where nitrogen and phosphorus are often limiting and thus constrain coastal productivity. However, when nutrient concentrations increase, associated increases in productivity drive elevated algal biomass, low oxygen zones, and the degradation of coastal systems. Thus, eutrophication significantly degrades water quality, which can negatively affect coastal organisms and hence recreational and economic benefits of coastal systems.

In response to eutrophication, federal and local stakeholders have made substantial socio-economic commitments to reduce nutrient loads responsible for water quality degradation. These restoration approaches have been informed by the paradigm that a decrease in watershed nutrient loads will subsequently decrease the frequency and extent of eutrophication to induce the process of oligotrophication (Nixon et al. 2009). Some of these restoration efforts have proven to be effective in coastal areas around the world (e.g. 25% nitrogen load decrease in the Chesapeake Bay, Lefcheck et al., 2018, 50% lower nutrients decrease in Danish coastal waters, Riemann et al., 2016) and have even decreased nutrient levels to pre-eutrophication states (e.g. Tampa Bay, Sherwood et al., 2017), with associated ecosystem improvements. However, efforts aimed at reducing nutrient loading might be insufficient for attaining restoration goals of improved water quality efforts due to several reasons. First, the reduction of nutrient loads from point sources certainly helps improve water quality where these loads dominate (Testa et al., 2022; Boynton & Bailey, 2008), however, many watersheds have large diffuse nutrient sources that make the management and mitigation difficult and expensive. Second, there are lag times between

groundwater nutrient inputs and diffuse nutrient sources (Boynton et al. 2014), leading to uncertain effects of the management actions that may be difficult to discern from monitoring data. In addition, eutrophication can induce a self-perpetuating state once a critical threshold of external nutrients loads has occurred, particularly, in shallow water bodies (Scheffer, 2004; Søndergaard et al., 2001). Thus, past and current watershed nutrient reduction efforts may be insufficient in order to reach water quality restoration goals.

In an effort to target diffuse nutrient sources, lag responses, and accelerate oligotrophication of coastal waters, federal and local stakeholders have also implemented alternative restoration approaches that complement point and non-point source nutrient load reduction. Traditional approaches to mitigate diffuse nutrient sources include the regulation of agricultural practices like manure management and the use of winter cover-crop to decrease nutrients in overly fertilized soils (Andersen et al. 2014). Other approaches that target diffuse and non-point sources include stream and freshwater marsh restoration (Filoso and Palmer 2011) and coastal wetland restoration (Hassett et al. 2005). Restoration of these systems aims to enhance and/or restore the nutrient removal capabilities and increase organic matter removal (Vymazal 2007) , although the effectiveness of these interventions varies widely (Passeport et al. 2013).

In urban areas with a high percentage of impervious surfaces, local stakeholders have implemented wet retention ponds as an effort to reduce storm event flows, sequester nutrients, and reduce overall runoff to coastal waters (Hancock et al. 2010). These retention ponds contribute to the improvement in water quality by allowing suspended solids to settle in the bottom and promoting nutrient uptake by surrounding pond vegetation (USEPA 1999). However, research has shown that these systems vary widely in their effectiveness (Booth et al., 2002; Fennessey et al., 2011; McCuen, 1979; Emerson et al., 2010) and oftentimes fail to achieve regulatory goals due to

underestimation of precipitation intensity and inability to decrease storm flow due to design flaws (Hancock et al. 2010). In general, these systems have achieved some nutrient load reduction, however, the effectiveness of these technologies depend on storm events, effective design, and implementation.

Floating treatment wetlands (FTW) have been utilized as a tool to further increase the nutrient removal potential of wet retention ponds (Wang & Sample, 2014). Research has shown that floating wetlands can increase the nutrient removal efficiency in retention ponds treating urban runoff (Wang & Sample, 2014), wastewater (Barco and Borin 2020), and agricultural runoff (Spangler et al. 2019). FTWs are made of floating porous media and wetland plants known to have a high rate of nitrogen assimilation and resiliency to anoxic waters and soils. Removal mechanisms of an FTW encompass the interaction between plants, the atmosphere, and ambient water. Extensive root systems suspended in the water column trap sediment and increase sedimentation rates, while biofilm growth in the porous media and the roots provide additional transformation and assimilation of nutrients and pollutants beyond that of plant assimilation (Yeh et al. 2015). However, there is no research available on their potential to remove nitrogen from estuarine systems.

This dissertation aims to estimate N uptake rates of floating wetlands and explore the possibilities of using them as a tool for nitrogen removal in estuarine waters. Mesocosm experiments will be used to track nitrogen loss associated with denitrification and plant uptake. Afterward, I will implement a mass balance approach to identify the main nitrogen removal pathways and estimate nitrogen removal potential. Finally, I will construct a numerical model to represent nitrogen cycling within the floating wetlands to understand

Objectives

Each objective of my dissertation research is listed below and will be addressed as a chapter of the dissertation.

Chapter 2: Quantify the dynamics of nitrogen cycling in floating wetlands in estuarine-like environments and identify major nitrogen removal pathways beyond plant nitrogen assimilation

Chapter 3: Develop a nutrient budget for floating wetlands in estuarine mesocosm experiments

Chapter 4: Develop a numerical deterministic model that explains and predicts nitrogen removal dynamics in a floating wetland deployed in estuarine-like conditions

Chapter 5: Synthesis of floating wetland research and procedures for future submission and evaluation of technologies for BMP review and approval

Chapter 2: Floating wetlands beyond retention ponds: estimating nitrogen cycling and removal in tidal waters

Abstract

Efforts to meet nutrient reduction goals in the Chesapeake Bay watershed involve a variety of practices that remove nutrients before they are delivered to estuarine systems. Floating treatment wetlands (FTW) have been a certified best management practice (BMP) implemented for decades in retention ponds and wastewater treatment plants but have only recently been placed in tidal waters to remove nutrients directly. Given the paucity of data on nitrogen cycling within tidal FTW, I measured nitrogen transformation and removal within FTW deployed in estuarine-like mesocosms during a 12-week experiment in summer 2019, and a 10-week experiment in spring 2021. Results indicate a comparable, net removal of TN for both summer of 2019 and spring 2021, but substantial transformations of nitrogen within the FTW. Nitrate (NO_{2+3}^-) was generated while ammonium (NH_4^+) and particulate nitrogen (PN) were removed from the mesocosm. Nitrogen concentrations measured in different parts of the mesocosms and wetland media also indicate signs of transformation, where NO_{2+3}^- concentrations were 0.2 mg L^{-1} higher in the media porewater than the inflowing water for both control and experimental mesocosms. This suggests relatively high rates of nitrification within the media. This nitrification could support measured denitrification rates (2.4 - 10.9 mg N_2-N m^2 h^{-1}), which were at least four times higher than in oligohaline marshes and almost half the rates reported in restored oyster reefs that are also considered as a BMP. This research has shown that floating wetlands have the capability to transform and remove nitrogen in estuarine-like environments, potentially expanding the areas in which floating wetlands can be deployed. Furthermore, this study provides measurements of these transformation and removal rates to inform future estimates of impact and remediation following floating treatment wetland use in estuarine environments.

Introduction

Nutrient pollution and eutrophication remains a problem globally, degrading coastal ecosystems through excess phytoplankton biomass and associated depletion of dissolved oxygen and food web disruption. Nutrients are essential for plants and animals to grow, but may constrain coastal productivity in pristine environments where nitrogen and phosphorus are often limiting. However, when nutrient concentrations increase, associated increases in productivity drive elevated algal biomass (Nixon 1995), low oxygen zones (Diaz and Rosenberg 2008), and the degradation of coastal systems (Deegan et al. 2012). High rates of productivity and organic matter degradation also stimulate microbially-mediated nutrient regeneration and transformation, including oxygen sensitive processes like nitrification and denitrification (Kemp et al., 1990 Cornwell et al., 1999). This nutrient-enrichment driven eutrophication significantly degrades water quality, which can negatively affect coastal organisms and hence recreational and economic benefits of coastal systems. To try and reverse this pollution problem, many socio-economic commitments to reduce watershed nutrient loading have been put into place worldwide (e.g. Backer et al. 2010, NRC 2009).

Efforts to meet watershed nutrient reduction goals in the Chesapeake Bay watershed (i.e., total maximum daily loads, or TMDLs) involve a variety of practices. Known as best management practices (BMPs), these range from cover crops and conservation tillage for managing diffuse pollution sources from agricultural lands, to biological nitrogen reduction technologies implemented for point sources from single wastewater treatment facilities. Improvements to wastewater treatment plants have allowed for a considerable reduction in nitrogen load to the Chesapeake Bay since 1985 (Clune et al. 2021). However, watershed model estimates suggest that there are still 42 million lbs./year in nitrogen point sources and 209 million lbs./year of non-point sources of nitrogen (CBP 2017) still entering the Chesapeake Bay. In the

coming decades, additional nutrient load reductions will have to be made from these diffuse sources, which range from agricultural fields to urban stormwater. Many of these reductions will need to come from technologies involving land management practices approved by the Environmental Protection Agency (EPA) that mitigate the polluted water from nearby surface and groundwater (Choi et al. 2020). However, issues of cost and limited adoption of these BMPs present a challenge to reaching land-based nutrient removal goals.

Alternatives to land based BMPs in the Chesapeake Bay TMDL framework include floating treatment wetlands (FTW), which are a certified BMP technology evaluated and approved by the US Environmental Protection Agency (EPA), academic researchers, engineers, and implementers, in which macrophytes are grown on a floating raft and/or media within a retention pond. The roots are in contact with the water column and remove nutrients and other pollutants via several physicochemical and biological processes (Sharma et al. 2021). The implementation of FTW has primarily occurred in retention ponds as a way to increase their efficiency at treating runoff and overcome operational challenges and flaws such as inconsistent hydrologic loads of nutrients and other pollutants. The buoyant nature of FTW allows for the constant removal of nutrients and pollutants regardless of the water level in the retention pond. Previous research exploring the effectiveness of FTW in retention ponds has employed the use of in-situ measurements (Nahlik and Mitsch 2006) and mesocosm experiments (Tanner and Headley 2011). While the relatively simple design of retention ponds allows for the quantification of nitrogen removal via input-output analysis (i.e., differences between inflow and outflow concentrations), this approach limits deeper understanding of nitrogen transformations and removal mechanisms that drive these reductions. FTW technology and research have evolved and expanded to engineered FTW to treat other polluted waters, including urban and

agricultural runoff (Stewart et al. 2008; Sample and Wre 2017), secondary effluent (Gao et al. 2018), greywater (Faulwetter et al. 2011), mine tailings water (Gupta et al. 2020), and industrial wastewater (Knight et al. 1999).

In contrast to the common implementation of FTW in retention ponds, implementation of FTW in estuarine systems has not been widely employed or studied. In those places that have deployed FTW, the same technology developed for retention ponds has been applied but utilizing coastal wetland plants like *Phragmites australis* (Sanicola et al. 2019). Microcosms installed in the floating wetlands deployed in the Inner Harbor of Baltimore, MD, US in 2009 provided evidence of nutrient transformation and potential removal, but extrapolation of these impacts, accounting for the fate of the nutrients, or the details of their transformation was not clear (Streb 2013). Research performed in FTW deployed in the Southern Baltic Sea's tidal lagoons indicates that FTW serve as protection for shorelines, as well as nursery habitats for shrimp and eels (Karstens et al. 2021). However, measurements of nutrients around those FTW did not indicate any nutrient reductions in the surrounding waters (Karstens et al. 2021). Other research performed by Sanicola et al. (2019) in Queensland, Australia explored shoot and root growth of suitable FTW plants species under different salinity environments. Research identified two plant species, *Isolepis nodosa* and *Baumea juncea,* with the potential to significantly reduce phosphorus as long as the plant is harvested (Sanicola et al. 2019). Thus, despite recent efforts to understand the role of FTW as a habitat provider for local wildlife, a detailed understanding of the biogeochemical transformations in these wetlands is lacking.

To increase our understanding of the mechanisms of nitrogen removal and transformation in estuarine FTW, I explored the potential of FTW to remove nitrogen from estuarine waters by measuring a comprehensive suite of nitrogen removal processes using mesocosm experiments

under brackish water conditions. One experiment focused on measuring nitrogen removal and transformations in summer of 2019 while the second experiment focused on measuring nitrogen removal and transformations in the spring of 2021. The experiments included triplicate mesocosms with vegetated FTW and control tanks that only included the floating wetland media. The mesocosms allowed for a high degree of control, daily sampling frequency, and ease of measuring process rates (denitrification, plant uptake) that allowed us to assess nitrogen transformations and associated nitrogen losses. We hypothesized that treatments with vegetated media would remove a higher fraction of the nitrogen inputs than the control treatments with only the wetland media, as a result of enhanced nutrient removal through plant uptake and plant-associated denitrification.

Materials and Methods

Experimental Design

We designed and executed two mesocosm experiments to measure nitrogen removal and transformation during the spring and summer. The first experiment was performed from June 21 to September 9, 2019. The second experiment was performed from April 16 to July 22, 2021. These experiments were carried out in different years due to COVID-19 interruptions as well as logistics. The mesocosm design consisted of a flow-through system, with three control tanks and three experimental tanks. Control tanks consisted of unplanted floating wetland media, while the experimental tanks consisted of the floating media planted with *Spartina patens*. To measure the effects of the floating wetland nitrogen removal, we measured nitrogen accumulation in plant material (roots, shoots, flowers, and seeds), periphyton and detritus within the mesocosm tanks, as well as rates of nitrogen removal (denitrification) within the floating wetland matrix. Dissolved and particulate nitrogen concentrations from the inflowing water and outflowing water

were collected weekly for both experiments (summer 2019 and spring 2021). For the spring 2021 experiment, nitrogen concentrations were also measured within the tank water column and within the media pores. Water temperature, dissolved oxygen, salinity, specific conductivity, pH, and chlorophyll-a in the tank water column were monitored on a daily basis between 12:00 PM and 3:00 PM. See appendix A for average environmental characteristics of the tanks (table S1). Hourly precipitation and photosynthetically active radiation (PAR) data were collected from the Chesapeake Biological Laboratory (CBL) monitoring station in Solomons, MD, US (https://cblmonitoring.umces.edu/). Plant material accumulation was measured at the beginning and at the end of the experiment, separated into above-ground and below-ground biomass. Denitrification was measured once a month during the course of each experiment.

Experimental Setup

Six mesocosm tanks that were 0.9 m in depth and 1.82 m in diameter were deployed in an outdoor setting at the Chesapeake Biological Laboratory, Solomons Island, Maryland (38.3194° N, 76.4540° W). The Chesapeake Biological Laboratory is located in the lower portion of the Patuxent River and is known to be mesohaline (salinity ranges from 5-18 ppt). Pumped Patuxent River water (222 meters from shore) (Fig. 1), entered the tanks from the bottom and exited the tanks at the surface through a standpipe (Fig. 1). Outflow discharge from each of the tanks went directly back into the Patuxent River. The flow rate was measured and adjusted daily via valves on the inflowing pipes to attain a residence time of 6 hours, which is consistent with a semi-diurnal tidal cycle of 6 hours. The 6-hour residence time was meant to characterize the time it would take a given parcel of water to move through a given location in a tidal estuary with a semi-diurnal tide. In this case the parcel of water is moving through our mesocosm tanks. Three control tanks consisted of unplanted FTW media covering the surface area of the tanks to reduce

light availability and associated water column photosynthesis that would lead to mesocosm artifacts. Experimental tanks consisted of the floating media with 19 *Spartina patens* plants, 88 kg of GardenPro top-soil, and approximately 44 kg of Premier Sphagnum peat moss. As in the control tanks, the FTW covered the entire surface area of the tanks. During the experiment, the FTW were designed to be partially submerged to simulate the high-marsh environment common to *Spartina patens*, commonly known as salt hay. This high-marsh grass was selected in the experiments because it is a common species in the tidal wetlands of the region, has the ability to withstand partial flooding and a wide range of salinity from 0 - 30 ppt (Merino et al. 2010), and is readily available in local nurseries. Recent studies have also shown *S. patens* as a suitable plant for floating wetlands deployed in brackish environments (Landaverde et al. 2024). After the FTW were installed and planted, they were left for two weeks before taking the first measurements in order for the wetland plants to establish and for conditions within the tanks to stabilize.

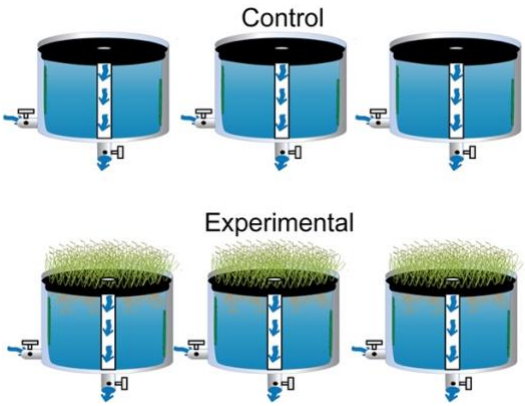

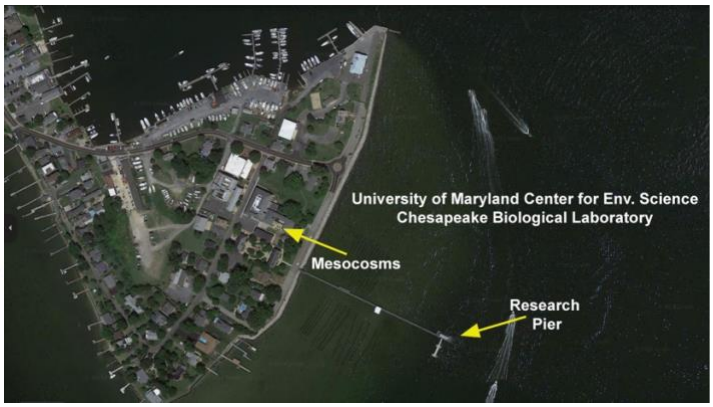

Figure 1. (left) Diagram of the experimental design in triplicate mesocosms tanks with and without floating wetlands. The flow of water enters through the bottom and exits the tanks through a centrally located standpipe. (right) Research pier at the University of Maryland Chesapeake Biological Laboratory, Solomons Island, Maryland, USA where source water for the mesocosm tanks was obtained. (bottom) Picture of control and experimental tanks on July 2, 2021.

Sample measurements and analysis

Dissolved (NH_4^+, DON, NO_{2+3}^-) and particulate (PN) nitrogen concentrations were measured on a weekly basis from the inflow and outflow for summer 2019. For spring 2021 we included dissolved nutrient measurements from within the floating media (i.e. the porewater within the media), as well as the water column inside each tank. Porewater was collected using a syringe to extract the water from the media, while inflow and outflow water was collected directly from the pipes just downstream from the valves that controlled water flow in and out of the tanks. Water samples from the different parts of the tanks were collected in 2L Nalgene bottles that were previously acid washed. Inflowing water was measured at one valve where water entered the plumbing for the entire mesocosm system, and the nitrogen concentration at this the inflow was assumed to be representative for the water entering at the valves for all tanks. Prior to starting the experiment, dissolved nitrogen was measured from two different valves to confirm that the inflowing concentration of dissolved nitrogen was not substantially different

between all tanks (i.e., nitrogen was not transformed within the plumbing system). The mean ± standard deviations of measurements for NH_4^+ (0.034 ± 0.0004 mg L^{-1}), and NO_{2+3}^- (0.02 ± 0.002 mg L^{-1}) of the two valves indicate highly comparable concentrations (low standard deviation) indicating no significant difference between the inflow pipes. Samples were sent to the Chesapeake Biological Laboratory Nutrient Analytical Services for analysis. Ammonium (NH_4^+) was analyzed using standard methods (4500-NH3 G-1997, MDL 0.009 mg L^{-1}), nitrate + nitrite (NO_{2+3}^-) was analyzed using the catalyzed enzyme reduction method (ASTM D-7781, MDL 0.0057 mg L^{-1}), dissolved organic nitrogen (DON) was analyzed following the EPA 365.1 method (MDL 0.05 mg L^{-1}), and particulate nitrogen (PN) was analyzed following the EPA 440.0 method (MDL 0.0263%). Discrete sampling of water temperature, dissolved oxygen, salinity and specific conductivity was measured on a daily basis using a YSI Sonde MPS 556 just below the floating matrix (table S1). Chlorophyll-a was monitored on a daily basis and analyzed within 28 days of collection using 90% acetone extraction technique and fluorometric analysis (EPA 445.0, MDL 0.68 μg L^{-1}). Water volumes for chlorophyll-a analysis ranged between 60mL and 180mL depending on the location (inflow, outflow, water column and media porewater). YSI Sonde calibration was performed weekly, whereas fluorometric calibration was performed every 60 days. We measured whole-tank above- and below-ground biomass at the beginning and end of the experiments. Above-ground and below ground biomass was collected following Kreeger (2014a; 2014b). Initial above and below-ground biomass was calculated by randomly selecting three plants before planting. Since plants were all the same size, we assumed all three tanks started with the same above and below ground biomass. Plant material was rinsed with DI water and dried at 60˚C to constant weight. Then, plant material was ground and analyzed for nitrogen content (Zimmermann et al. 1997, MDL 0.01%), to estimate whole-tank plant nitrogen content.

To estimate final above-ground biomass, nine *S. patens* plants per tank were collected, rinsed with DI, and dried at 60 ˚C to constant weight and further analyzed for nitrogen content. The rest of the above-ground material from each tank was harvested, rinsed with DI water, and dried at 60 ˚C until the material reached a constant weight. The nitrogen content of all sampled plants was averaged and multiplied by the total amount of above-ground biomass in each tank to obtain the total above-ground biomass in milligrams of nitrogen per tank. For final below-ground biomass, three randomly selected squares from each floating matrix were cut out and their area was measured (between 40 cm^2 and 40.5 cm^2 per square). All root material was extracted from the matrix in each square, rinsed with DI and dried at 60˚C, and further analyzed for nitrogen content. These subsamples are assumed to represent the whole tank, and the subsampled belowground biomass and N content were extrapolated to compute a whole-tank N content.

Denitrification rates (which are actually measured N_2-N fluxes) were measured in summer 2019 and spring 2021, while nutrient fluxes (NH_4^+ and NO_{2+3}^-) were only measured during the spring of 2021. These fluxes were measured at two randomly selected, pre-defined locations within each FTW media in both the control and experimental mesocosms. Once a month, two pre-cut cores of floating wetland matrix from each tank were collected, placed on a 6.5 cm plexiglass core, gently filled with ambient water, and capped with an O-ring sealed top. One core containing water from the tanks was used as a blank to distinguish between the denitrification happening in the water column and the media. The cores were then placed in the dark in a temperature-controlled water bath to attempt to simulate in-situ conditions. After reaching in-situ conditions, the cores were incubated for three hours in the dark. This method is an adaptation of a method used to measure denitrification and nutrient fluxes from bottom sediments (Testa et al. 2022). Every hour, samples were collected in 12mL exetainers (Labco,

UK) from each core and fixed with 60µL of a saturated mercuric chloride solution (Fulweiler et al. 2007). Samples were analyzed for the N_2/Ar and O_2/Ar ratio of gases using a membrane inlet mass spectrometer (MIMS, Bay Instruments, Easton, Maryland) and the N_2/Ar technique (Kana et al. 1994). The N_2/Ar technique measures the net N_2 production in the sample core, thus denitrification rates and nitrogen fixation rates cannot be separated. Thus, the linear increases in N_2 concentration were used to estimate net N_2 production during the experiment as net N_2 flux, or net denitrification (Kana et al. 1994; Cornwell et al. 2016). Detailed calculation on how flux rates were estimated can be found in appendix A Section 1.

Measuring and removing periphyton

Mesocosm walls can substantially alter experimental conditions by limiting water exchange, absorbing downwelling light, and providing substrate for a myriad of organisms to grow (Kemp et al. 2009). Because the ratio of wall surface to water column is high in mesocosms, and because periphyton accumulate on tank walls, we sought to directly measure the relative contribution of periphyton to the biomass and N budget of each tank (Chen et al. 1997; Chen et al. 2000). To prevent excess periphyton accumulation, all periphyton in each mesocosm tank was scrubbed from the walls and collected on a weekly basis. To collect the periphyton, the floating media was lifted using a gantry crane. A 500 µm mesh was added to the outflow pipe and then the tank was drained. Wall and tank bottom were scrubbed using a clean brush and all material gathered. The collected periphyton was then brought to the laboratory, rinsed with deionized water, and dried at 60˚C until a constant weight was reached. All the periphyton collected was analyzed for PC and PN to quantify how much nitrogen was being removed by tank artifacts.

Results

Nutrient Removal

To identify the overall amount of nitrogen being removed from the mesocosms, we calculated differences in total nitrogen (TN) between the inflow and the outflow rates. Total nitrogen concentrations were estimated by adding all pools of nitrogen together. Overall, experimental mesocosms for summer 2019 and spring 2021 showed the highest removal of TN (i.e., outflow < inflow) when compared to the control mesocosms. Experimental mesocosms removed a total of 23.7 g TN during the summer 2019, and 17.3 g TN during spring 2021 experiments. Meanwhile, the control removed a total of 17.1 g TN during the summer 2019 experiments and 8.3 g TN during spring 2021 experiments. On two occasions during summer 2019 and spring 2021the control mesocosms became sources of TN, meaning that the concentrations of TN were higher in the outflow than in the inflow.

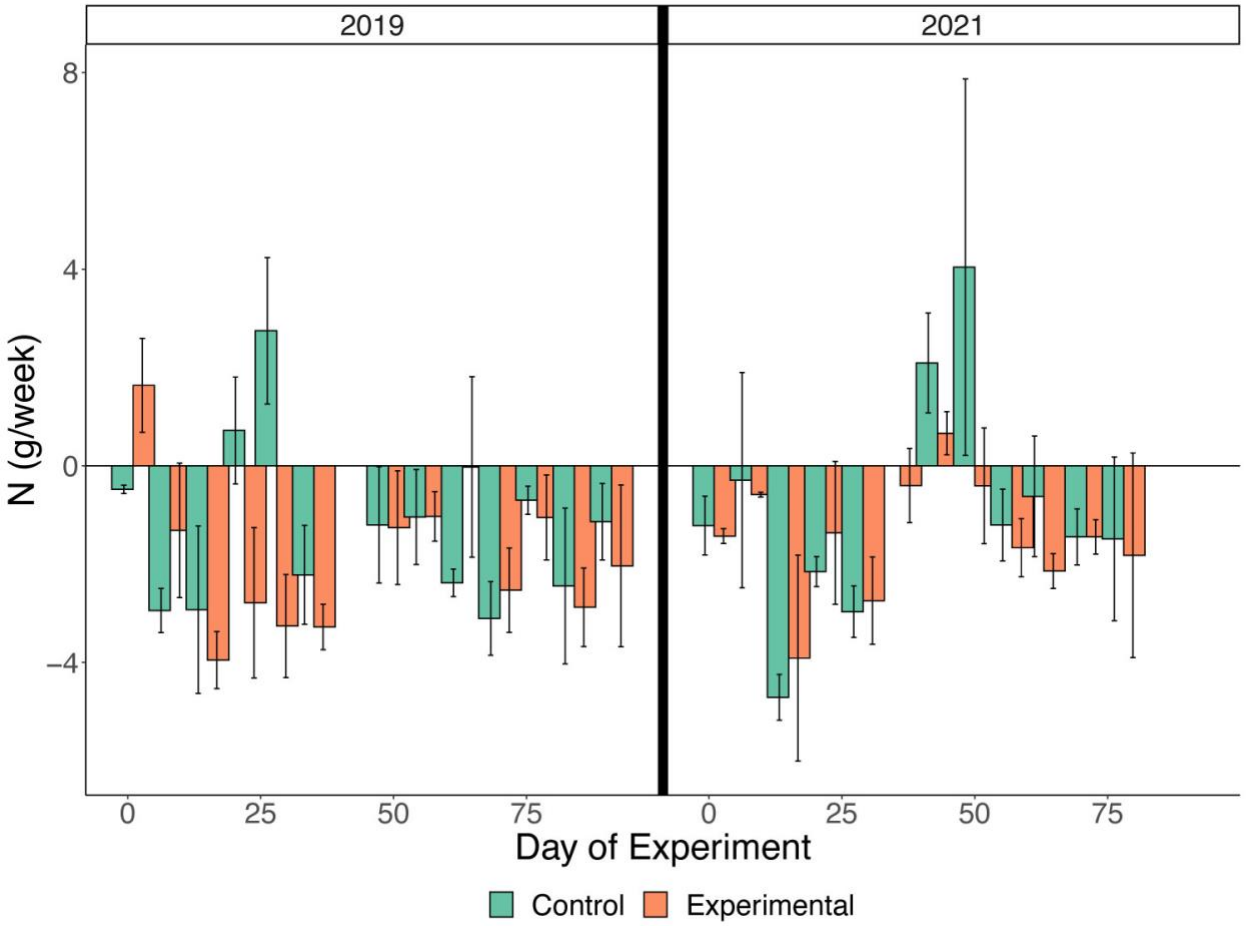

Figure 2. Total nitrogen weekly removal rates from mesocosm experiments in summer 2019 and spring 2021. Positive values indicate an overall addition and/or production of nitrogen in the mesocosm tank, while negative values indicate an overall removal of nitrogen. Error bars represent the standard deviation from the mean.

To further understand nitrogen cycling within the tanks, we computed differences between the inflow and the outflow of NH_4^+, NO_{2+3}^-, DON, and PN to determine if there was a net production (outflow>inflow) or net consumption (outflow<inflow) of each analyte. These net production/consumption calculations quantify the balance of processes that produce and consume each analyte, and thus represent a net transformation, not a permanent removal or production. We hereafter define a net transformation that increases the concentration of an analyte as "production" and a net transformation that decreases the concentration of an analyte as "consumption".

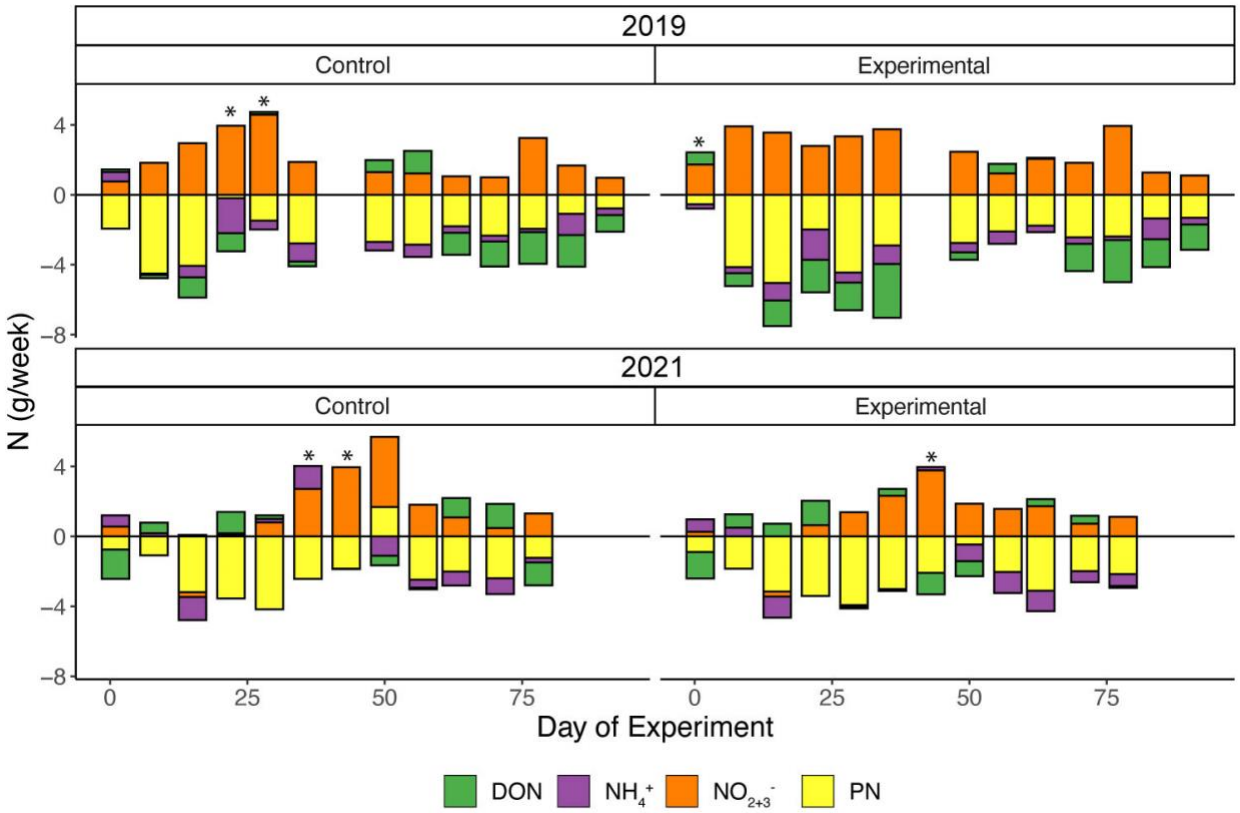

Figure 3. Weekly removal rates of DON, NH_4^+, NO_{2+3}^- and PN for summer 2019 and spring 2021. Negative values indicate a net removal of particulate nitrogen species. Asterisks indicate where the tanks experienced a production of TN.

Data suggest a substantial nitrogen transformation in both control and experimental mesocosms and years given the observed decrease in NH_4^+ and subsequential increase of NO_{2+3}^- inside the tanks. During the summer 2019 experiments, the control mesocosms produced 26.4 g NO_{2+3}^-, while the experimental mesocosms generated 33.0 g NO_{2+3}^- (fig 3). In contrast, both treatments showed consumption of DON, NH_4^+, and PN. Similarly, in the spring 2021 experiments, the control mesocosms produced 16.5 g NO_{2+3}^-, while the experimental mesocosms produced 15.1 g NO_{2+3}^- (fig. 3). Both, control and experimental mesocosms, during the spring consumed PN and NH_4^+. Because there is a substantial amount of NO_{2+3}^- being produced in the system for both years, we further grouped the dissolved inorganic pools (DIN = NH_4^++ NO_2 +

NO_3). The results shown in (fig. 4) indicate that for both years the control and experimental mesocosms consumed PN but produced inorganic forms of nitrogen. During the spring 2021 experiment (fig. 4), DON was produced in both control and experimental.

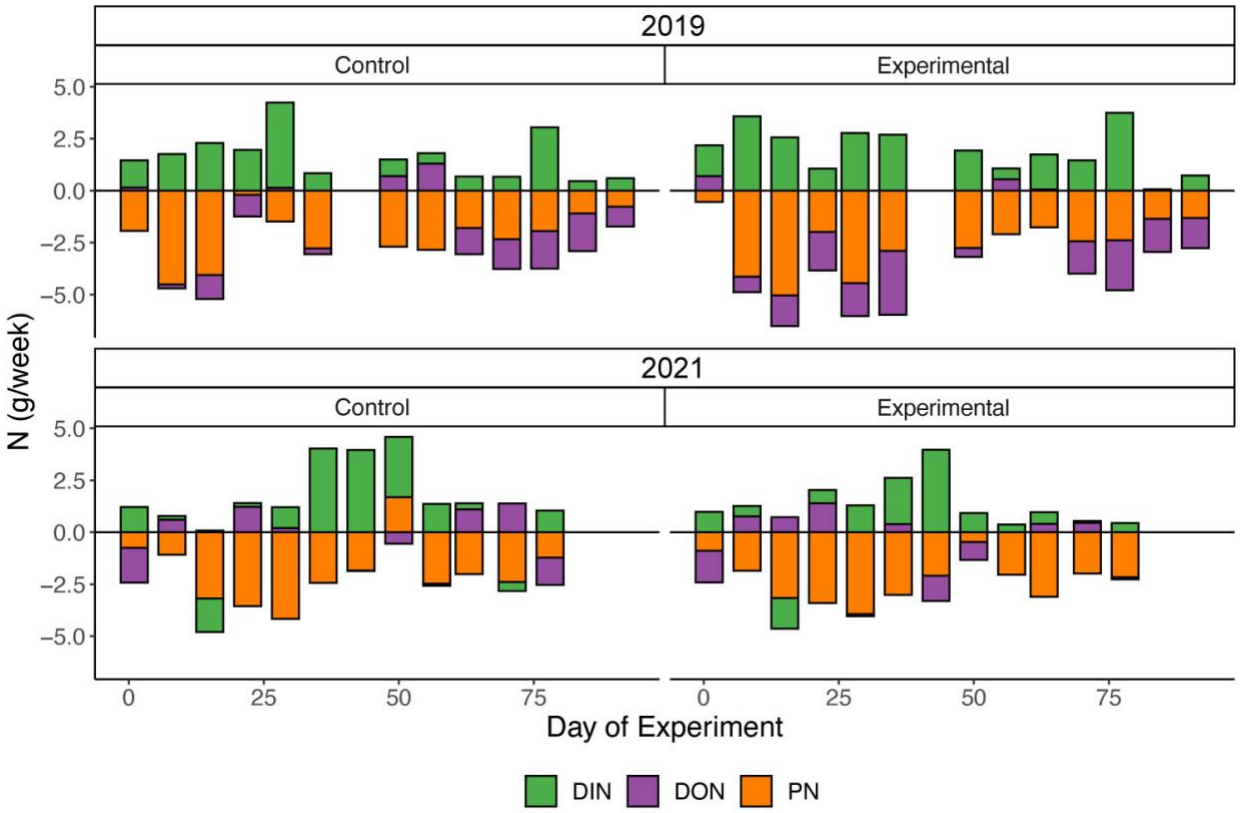

Figure 4. Weekly removal rates of organic, inorganic, and particulate forms of nitrogen. Negative values indicate a net consumption. 2019 values (top) and 2021 values (bottom).

During the spring 2021 experiments measurements of nitrogen concentrations from the tank's water column and FTW media porewater suggest temporal variation in nitrogen transformations. NO_{2+3}^- concentrations from the different parts of the mesocosm for both control and experimental showed no difference at the beginning of the experiment (initial 20 days), but beginning on day 20 (mid-May), NO_{2+3}^- increased in the porewater (fig. S2). The outflow NO_{2+3}^- concentration was 0.1 mg L^{-1} higher than the inflow during this period (i.e., net production). The opposite pattern was measured for NH_4^+ in both control and experimental mesocosms, which

increased inside the media during the first part of the experiment (and prior to nitrate increase) and then decreased in concentration during the second half of the experiment (~day 30). The NH_4^+ concentrations at times differed by 0.03 mg L^{-1} between the inflow and the media. By the latter half of the experiment, NH_4^+ concentrations were lower in the media than in the water column, while media NO_{2+3}^- concentrations were higher than other pools. Lastly, when exploring DON concentrations at different locations in the tanks (fig. S2), there is not a substantial difference in concentrations either between tank location or the treatment type.

Nitrogen transformations and oxygen consumption

Denitrification (N_2-N) rates varied throughout the length of summer 2019 and spring 2021 experiments. During the summer 2019 experiment N_2-N removal rates increased towards the end of the experiment with the highest flux being 13.4 mg N_2-N m^{-2} h^{-1} for the control mesocosm and 10.3 mg N_2-N m^{-2} h^{-1} for the experimental mesocosm (fig. 5). The spring 2021 experiments showed a slightly different behavior with the control mesocosms having the highest N_2-N removal rate at the end of the experiment (14.71 mg N_2-N m^{-2} h^{-1}, this includes an outlier) while the experimental mesocosms had the highest N_2-N removal rate at the beginning of the experiment (10.9 mg N_2-N m^{-2} h^{-1}; fig. 5). Repeated measures ANOVA indicated a significant difference in rates between months ($p<0.05$) but no significant difference between treatments ($p>0.05$) for 2019 and 2021.

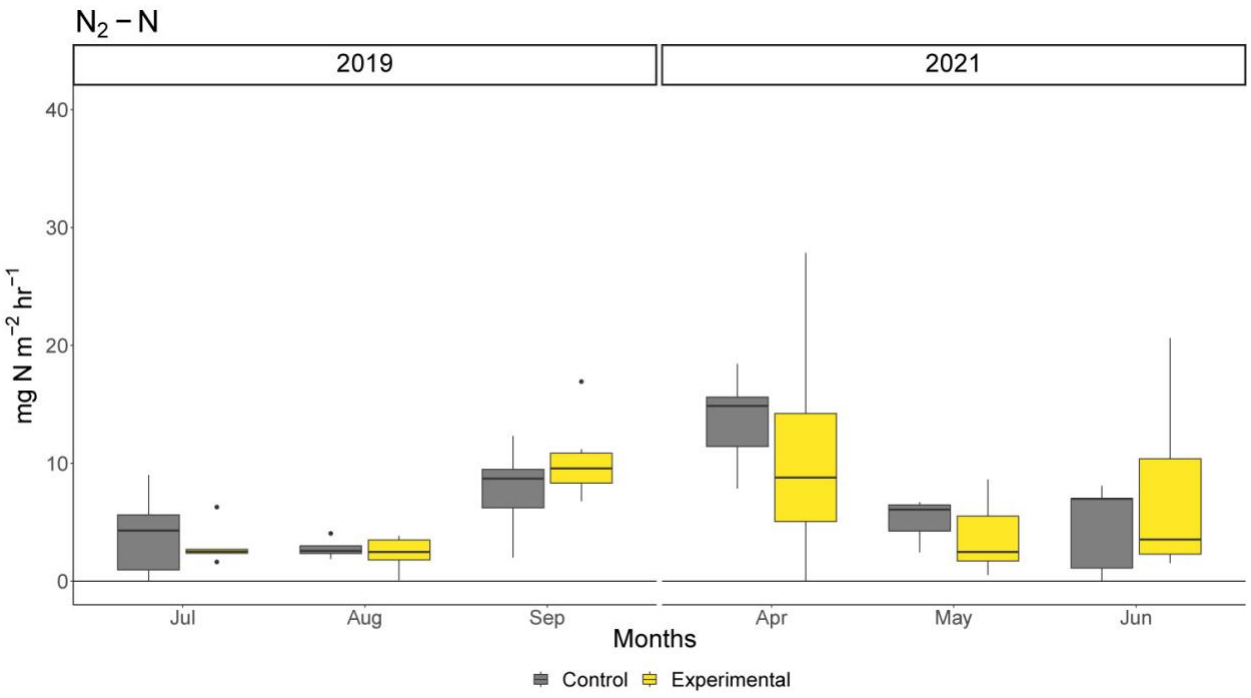

Figure 5. Denitrification measurements made monthly during the summer 2019 (left) and spring 2021 (right) experiments. Boxplot of denitrification fluxes (thick horizontal bars are median rates) illustrate peak fluxes in September and similarity between control and experimental mesocosms. Spring 2021 denitrification fluxes were similar to the summer rates from 2019, however higher fluxes can be seen happening in April rather than in September. Note circles represent outliers.

Oxygen consumption fluxes also varied in between summer 2019 and spring 2021 experiments. During summer 2019 there was an increase in oxygen consumption in both the control and experimental mesocosms over the course of the experiment (fig. 6). However, the variability was lower in the experimental mesocosms. The highest oxygen consumption was reported at the end of the experiment for the control was -391 mg O_2 m^{-2} h^{-1} while the experimental mesocosm was -232 mg O_2 m^{-2} h^{-1}. Oxygen consumption fluxes recorded for spring 2021 (fig. 6) indicated a slightly different behavior than those from 2019. During the month of April, the oxygen fluxes were close to zero, then increased over May and June. Repeated measures ANOVA indicated a significant difference in oxygen fluxes between months (p<0.05)

but no significant difference between control and experimental mesocosms (p>0.05) for 2019 and 2021.

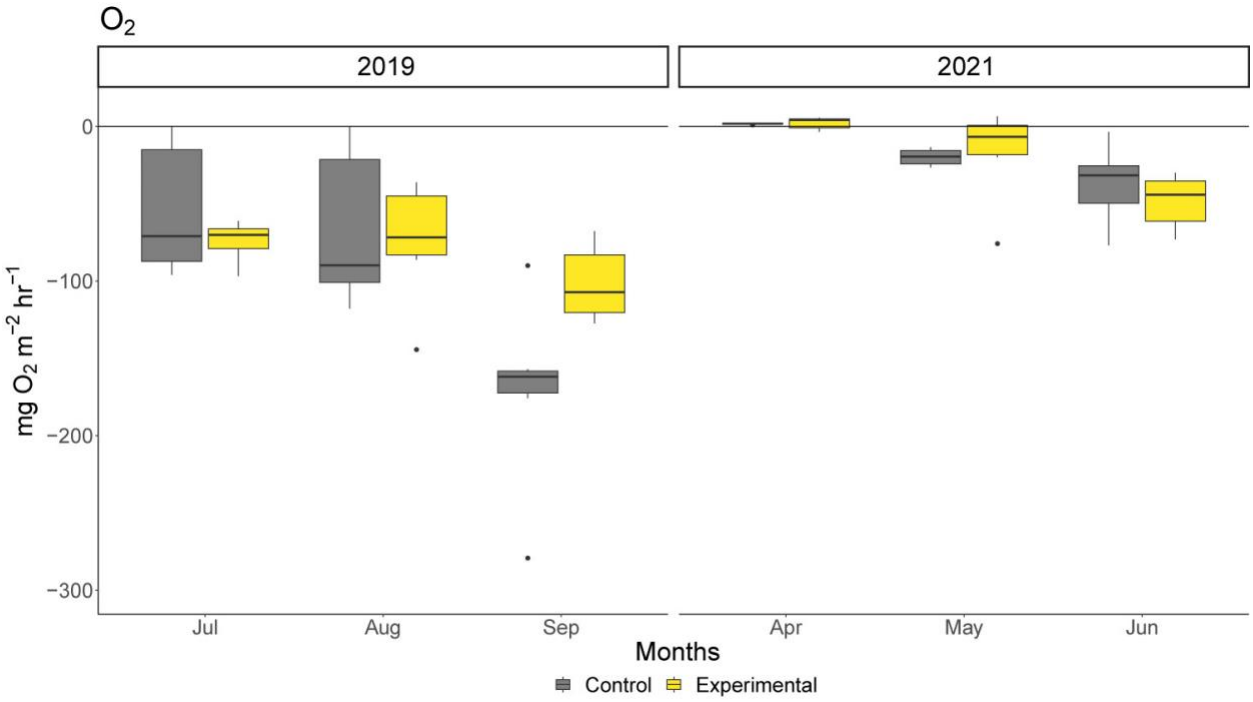

Figure 6. Oxygen consumption fluxes measured for the control and experimental mesocosms in 2019 (left), and 2021 (right). Boxplot of the oxygen fluxes (thick horizontal lines are median rates) measured monthly indicate highest oxygen consumption for the month of September. April fluxes indicate little oxygen consumption however demand increases throughout the experiment. Note circles represent outliers.

In addition to measuring denitrification and oxygen fluxes, we also measured NO_{2+3}^- and NH_4^+ fluxes from all the cores in 2021 (fig. 7). During the months of April and June fluxes of nitrate indicated an overall removal (fig. 7) whereas the month of June indicated an overall production of nitrate. Repeated measures ANOVA indicate a significant difference between months (p=0.01 for NO_{2+3}^-) but no significant differences between treatments. Lastly, ammonium fluxes (fig. 7) also show high variability, but fluxes tended to be negative. Statistical analysis indicated no significant differences in fluxes between months and between treatments (p=0.55). To quantify metrics of nitrogen cycling associated with the media, we derived a series of indices

of nitrogen transformations (appendix A Section 1). First, we computed the nitrification needed to support denitrification. This metric assumes that any N that was denitrified in excess of the NO_{2+3} influx was generated through nitrification. Computed nitrification ranged between 12.5 mg N m^{-2} h^{-1} and 300 4.2 mg N m^{-2} h^{-1} for the control and 5.3 mg N m^{-2} h^{-1} and 10.3 mg N m^{-2} h^{-1} for the experimental treatment. To further understand these fluxes, we calculated the denitrification efficiency and ammonium recycling index (see appendix A). The computed denitrification efficiency was near 100% for all fluxes, and the ammonium recycling near zero, suggesting a very efficient conversion of available nitrogen to N_2.

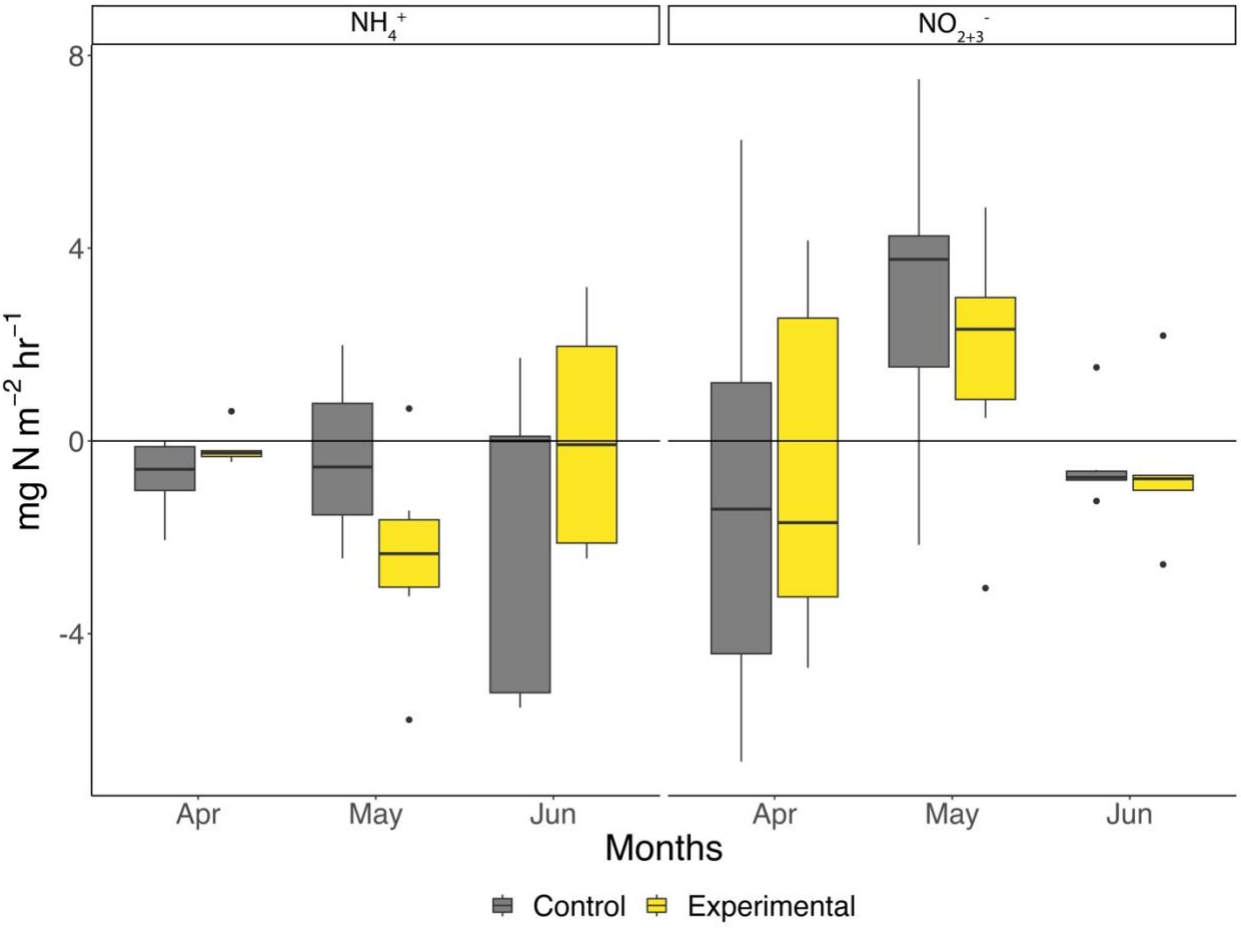

Figure 7. (left) NH_4^+ fluxes measured during 2021 mesocosm experiments. (right) NO_{2+3}^- fluxes measured during 2021 mesocosm experiments. April fluxes indicate a decrease in NO_{2+3}^-. However, as the experiment continues fluxes seem to transition from consumption to production

and then to almost no flux of nutrients. Error bars represent one standard deviation of the mean of three tanks and circles are considered outliers.

Plant biomass and periphyton N assimilation

In terms of N accumulation, above ground biomass at the end of the experiment accumulated higher quantities of nitrogen when compared to the below ground (table 3). This behavior happened during both experiments in 2019 and 2021. Physically, the plants appeared to have developed very tall stems while the root mat development was modest. We removed 5-70 g and < 10 g of periphyton in the experimental and control tanks, respectively (fig. S3), accounting for less than 0.5 g N/week. A higher mass of periphyton was collected in the experimental tanks, but this material was around 1 % N, compared to 2-3 % N in the control tanks (fig. S3).

Table 1.1. Biomass mg N accumulation for both experiments in summer 2019 and spring 2021. Accumulation includes the standard deviation from the mean. These are overall accumulation values not extrapolated to surface area.

Experiment year	**Above/Below**	**Initial**	**Final**	**Accumulation**
Summer 2019	Above	0.67 g N	12.6 g N	11.9 g N (±2.6 mg N)
Summer 2019	Below	0.98 g N	2.6 g N	1.6 g N (±0.35 mg N)
Spring 2021	Above	0.33 g N	1.5 g N	1.2 g N (±0.45 mg N)
Spring 2021	Below	0.50 g N	1.3 g N	0.8 g N (±0.17 mg N)

Discussion

Nitrogen removal was N-species specific

Overall, our results indicate that floating wetlands are capable of removing TN from estuarine-like environments (fig. 2). These removal effects are consistent and/or similar with previous FTW research that found removal of TN in retention ponds (White and Cousins 2013; Lucke et al. 2019). Previous research has focused on overall TN changes and plant assimilation

alone. Our research goes one step further and explores the changes of nitrogen. Our results indicate that FTW N removal results from nitrogen-species specific transformations associated with microbial remineralization, nitrification, and denitrification. Overall, PN, DON, and NH_4^+ were consumed in the tanks, but NO_{2+3}^- was produced. During both summer 2019 and spring 2021, the FTW seemed to have supported overall nitrification with a decrease in NH_4^+ and a subsequent increase in NO_{2+3}^- (fig. 3). This apparent production of NO_{2+3}^- is not consistent with previous studies, where (Messer et al. 2022) reported that FTW are capable of removing NO_{2+3}^- and (Chang et al., 2012) showed that under specific retention pond conditions and areal coverage, FTW can remove 100% NH_4^+-N and up to 73% NO_3-N. Our data suggest that transformations of NH_4^+ to NO_{2+3}^- could be supported by biofilm and root-associated microbial communities (see Chapter 4). Root-associated microbial communities have long been an important part of floating wetland technology (Urakawa et al. 2017; Gao et al. 2019; Choudhury et al. 2019), whose activity leads to the cycling and removal of nutrients through assimilation, nitrification and denitrification in concert with microalgae that assimilate inorganic forms of nutrients. Our measured rates of net NH_4^+ (fig. 7) production in the floating media, although variable, remained close to, or below zero, which indicates potential nitrification given that we would expect high rates of remineralization in the media (e.g., oxygen consumption was substantial; fig. 6). Furthermore, the fact that the net NO_{2+3}^- fluxes were positive in May (and somewhat in April; fig. 7) support the idea of active nitrification, which in turn, supports denitrification (Kemp et al. 1990) and nutrient removal.

Denitrification - the main nitrogen removal pathway

Denitrification in FTW has previously been assumed to be an important contributor to nitrogen removal, but this process has rarely, if ever, been directly measured in FTW. Researchers have typically used an acetylene inhibition technique to estimate the potential for denitrification in roots. Results from these experiments indicate that root-associated denitrification was the major N removal pathway in floating wetlands in freshwater, sub-arctic regions, removing between 0.4 and 30 mg N_2O-N m^{-2} h^{-1} (Choudhury et al. 2019). Other studies in freshwater conditions have developed FTW with carbon amendments to stimulate denitrification (Messer et al. 2022) and thiosulfate additions to stimulate autotrophic and heterotrophic denitrification (Gao et al. 2018). Messer et al., (2022) showed no significant differences in denitrification between the carbon amendment and control. Meanwhile, Gao et al., (2018) indicated that increased denitrification and plant assimilation with a peak TN removal of 636 mg TN m^{-2} h^{-1} because thiosulfate increases anoxia and allows denitrification. Our results indicate that denitrification played a major role in removing nitrogen from our FTW under mesohaline conditions. The lowest denitrification rate we measured was four times higher than the rates reported for tidal and brackish sediment by Cornwell et al. (2016) (0.8 mg N_2-N m^{-2} h^{-1}) while our highest denitrification flux was half of those reported for restored oyster reefs by Kellogg et al. (2013) (21.8 mg N_2-N m^{-2} h^{-1}). When comparing our results to oligohaline marshes, our rates are also four times higher than those reported by (Merrill and Cornwell 2000) (0.8 mg N_2-N m^{-2} h^{-1}). Regardless of the experimental period (summer 2019 or spring 2021), our denitrification rates suggest that FTW are efficient at removing nitrogen.

Interestingly, our results also indicate that the control (unplanted media) were also able to sustain rates of denitrification that were comparable to wetland-planted mesocosms.

Denitrification in the control ranged from 2.5 mg N_2-N m^{-2} h^{-1} to 13 mg N_2-N m^{-2} h^{-1} in the summer and from 4.1 N_2-N m^{-2} h^{-1} to 25.6 mg N_2-N m^{-2} h^{-1}. Past research investigating the contribution of the media to nutrient transformations and/or removal have shown mixed results. Stewart et al. (2008) indicated that Bio-Haven media successfully promoted nitrification and denitrification, removing 10.6 g day^{-1} of NO_3^--N and 0.2 g day^{-1} of NH_4^+-N. Garcia Chance et al. (2019), reported that their control performed better than the unplanted and planted treatments but acknowledged that periphyton might have played a role in nutrient transformations and assimilation. Wang et al. (2014) reported that their media facilitated the removal of nutrients in a similar fashion to the planted media. Lastly, Hu et al. (2010) found no difference between a media and no media treatment in an ecological sludge floating-bed artificial ecosystem. Nonetheless, our results indicate that the porous media and associated biofilm in the FTWs we examined has the potential to support an environment ideal for nitrification and denitrification (Garcia et al. 2022).

The high denitrification we measured were also associated with comparably low NO_{2+3}^- and NH_4^+ fluxes, suggesting internal N cycling to support the observed denitrification. For example, the computed denitrification efficiency was near 100%, while the NH_4^+ recycling efficiency was near zero, suggesting very efficient conversion of available nitrogen to N_2. One explanation for this efficiency is the rapid conversion of DON to NH_4^+ and NH_4^+ to oxidized nitrogen, and the apparent nitrification flux we derived are of the same order of magnitude as the denitrification rate (4,200-11,200 mg m^{-2} h^{-1}). Nitrification measured in estuaries is often higher than in open oceanic waters (Damashek et al. 2016), however, it is highly variable within and between estuaries (Damashek et al. 2016). Although nitrification fluxes in wetland sediments have rarely been reported, our apparent fluxes are higher than nitrification measured in estuarine

sediments (Kemp et al. 1990) and comparable to water-column nitrification rates measured in the York River and mid-Chesapeake Bay during destratification events (McCarthy et al. 1984), and nutrient-rich estuaries like San Francisco Bay (Damashek et al. 2016).

Variability in Denitrification fluxes

Although our measured estimates of denitrification are high relative to other estuarine environments, including tidal wetlands, the fluxes were also highly variable. This suggests that there is a range of conditions within the floating wetland media that are more or less supportive of denitrification. Root development (and thus root content) was not evenly distributed throughout the media, and the algal biofilms that developed on the media were patchy. Plant-root presence might have affected the microbial community composition and thus contribute to variability in nitrogen cycling. Tanaka et al. (2012) and Urakawa et al. (2017) found the microbial composition of roots to be more diverse than unplanted media, and was dominated by Alphaproteobacteria, Betaproteobacteria and Cyanobacteria. Thus, plant presence plays a role in selecting and or dictating the microbial composition in the floating media (Urakawa et al. 2017). More research is needed to better understand the differences in microbial-periphyton composition in planted and unplanted media.

Plant N assimilation

Plant N assimilation is the way stakeholders, in the Chesapeake Bay, provide credit for the amount of nitrogen removed from a retention pond by a FTW (Schueler et al. 2016). Our results show a higher nitrogen accumulation in the summer 2019 than spring 2021 experiment. *Spartina patens* has been shown to effectively assimilate N from brackish systems when compared to *S. alterniflora* and other wetland plants (Landaverde et al. 2024), making it suitable for use in FTW technology in estuarine-like environments. However, research indicates that

although plants assimilate nitrogen during the growing season, it will leach back to the system if not harvested entirely (Wang et al. 2014). Previous research shows that even when harvesting twice during the growing season, plant N assimilation is only a small fraction of the nitrogen that is transformed and or potentially removed from the retention pond (Wang et al. 2014). As our results indicate, the media is capable of removing higher amounts of nitrogen through denitrification for both summer 2019 and spring 2021 (29 and 37 g N, respectively), when directly compared to plant N assimilation (15 and 1.7 g N, respectively). These results are consistent with previous studies that suggest most of the removal is done by the periphyton and root-associated biofilm (Wang and Sample 2014).

Floating wetlands: beyond retention ponds

FTWs have been implemented as a way to overcome nutrient removal limitations of retention ponds and wastewater treatment plants for decades. Since 2016, FTWs have been certified as a best management practice (BMP) thanks to their removal efficiency and increased contribution to nutrient and sediment removal from multiple sources of runoff and wastewater (Schueler et al. 2016). For decades this technology has been implemented with the idea that plant growth is the main facilitator of nutrient and sediment removal. However, new research has suggested that the bulk of the nutrient removal happens thanks to the associated microbial communities growing in the floating media and dense root system. Our results, combined with previous research, contribute to the idea that bulk nitrogen removal happens effectively and permanently through microbial transformations. More importantly, these results are indicative that floating wetlands have capabilities of removal efficiency through plant and microbial communities in tidal systems. These results can help expand the FTW BMP credit and go beyond retention pond installations. Implementation of this technology in tidal systems can help expand

and improve nutrient management efforts beyond land nutrient management in coastal areas where shoreline is highly developed, and the restoration of wetlands is not an option. More importantly, the installation of these FTW along developed coastlines can help abate nutrient in an era where population, land development, and temperatures are expected to increase.

Conclusion and Future Work

Our mesocosm study in estuarine-like environments revealed that FTW foster an environment suitable for the transformation and removal of nitrogen through multiple pathways. The transformation and removal of nitrogen was form-specific, where the FTW removed dissolved organic, particulate, and NH_4^+, but generated high quantities of NO_{2+3}^-. The net NO_{2+3}^- production appeared to sustain high rates of denitrification in the wetland media in excess of plant tissue uptake. The control treatment (un-planted media) transformed and removed nitrogen in ways comparable to the planted media, identifying microbial communities as a major player in the nitrogen transformation and removal in FTW. Thus, this technology seems to foster a suitable environment for nitrogen removal beyond plant assimilation and subsequent harvest. These results are encouraging and support the potential for expansion of current BMP crediting and implementation of FTW in urban tidal systems where restoration of natural wetlands is not an option. Future research could address some of the limitations of this study, including additional studies to understand the performance of floating wetlands in the fall and winter, experimentation with different species, and perhaps longer experiments that include the entire growing season. *In situ* studies of FTW performance in small estuaries could help develop methods that allow for accurate measurements of nitrogen transformations and changes in concentrations in, and around, the FTW. Additionally, future research should also include the evaluation of current implementation methods like anchoring techniques, evaluation of estuarine

plant performance, and FTW designs better suited for tidal systems and thus maximize nitrogen transformation and removal potential.

Chapter 3: Partitioning nitrogen removal potential in floating wetlands using a mass balance approach

Abstract

Floating wetlands have been extensively applied as a nutrient removal technology in retention ponds and other freshwater systems. Despite this long history, surprisingly few studies have attempted to directly quantify the removal rate of nitrogen contributed by specific processes. The need to better quantify these nitrogen removal processes is underscored by a growing desire to identify novel ways to remove nutrients from eutrophic ecosystems, and to certify technologies as Best Management Practices. We therefore describe a series of mesocosm experiments executed under estuarine conditions to quantify the specific processes leading to floating wetlands' removal of nitrogen. We developed a nitrogen budget for two, 10-week experiments, one during the summer of 2019 and the other during the spring of 2021. Results indicate that floating wetlands remove nitrogen primarily through denitrification (15% and 39%, respectively), followed by plant nitrogen assimilation (8% and 2%, respectively) during both spring and the summer. These results reinforce the utility of floating wetland to remove nitrogen and provide specific information on removal mechanisms to support future design and certification frameworks.

Introduction

Although nutrients are essential for supporting the growth of plants and animals, when nutrient concentrations in aquatic ecosystems increase, associated increases in productivity drive elevated algal biomass (Nixon 1995), low oxygen zones (Diaz and Rosenberg 2008), and the degradation of coastal systems (Deegan et al. 2012). Decades of nutrient over-enrichment have led to degradation of water quality and habitats in a wide range of coastal ecosystems (Nixon

1995, Lefcheck 2018), leading to major commitments to reduce watershed nutrient inputs. Many efforts to meet watershed nutrient reduction goals have had limited success (Scientific and Technical Advisory Committee (STAC) 2023), in part due to the inherent challenges in reducing agricultural and urban non-point loads. Watershed nutrient reduction approaches involve a variety of practices known as best management practices (BMPs) (Choi et al. 2020), which are typically approved through a review process as accepted land management practices to mitigate pollution from non-point sources (Choi et al. 2020). Despite the fact that BMPs are intended to improve conditions in rivers, lakes, and estuaries, the vast majority of BMPs are land-based practices.

Floating treatment wetlands (FTWs) are an example of a water-based, certified BMP technology in which macrophytes are grown on a floating raft and/or media, typically in stormwater retention ponds. For most FTWs, the roots are in permanent contact with the water column and remove nutrients and other pollutants via several physicochemical-biological processes (Sharma et al. 2021). The implementation of floating wetlands is most common in stormwater retention ponds as an effort to increase the pond's efficiency at treating runoff and overcome operational challenges and flaws like an inconsistent hydrologic load of nutrients and other pollutants (Tanner 2006). FTW technology and research has evolved and expanded to engineered FTW to treat other polluted waters. Some of the polluted waters include urban and agricultural runoff (Sample & Wre, 2017; F. M. Stewart et al. 2008), secondary effluent (Gao et al. 2018), greywater (Faulwetter et al. 2011), mine tailings water (Gupta et al. 2020), and industrial wastewater (Knight et al. 1999).

Floating wetland efficiency and removal is generally estimated by doing measurements of nutrient concentrations in the inflow and outflow of retention ponds that are planted with floating

wetlands. These approaches estimate reductions in the outflow relative to the inflow as a metric of removal, and may be supported by measurements of nutrient and other water quality parameters in and around the floating wetland, and thus estimate a whole system removal of pollutant. Other studies have performed mesocosm experiments in a "batch" design, where floating wetlands are exposed to artificial runoff for a short period of time and water and plant biomass is analyzed for nutrients and other pollutants at the end of the experiment (Tanner and Headley 2011; Spangler et al. 2019). Results from the batch experiments are then extrapolated across the entire system of interest, depending on the size and density of wetlands (Tanner and Headley 2011). Although these approaches have allowed for an ecosystem-scale nutrient removal effect of floating wetlands in retention ponds, the specific pathways in which floating wetlands remove nutrients has not typically been explored.

Contrary to retention ponds, tidal waters are open systems consisting of tidal exchange, whereby nutrients available in any given location can have an uncertain origin. Due to the dynamic nature of tidal systems, measurements of the net effects of floating wetlands on nutrient uptake are difficult because the inflows and outflows of material cannot be constrained as they would in a retention pond and it is difficult to scale FTW nutrient removal to inflows. Mesocosm experiments provide a controlled system that allows for tracking of inputs and outputs, allowing for the development of constrained nutrient mass balance, which inform quantification of specific removal rates. Although mesocosm have constrains they still provide impactful data that allows for the understanding of floating wetlands as long as biases and limitations are acknowledged and addressed accordingly (Brisson et al. 2024). In the simplest way, a budget is the balancing of inflow and outflow of nutrients as well as estimating the magnitude of changes within the system of interest (Boynton and Nixon 2013). Budget analyses have been employed

on a large number of scales and for a variety of purposes in natural systems, including net watershed nutrient balances (e.g., Howarth et al., 1996), estuarine organic carbon budgets (e.g., Kemp et al., 1997), and oyster aquaculture nitrogen balances (e.g., Testa et al., 2015). Budgets allow the identification of the most important processes or stocks in a system, while also helping identify which processes or stocks are poorly constrained. Boynton et al., (2008) developed a nitrogen budget for the Patuxent River estuary that allowed for better understanding of the sources of nutrients and how loss processes, like wetland-derived denitrification and burial, were relative to external loads. Despite their utility to compare the relative magnitude of source and sink processes in ecosystems and inform nutrient management decisions, such budget analyses have not been performed for FTWs in estuarine waters.

Thus, the goal of this study was to utilize a budget approach using a wide-variety of measurements made during mesocosm experiments to identify and quantify the primary nitrogen loss terms in floating wetlands. We leveraged measurements of plant uptake, nutrient concentrations, denitrification, and inflow and outflow rates in experimental mesocosms to inform the budget approach. This budget will help assess the effectiveness of floating wetlands in removing nitrogen when deployed in estuarine-like environments and to compare nitrogen removal mechanisms within the floating wetlands to prior studies. Results from this research could potentially be used to update the current information on floating wetlands as a certified best management practice.

Materials and Methods

We designed and executed two mesocosm experiments, one in 2019 from June 21st until September 9th and a second in 2021 from April 16th until July 22nd, to measure nitrogen removal and transformation during the summer and spring. These experiments were carried out in

different years due to COVID-19 interruptions as well as logistics. The mesocosm design consisted of a flow-through system, with three control tanks and three experimental tanks (fig 1). Control tanks consisted of unplanted floating wetland media, while the experimental tanks consisted of the floating media planted with *Spartina patens*. To measure the effects of the floating wetland nitrogen removal, we measured nitrogen accumulation in plant material (roots, shoots, flowers, and seeds), periphyton and detritus within the mesocosm tanks, as well as rates of nitrogen removal (denitrification) within the floating wetland matrix. Dissolved and particulate nitrogen concentrations from the inflowing water and outflowing water were collected weekly for both experiments (summer 2019 and spring 2021). For the spring 2021 experiment, nitrogen concentrations were also measured within the tank water column and within the media pores. Water temperature, dissolved oxygen, salinity, specific conductivity, pH, and chlorophyll-a in the tank water column were monitored on a daily basis between 12:00 PM and 3:00 PM. See appendix A for average environmental characteristics of the tanks (table S1). Hourly precipitation and photosynthetically active radiation (PAR) data were collected from the Chesapeake Biological Laboratory (CBL) monitoring station (https://cblmonitoring.umces.edu/). Plant material accumulation was measured at the beginning and at the end of the experiment, separated into above-ground and below-ground biomass. Denitrification was measured once a month during the course of each experiment.

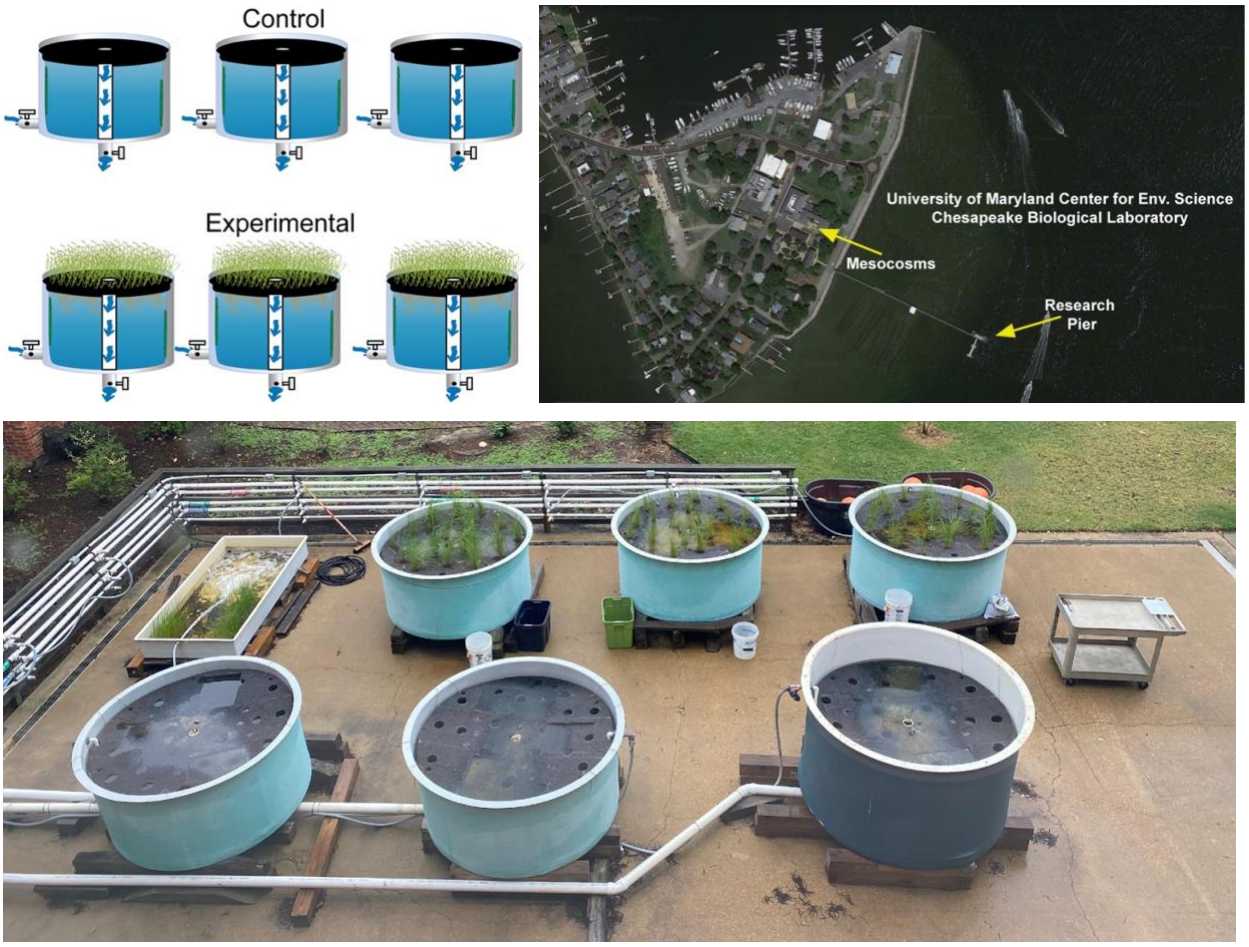

Figure 1. (left) Diagram of the experimental design in triplicate mesocosms tanks with and without floating wetlands. The flow of water enters through the bottom and exits the tanks through a centrally located standpipe. (right) Research pier at the University of Maryland Chesapeake Biological Laboratory, Solomons Island, Maryland, USA where source water for the mesocosm tanks was obtained. (bottom) Picture of control and experimental tanks on July 2, 2021.

Sample measurements and analysis

Dissolved (NH_4^+, DON, NO_{2+3}^-) and particulate (PN) nitrogen concentrations were measured on a weekly basis from the inflow and outflow for summer 2019. For spring 2021 we included dissolved nutrient measurements from within the floating media (i.e. the porewater within the media), as well as the water column inside each tank. Porewater was collected using a syringe to extract the water from the media, while inflow and outflow water was collected directly from the pipes just downstream from the valves that controlled water flow in and out of

the tanks. Water samples from the different parts of the tanks were collected in 2L Nalgene bottles that were previously acid washed. Inflowing water was measured at one valve where water entered the plumbing for the entire mesocosm system, and the nitrogen concentration at this the inflow was assumed to be representative for the water entering at the valves for all tanks. Prior to starting the experiment, dissolved nitrogen was measured from two different valves to confirm that the inflowing concentration of dissolved nitrogen was not substantially different between all tanks (i.e., nitrogen was not transformed within the plumbing system). The mean ± standard deviations of measurements for NH_4^+ (0.034 ± 0.0004 mg L^{-1}), and NO_{2+3}^- (0.02 ± 0.002 mg L^{-1}) of the two valves indicate highly comparable concentrations (low standard deviation).

Samples were sent to the Chesapeake Biological Laboratory Nutrient Analytical Services for analysis. Ammonium (NH_4^+) was analyzed using standard methods (4500-NH3 G-1997, MDL 0.009 mg L^{-1}), nitrate + nitrite (NO_{2+3}^-) was analyzed using the catalyzed enzyme reduction method (ASTM D-7781, MDL 0.0057 mg L^{-1}), dissolved organic nitrogen (DON) was analyzed following the EPA 365.1 method (MDL 0.05 mg L^{-1}), and particulate nitrogen (PN) was analyzed following the EPA 440.0 method (MDL 0.0263%) . Discrete sampling of water temperature, dissolved oxygen, salinity, specific conductivity, and pH was measured on a daily basis using a YSI Sonde MPS 556 just below the floating matrix. Chlorophyll-a was monitored on a daily basis and analyzed within 28 days of collection using 90% acetone extraction technique and fluorometric analysis (EPA 445.0, MDL 0.68 μg L^{-1}). Water volumes for chlorophyll-a analysis ranged between 60mL and 180mL depending on the location (inflow, outflow, water column and media porewater). YSI Sonde calibration was performed weekly,

whereas fluorometric calibration was performed every 60 days. We measured whole-tank above- and below-ground biomass at the beginning and end of the experiments.

Above-ground and below ground biomass were collected following Kreeger(2014a; 2014b). Initial above and below-ground biomass was calculated by randomly selecting three plants before planting. Since plants were all the same size, we assumed all three tanks started with the same above and below ground biomass. Plant material was rinsed with DI water and dried at 60˚C to constant weight. Then, plant material was ground and analyzed for nitrogen content (Zimmermann et al. 1997, MDL 0.01%), to estimate whole-tank plant nitrogen content. To estimate final above-ground biomass, nine *S. patens* plants per tank were collected, rinsed with DI, and dried at 60 ˚C to constant weight and further analyzed for nitrogen content. The rest of the above-ground material from each tank was harvested, rinsed with DI water, and dried at 60 ˚C until the material reached a constant weight. The nitrogen content of all sampled plants was averaged and multiplied by the total amount of above-ground biomass in each tank to obtain the total above-ground biomass in milligrams of nitrogen per tank. For final below-ground biomass, three randomly selected squares from each floating matrix were cut out and their area was measured (between 40cm^2 and 40.5 cm^2 per square). All root material was extracted from the matrix in each square, rinsed with DI and dried at 60˚C, and further analyzed for nitrogen content. These subsamples are assumed to represent the whole tank, and the subsampled belowground biomass and N content were extrapolated to compute a whole-tank N content.

Denitrification and nutrient fluxes were measured at two randomly selected locations within each FTW media in both the control and experimental mesocosms. The cores were drilled before the experiment started and then they were randomly selected. Once a month, two pre-cut cores of floating wetland matrix from each tank were collected, placed on a 6.5 cm plexiglass

core, gently filled with ambient water, and capped with an O-ring sealed top. A core containing only water from the tanks, was used as a blank and be able to distinguish between the denitrification happening in the water column and the media. The cores were then placed in the dark in a temperature-controlled water bath to attempt to simulate in-situ conditions. After reaching in-situ conditions, the cores were incubated for three hours in the dark. Nutrient fluxes (NH_4^+ and NO_{2+3}^-) were measured only during the spring 2021 experiment. This method is an adaptation of a method used to measure denitrification and nutrient fluxes from bottom sediments (Testa et al. 2022). Every hour, samples were collected in 12mL exetainers (Labco, UK) from each core and fixed with 60µL of a saturated mercuric chloride solution (Fulweiler et al. 2007). Samples were analyzed using a membrane inlet mass spectrometer (MIMS, Bay Instruments, Easton, Maryland) and the N_2/Ar technique (Kana et al. 1994). The N_2/Ar technique measures the net N_2 production in the sample core, thus denitrification rates and nitrogen fixation rates cannot be separated. Thus, the linear increases in N_2 concentration were used to estimate net N_2 production during the experiment as net N_2 flux, or net denitrification (Kana et al. 1994; Cornwell et al. 2016). Detailed calculations on how flux rates were estimated can be found in appendix A.

Measuring and removing periphyton

Mesocosm walls can substantially alter experimental conditions by limiting water exchange, absorbing downwelling light, and providing substrate for a myriad of organisms to grow (Kemp et al. 2009). Because the ratio of wall surface to water column is high in mesocosms, and because periphyton accumulate on tank walls, we sought to directly measure the relative contribution of periphyton to the biomass and N budget of each tank (Chen et al. 1997; Chen et al. 2000). To prevent excess periphyton accumulation, all periphyton in each mesocosm tank was scrubbed from the walls and collected on a weekly basis. To collect the periphyton, the

floating media was lifted using a gantry crane. A 500µm mesh was added to the outflow pipe and then the tank was drained. Wall and tank bottom were scrubbed using a clean brush and all material gathered. The collected periphyton was then brought to the laboratory, rinsed with deionized water, and dried at 60˚C until a constant weight was reached. All the periphyton collected was analyzed for PC and PN to quantify how much nitrogen was being removed by tank artifacts.

Mass balance

We computed a nitrogen mass balance for the entire length of the experiments in each tank by accounting for all measured nitrogen input and removal rates. The budget includes four classes of nitrogen inputs, including the inflowing nitrogen from the Patuxent River, atmospheric deposition, slow-release plant fertilizer included in each initial plant plug, and peat moss and topsoil added on top of the floating matrix in the experimental treatment tanks to support initial plant growth. Inflowing nitrogen was measured directly from one inflowing valve and was assumed to be the same at all other inflowing locations (see Butler-Viruet et al., 2025 for details). Atmospheric input was estimated by multiplying measured precipitation rates scaled to include only the deposition landing directly on the surface of each tank. Slow-release fertilizer is assumed to be a fixed amount of nitrogen per tank at the beginning of the experiment and we assumed that it completely dissolved by the end of the experiment. To estimate the amount of nitrogen contributed by the fertilizer, I assumed a uniform, one-time application to each of the 20 plant plugs that were placed in the media of each tank. I used the manufacturer-supplied concentration of N in the fertilizer and multiplied that by the suggested amount for batch application to each plant plug by the fertilizer company. Since fertilizer was deemed a small portion of the budget, I assumed that all fertilizer completely dissolved by the end of the

experiment. Peat moss and topsoil additions were assumed to be a fixed amount of nitrogen per tank at the beginning of the experiment, as we added 10 kg of peat moss (PREMIER Sphagnum peat moss) and 18 kg of topsoil (GardenPro by Harvest) to each experimental tank. We measured the % N content from each material (using same methods as above and below-ground biomass) to estimate the total input.

The budget also includes five nitrogen loss terms, including above-ground biomass nitrogen assimilation, below-ground biomass assimilation, periphyton biomass nitrogen assimilation, denitrification, and outflowing nitrogen. Above-ground and below-ground biomass nitrogen uptake was estimated by measuring initial and final nitrogen content of all harvested plant material. I measured whole-tank above- and below-ground biomass at the beginning and end of the experiments. Above-ground biomass was collected following Kreeger (2014a) whereas initial below-ground biomass was collected following Kreeger (2014b). Periphyton nitrogen assimilation was estimated by summing the weekly mass of harvested periphyton biomass from each tank multiplied by the % nitrogen content of the homogenized sample. Denitrification in the media was measured directly from each tank three times during the experiments following Butler-Viruet et al., 2025. To estimate the total nitrogen removed by each term, all weekly terms were added together over the course of the experiment. For denitrification we extrapolated measurements to represent monthly flux rates by assuming constant rates for each month where measurements were made, then added all three measurements together. A TN budget was calculated for each individual tank (3 control, 3 experimental), and then averaged together to compare treatment effect.

Finally, we also performed a 90 day mesocosm experiment in the summer of 2021 (July-September) where only the media was present. In this experiment, three tanks included the media

being submerged so that 50% of the media was submerged in water, and three tanks where media was 100% submerged. We measured denitrification once each month in all tanks using the same approach as Chapters 2 and 3. At the culmination of these experiments, we extracted the media cores that had been incubated for denitrification and performed a 12-day diagenesis experiment to estimate the accumulation of nitrogen in the media biofilm. In these experiments, we submerged each media core in water (using the same core liners as for denitrification) and deoxygenated the water by bubbling with nitrogen gas. Replicate cores were analyzed for each tank. We then extracted a 10 ml sample periodically over a 12-day period and replaced the water volume with N_2 gas to maintain anoxic conditions. Each sample was analyzed for NH_4, NO_{23}, and sulfide, where nitrogen species were analyzed as in Chapters 2 and 3 and sulfide ($H_2S + HS^- + S^{2-}$) samples were preserved with sulfide anti-oxidant buffer (SAOB), which raises sample pH such that H_2S and HS^- are converted to S^{2-}, and analyzed using the ion specific electrode method within 24 hours of sampling. The resulting concentrations were then multiplied by the core water volume at the time of sampling to compute the total mass that had accumulated. The time series of each solute mass was then fit with a linear regression (see appendix B) to estimate the rate of accumulation and the net accumulation (final –initial concentration) was computed for each core.

Uncertainty Estimates

To estimate the overall error in the budget terms, we followed Pennino et al. (2016). We first estimated the uncertainty and error propagation using the standard errors calculated for a subset of the rates that were measured separately in all tanks over multiple samplings over time, including denitrification, periphyton, and nutrient concentration in the outflow. We were unable to estimate uncertainty and error propagation in plant biomass accumulation since we only measured initial and final TN content. Similarly, inflow TN concentration does not have an

associate estimated uncertainty and error since we assumed that one inflow was representative of all inflow in the tanks. Details and equations on how we estimated the standard error and overall budget error can be found in appendix B.

Results

Results of the budget will be presented in terms of grams of total nitrogen (g TN) per length of each experiment. Results from the 2019 budget represent TN removal of floating wetlands during the summer experiments (June – August), while the 2021 budget represents the TN removal of floating wetlands for the spring experiments (April – June).

The control nitrogen budget for summer 2019 indicates an overall difference of 17 g TN between the inflow and the outflow (fig. 2), which equates to a net removal by the floating wetland. In the control budget, denitrification removed 32 ± 7 g TN, which exceeded the difference between the inflow and the outflow. When considering the difference between the sources of nitrogen and all the sinks of nitrogen (outflow plus all other loss terms) in the control treatment, a net source of 16 g TN was unaccounted for. The wall periphyton loss term was minimal with only a removal of 0.9 ± 2 g TN. The experimental treatments for summer 2019, on the other hand, show a difference (i.e., an uptake) of 129 g N between the inflow and the outflowing concentrations (fig. 2, bottom). Denitrification over the experiment removed a total of 29 ± 4 g TN, while the plant sequestered 12 g N for above ground biomass and only 3g N for below ground biomass. Wall periphyton TN assimilation removed 3 ± 2 g TN from the mesocosm. When considering the difference between the sources of nitrogen and all the sinks of nitrogen (outflow plus all other loss terms) in the experimental treatment, a net source of 82 g TN was unaccounted for.

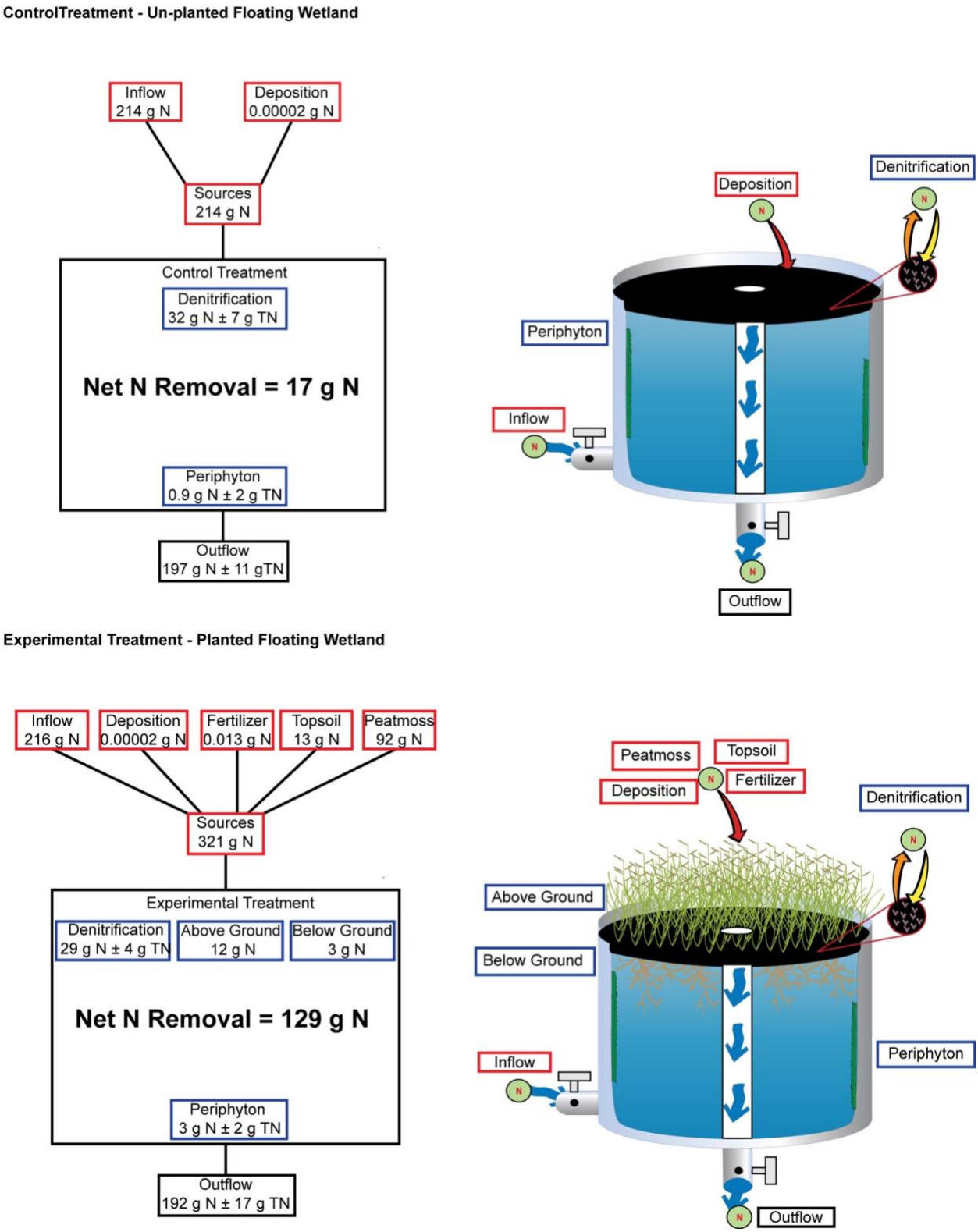

Figure 2 Control tank nitrogen budget. (top) Nitrogen budget for the experimental tank. (bottom) Diagram of the sources (red) and losses (blue) of nitrogen in the mesocosm tank. ± represent the uncertainty for each term.

For spring 2021, the control budget included an average removal of 13 g TN from the system (fig 3, top). Denitrification removed on average 45 ± 18 g TN and periphyton played a minimal role, removing 0.9 ± 2 g TN. Meanwhile, the experimental budget (fig. 3, bottom) indicates a net loss of 122 g TN, and denitrification accounted for an average removal of 37 ± 7 g TN, above ground biomass removed 1.1 g TN and below ground removed 1 g TN from the mesocosm system. Periphyton was responsible for the removal of 2 ± 2g TN.

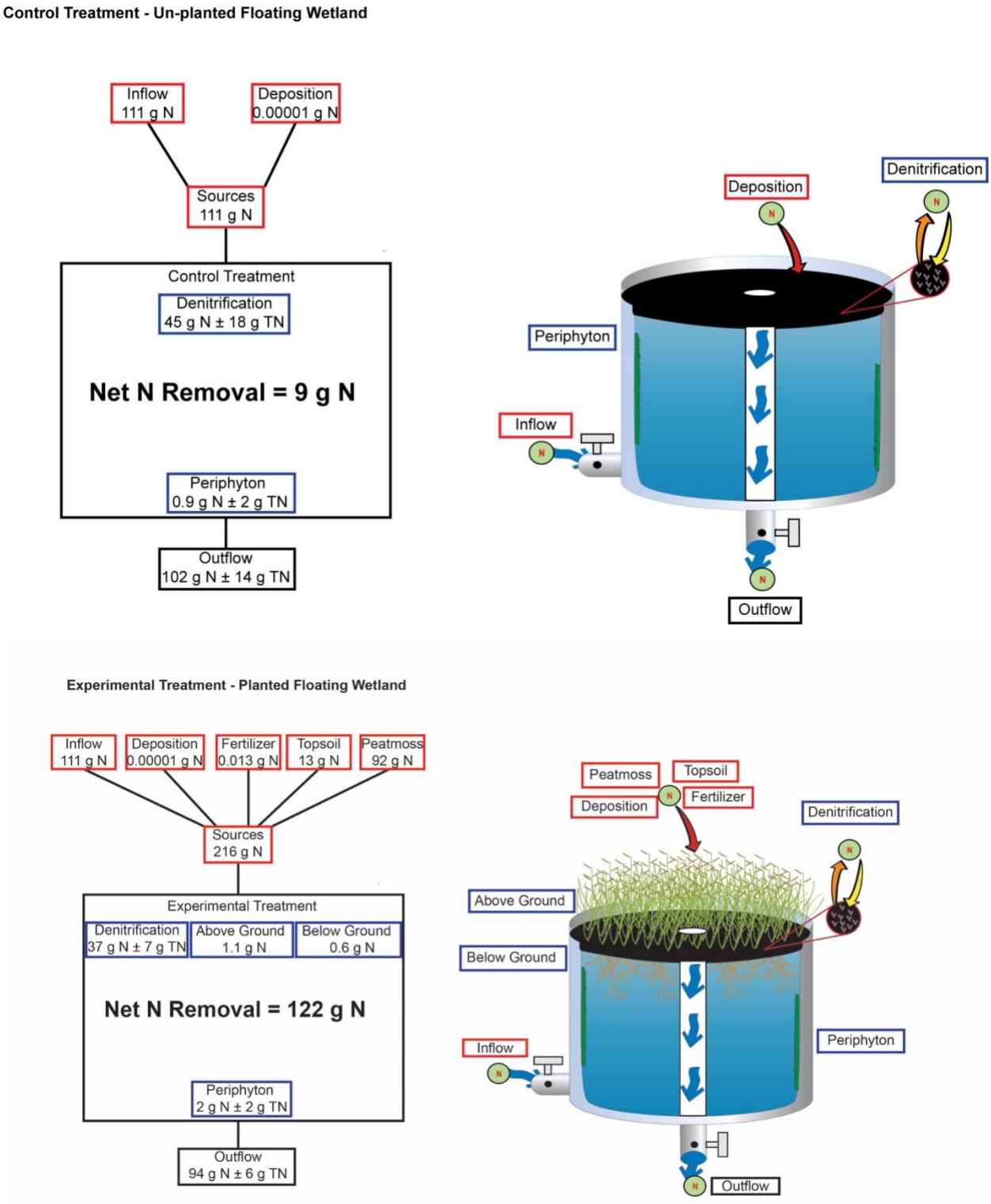

Figure 3. Control budget for Spring 2021 (top) and experimental budget for Spring 2021 (bottom). Diagram of the sources (red) and losses (blue) of nitrogen in the mesocosm tank. ± represent the uncertainty for each term.

Discussion

During both years and seasons denitrification was the primary nitrogen sink in our budgets. Denitrification removed 16% of the TN input during summer 2019 in the controls, and 15% in the experimental treatment. Meanwhile for spring 2021, denitrification removed 44% of the TN input in the controls and 39% of the TN in the experimental treatment. The relative contribution of denitrification to total N losses in the mesocosm tanks during summer was comparable to natural systems with low residence times 10-15%, (Shen et al. 2022) but lower than longer residence time systems, where denitrification in sub-tidal sediments removed 60% of the watershed load to the Patuxent River estuary (Boynton et al. 2008). Regardless of the relative removal rate, denitrification was the largest removal process in our wetlands, exceeding removal via plant biomass by a factor of two during the peak growing season (June to August) and by a factor of >20 during the low-biomass period.

A relevant result of our budget analysis was the fact that we measured substantial denitrification rates in the control treatments, where no wetland plants were added. Our control treatment consisted of a floating media with a surface area of 2.5 m^2 and a thickness of 17.8 cm and is made of PET fibers that create high porosity and internal surface area of 656.2m^2/m^3. Throughout the course of our experiment noticeable amounts of biofilm developed within the media pores (fig. 1) which possibly created substantial areas of oxic and anoxic interfaces that could support coupled nitrification and denitrification. Recent research has demonstrated that unplanted media also has the potential to remove nitrogen through the activities of microbial communities that develop within the complex matrix within the media. Stewart et al., (2008) indicated that BioHaven media (made of PET fibers) successfully promoted nitrification and denitrification, removing 10.6 g day^{-1} of NO_3^--N and 0.2 g day^{-1} of NH_4^+-N. Wang and Sample, (2014) reported that their media (PVC frame with plastic mesh) facilitated the removal of

nutrients in a similar way to the planted media, while Zhao et al. (2013) reported that their floating beds with rhizo-bags performed better than the no-media treatments but worse than their floating beds planted media with tall fescue (*Festuca arundinacea*) thanks to bacterial development throughout the course of their experiment. These results support the hypothesis that floating media -sustain an environment ideal for microbially-mediated nitrification and denitrification (Garcia et al. 2022).

In comparison to denitrification, plant nitrogen assimilation removed a comparably low amount of nitrogen in our experiments. Plant assimilation removed a combined 15 g TN (8%) of TN in the summer, and 1.7 g TN (1.8%) of the TN in the spring. Summer values are comparable to other floating wetland studies, where for example, Garcia Chance et al. (2019) reported that *P. cordata* and *J. effesus* removed higher rates of N during the months of August and September when deployed in a high nutrient runoff (8.6 g TN and 88 g TN, respectively when extrapolated to the same amount of time elapsed in our experiment). When comparing these sinks to natural systems, Anderson et al. (1997) reported a removal of 14 g TN m^{-2} y^{-1} for *Spartina alterniflora* in a marsh located in Eastern Shore Virginia. Again, these ranges are indicative that the removal of TN by *Spartina patens* in our mesocosm (37.5 and 4.3 g TN m^{-2} for 2019 and 2021) is comparable to rates found in natural systems. Above ground assimilation was higher than below ground assimilation, indicating that wetlands planted for nitrogen removal *in situ* could be managed with above ground harvest occurring in fall to remove the nitrogen completely from an estuary. This high above ground to below ground N ratio can be seen in natural marshes that are experiencing high levels of nitrogen input, as for example, where *Spartina* spp. allocate biomass primarily to above ground tissue under nitrogen enrichment (Deegan et al. 2012). This allocation to above ground biomass seen in the experimental treatments can be due to the use of fertilizer at

the plant nursery that provided the plants for the experiment, or due to the relatively high background N concentrations in the Patuxent River water we used in our experiments. Floating wetland budgets from both the 2019 and 2021 mesocosms indicated that 85 g TN (2019) and 83 g TN (201) were unaccounted for in the experimental tanks, suggesting an unaccounted for sink of N. One potential sink of N that we did not explicitly include in our budgets was incorporation of N into the biomass of the biofilms that developed in both experimental and control media.Data from the diagenesis experiments showed that after 12 days, the media released an average of 4 g ± 1.2 g of highly degradable N, but this duration was not long enough to decompose all of the biofilm. However, the modeled total N that would be released given all of biofilm degraded ranged from 6 g TN up to 16 g TN of highly reactive N after a year. These experiments suggest that the biofilm likely accounted from 6% up to 19% of the missing N in the budgets.

There could be other sources of error in the budget calculations that led to the mass imbalances we measured. For example, in the experimental treatments, we effectively assumed that all of the topsoil and peatmoss was removed, despite the fact that it is likely that substantial portions of this material remained at the end of the experiment, especially given its low N content (1% for peatmoss and 0.7% for topsoil). We also observed that a portion of this material sunk to the bottom and was removed when we cleaned the tanks to sample the periphyton, or some left the tank through the standpipe. All of these uncertainties might be causing the discrepancies in the budget, especially since the peatmoss and topsoil inputs were nearly 30% of the overall input to the tanks.

In contrast to the experimental tanks, there was more nitrogen being removed than the difference between the inflow and the outflow, indicating an unidentified net source of nitrogen.

indicates. This source is potentially necessary to support the denitrification we observed in the control treatments. We hypothesize, that the high surface area of the media allows for adjacent anoxic and oxic microzones to develop throughout the media, which has a very high surface area (132 m2/m2), allowing for extensive environments for both nitrification and denitrification. These potential microzones, although difficult to measure directly, have been suggested to occur in aerobic marine sediments (Testa et al. 2013) and within the pore spaces of oyster shells (Caffrey et al. 2016). Indeed, we measured a gradual accumulation of NO_{23}^- and reduction in NH_4^+ within the porewaters of the media in the summer 2021 experiments (Butler-Viruet et al. 2024), supporting the notion of nitrification. Future studies should more explicitly quantify the potential for these N transformation rates coupled with identification of the relevant organisms.

Conclusion and Future Work

Floating treatment wetlands seems to remove TN through denitrification during the summer and spring season in two different years. However, imbalances in the budget indicate that there are internal processes and external artifacts affecting the accurate estimation of these budgets. From previous research focusing on the N dynamics and internal N transformations in floating treatment wetlands, we gathered results that indicate floating wetlands are capable of supporting nitrogen transformations ranging from ammonification to denitrification. We suspect that nitrification serves as a source of nitrogen in both control and experimental treatments. For the experimental imbalances where we have higher sources of TN than sinks, we suspect insufficient accounting for the peat moss and topsoil and accumulation of N in biofilms led to the discrepancies. Future work should include higher frequency in sampling of inflowing and outflowing nutrients as well as more detailed measurements of nitrogen cycling.

Chapter 4: Modeling nitrogen cycling and removal pathways in a temperate *Spartina patens* floating wetland

Abstract

We implemented a process-based model to quantify the plant nitrogen assimilation and nitrogen dynamics occurring in the water column and floating media of tidal floating wetlands. This process-based model included a plant growth sub model that is nitrogen based, a water column nitrogen sub model, and a floating media nitrogen sub model to describe the internal nitrogen processes happening in floating wetlands. We developed a media amplifier to represent the three-dimensional space of the media in our one-dimensional model and be able to represent its effects on nitrogen cycling within the media. The model was calibrated using mesocosm experiment data collected during a 90-day summer period and validated using mesocosm data from a 90-day spring experiment conducted the following year. Results indicated an overestimation of plant biomass and underestimation of nitrogen outflows during the spring season. Sensitivity analysis shows that the model was sensitive to plant biomass allocation from the shoots to the roots parameter as well as the presence of the amplifier to represent the biofilm and algal mats in the media. On the other hand, the model performed better when predicting denitrification during the spring months with some overestimation happening but following the existing downward trend observed in the measured rates. This indicates that overall, the model performance is sensitive to plant growth characteristics as well as the media amplifier and there is a need to improve the modeling approach of the biofilm and algal mats to in the model. Further improvement can improve predicting capabilities and help implementers in decision making process on when and where to deploy these floating wetlands in coastal systems in need of additional approaches to address eutrophication problems.

Introduction

Floating wetland technology was originally designed to be implemented in stormwater retention ponds to improve their contaminant removal efficiency and overcome the operational limitations (i.e., maximum nutrient removal potential) of existing retention ponds (Tanner 2006). Floating wetlands are typically composed of floating rafts (made of recycled PET plastic fiber or a biodegradable material) planted with macrophytes (Sharma et al. 2021). These macrophytes remove contaminants and excess nutrients from the water by direct nutrient uptake, and by maintaining permanent contact with the water to slow flow velocities, hence increasing particle settlement rates and magnitude (Sharma et al. 2021).

Many approaches have been used in the past to quantify floating wetland nutrient removal. Harvest of above-ground vegetation is a relatively integrative, easy-to-measure quantity that contributes to the effectiveness of a floating wetland by directly removing tissue nutrients from a system. In the northern temperate zone, research recommends harvesting biomass in June to maximize nutrient assimilation or early fall to prevent nutrient leaching (Wang et al., 2014). However, floating wetlands deployed in the subarctic region of the world showed a lower N plant accumulation when compared to the efficiency of floating wetlands deployed in temperate, tropical and sub-tropical areas (Choudhury et al., 2019), so measurements from one type of wetland in one region may not have wide applicability. Furthermore, because floating wetlands are small in size and are seasonally dynamic, extrapolating the effects of one wetland sampled a few times to ecosystem-scale effects is problematic. In addition to plant biomass nutrient uptake, floating wetland effectiveness in retention ponds is reliant on many different factors. Temperature (Van De Moortel et al. 2010), water flow, retention time (Yang et al., 2008), floating wetland size and plant species (Garcia Chance and White 2018), as well as microbial composition and activity (Gao et al. 2019), all interact to control nitrogen removal rates. All

these variables may vary on time scales ranging from hours to seasons, and each controls plant productivity and the biogeochemical processes that control the cycling and loss of nutrients from a wetland ecosystem. Thus, incomplete sampling of wetland processes combined with irregular sampling over time may not capture the seasonal and spatial dynamics of wetland nutrient removal.

To overcome these challenges, models have previously been created to represent and explain the mechanisms underlying floating wetland nutrient removal dynamics. Two types of models have previously been implemented to quantify nutrient loss in floating wetlands; (1) empirical models that employ empirical relationships to estimate nutrient loss at the system-scale, and (2) process-based models that seek to represent the detailed plant physiology and nutrient cycling rates that contribute to nutrient removal. Examples of empirical models include that of Wang & Sample (2013), who developed a first-order kinetic model that attempts to describe the performance of a floating treatment wetland in isolation, separated from the performance of the pond/lake in which it is deployed. Meanwhile, Headley and Tanner (2012), used the *P-k-C** model proposed by Kadlec & Wallace (2009), to estimate the areal removal rate coefficient of nutrient removal by the wetland. Kadlec & Wallace (2009) developed the *P-k-C** to predict the outflowing concentration of contaminants and other pollutants based on the inflowing concentration, the number of ponds/tanks in series (*P*), and the volumetric rate constant (*k*) based on the inflowing concentration (*C**). Despite the utility of these models, they may lack mechanistic dynamics to represent nutrient allocation, seasonality of plant growth, and energy distribution, and thus their potential for N removal.

Process-based models include the mechanisms needed to model nutrient removal, like nitrification and denitrification. Marimon et al., (2013) developed a process-based model that

included the physical-chemical and biological processes of nitrogen removal (e.g., sedimentation, deposition, plant assimilation, nitrification, ammonium, and nitrate uptake). Their model attempted to improve the understanding of nitrogen dynamics of floating wetlands deployed in a sub-tropical stormwater wet retention pond. On the other hand, McAndrew & Ahn, (2017) developed a process-based model composed of a hydraulic retention time, plant growth, and a nitrogen sub-model. They utilized the model to explore the impact of three design elements of a floating wetland and concluded that floating wetland efficiency (with low macrophyte coverage) increases with an increase in hydraulic retention time and surface area coverage. More importantly this model indicated that efficiency can be attained with the appropriate retention time and high macrophyte coverage. Wang et al., (2019) also developed a process-based model composed of nitrogen, phosphorus, and plant growth sub-models to describe the floating wetland nutrient removal dynamics more accurately. Despite these relatively complex ecosystem-like models of floating wetlands, these models have not been incorporated into a water column modeling framework to explore impacts on estuarine biogeochemistry and wetland-water interactions. These models have also not represented the dynamics of nutrient cycling in the wetland matrix or the impact of floating wetlands on the cycling of nutrients and oxygen in the water column they inhabit. More importantly, these models have only been applied in retention ponds and/or lakes.

Thus, the purpose of this chapter is to (1) build a mechanistic model of a floating wetland, (2) estimate the dynamics of nitrogen cycling within the media of the floating wetland, and (3) implement this model in areas of interest in the Chesapeake Bay region. The model was calibrated against measurements made in a mesocosm experiment in the summer of 2019, and validated against the same type of experiments in the spring of 2021. A sensitivity analysis was

performed using STELLA 10.1 to identify the parameters and processes that closely affect the nutrient removal performance of the floating wetland. In particular, I sought to incorporate the effects of the complex three dimensional media structure as it creates additional surface area to support coupled nitrification-denitrification.

Methods

Model Description

The model applied in this study was based upon a previously published process-based model by Wang et al., (2019). The model comprises two sub-models, a plant sub-model that includes representations of above-ground and below-ground biomass, and a nitrogen dynamics sub-model that represents organic and inorganic nitrogen pools, and the processes of nitrogen uptake, release, remineralization, nitrification, and denitrification. The model in Wang et al., (2019) was based on floating wetlands deployed in retention ponds and was employed for a relatively short duration in the peak of the summer growing season. In this study, we applied the model against a pair of 70-day experiments, where floating wetland media planted with *Spartina patens* were grown in flow-through mesocosms at the Chesapeake Biological Laboratory in Solomons, Maryland, USA (38.3185° N, 76.4541° W). The experiments and model simulations were carried out between June 21st and September 9th, 2019, and April 16 to July 22nd, 2021.

Model Setup and Forcing Data

The model was structured as a 2.5 m^2 domain with a media with a volume of 2 m^3 deployed within a water column of 4.1 m^3. Model forcing includes an inflow of three nitrogen species (DON, NH_4, NO_{23}) based on weekly measurements made during the experiment (Butler-Viruet et al. 2024). Water temperature and daily integrated PAR were derived from measurements made in the nearby Patuxent River (<300 m from the experimental location). Initial conditions for above and below ground biomass were derived from direct measurements

of plant tissue at the initiation of the experiments, and initial nutrient concentrations came from measurements made in the mesocosms at the outset of the experiment (Butler-Viruet et al. 2025). Major model assumptions include (1) plant biomass can be represented by two homogenous above-ground and below ground pools; (2) organic nitrogen can be represented as a single state variable with a single decomposition rate; and (3) water column algae is insignificant (and omitted) as algae concentrations are generally low (West et al., 2017). A diagram of the model is shown in (fig.1). All simulations were run in STELLA software, with a daily time-step using a 4th order Runge-Kutta integration.

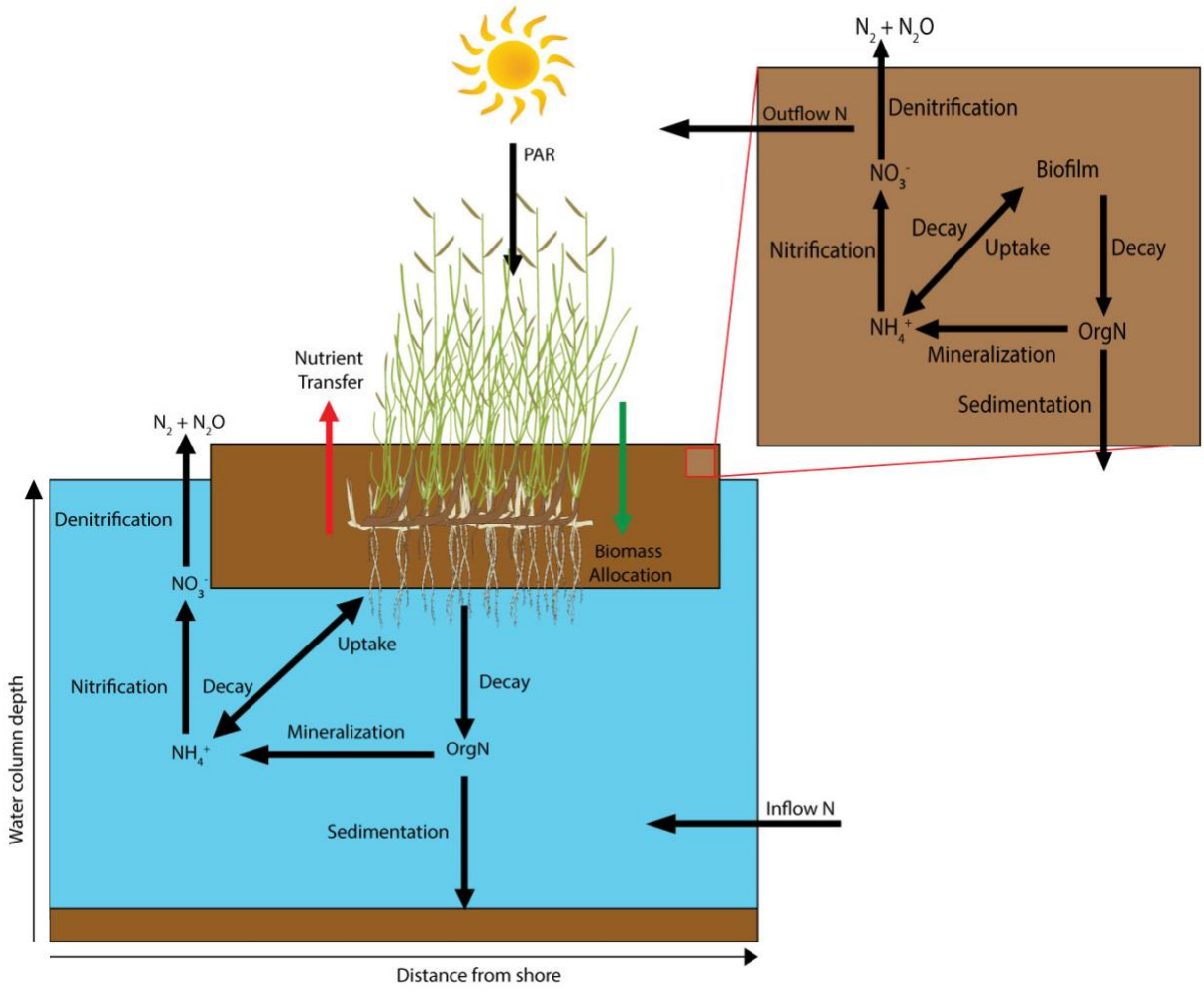

Figure 1. Conceptual diagram of the floating wetland nitrogen cycling model to fit mesocosm flow-through experiment.

Plant growth model

The plant sub-model is composed of two state variables: shoot (above-ground) biomass and root or below-ground biomass. In this part of the model, the shoots generate biomass during photosynthesis and translocate nitrogen to roots, while the roots assimilate nitrogen from the water column to increase its biomass and decay to release DON. Shoot litter was not considered in this model as it is assumed to stay on top of the floating raft. Root litter is transformed into organic matter via hydrolysis. The shoot and root growth equations are expressed as Eqs. (1) and (2):

$$\frac{dB_{SH}}{dt} = ((1 - FSTR)\ P_{SH}\text{-}R_{SH})\ B_{SH} \quad (1)$$

$$\frac{dB_{RO}}{dt} = FSTR \cdot P_{SH} \cdot B_{SH} - R_{RO} \cdot B_{RO} \quad (2)$$

where B_{SH} and B_{RO} are the shoot and root biomass of the plants (g DW m^{-2}), respectively; P_{SH} is the growth rate of shoots (day^{-1}); R_{SH} and R_{RO} are the decay rate of the shoots and roots respectively (day^{-1}), and FSTR is the fraction of shoot photosynthetic products directly transferred to the roots based on the availability of inorganic nitrogen and coefficient and max allocation of photosynthetic product from the shoots to the roots (Eq 3):

$$FSTR = FSTR_{max} \cdot \left(\frac{DIN}{DIN + kFSTR}\right) \quad (3)$$

The growth rate (P_{SH}) of the plants in floating treatment wetlands was limited by nutrient concentration in the water column, water temperature, and daily integrated light availability. P_{SH} can be calculated by Eq. (4).

$$P_{SH} = PM_{SH} \cdot f_1(N) \cdot f_2(T) \cdot f_3(I) \quad (4)$$

$$f_1(N) = min\left(\frac{NH_4+NO_3}{KHN_{PL}+(NH_4+NO_3)}\right) \quad (5)$$

$$f_2(T) = \begin{cases} e^{-KT1_P(T-TP1_P)^2} & if \quad T \le TP1_P \\ 1 & if \quad TP1_P < T < TP2_P \\ e^{-KT2_P(T-TP2_P)^2} & if \quad T \ge TP2_P \end{cases} \quad (6)$$

$$f_3(I) = \left(\frac{PAR}{PAR_{max}}\right) \quad (7)$$

PM_{SH} is the maximum shoot growth rate under optimal conditions (day^{-1}); $f_1(N)$ and $f_2(T)$ are the nutrient and temperature limitation coefficients, respectively; KHN_{PL} is the plant half-saturation constant for nitrogen uptake from the water column in (mg L^{-1}); T is the water temperature deg C; $TP1_P<T<TP2_P$ is the optimal temperature range for plant growth deg C; $KT1_P$ is the effect of temperature below $TP1_P$ on plant growth (C^{-2}); and $KT2_P$ is the effect of temperature above $TP2_P$ on that plant growth (C^{-2}); $f_3(I)$ is the daily integrated light availability as a function of the annual daily maximum light availability.

The decay of the shoots and roots can be calculated by Eqs (8) and (9)

$$R_{SH} = RM_{SH} \cdot e^{KTR_{SH}(T-TR_{SH})} \quad (8)$$

$$R_{RO} = RM_{RO} \cdot e^{KTR_{RO}(T-TR_{RO})} \quad (9)$$

where TR_{SH} and TR_{RO} are the reference temperatures for shoots and roots deg C, respectively; RM_{SH} and RM_{RO} are the reference decay rates for shoots and roots at the reference temperature (day^{-1}), respectively; and KTR_{SH} and KTR_{RO} are the effects of temperature on the shoots and root decay rates (C^{-1}), respectively.

Nitrogen dynamics sub-model

The nitrogen dynamic sub-model is based on traditional representations of nitrogen dynamics in estuarine water columns. Total organic nitrogen (OrgN) sources include root decay and water inflow supply, whereas sinks and/or removal mechanisms of OrgN are mineralization, sedimentation, and outflow from the tank. Ammonium nitrogen (NH_4^+-N) sources include inflowing water, root and organic matter decay, while the sinks include nitrification, plant uptake, and outflow from the tank. For nitrate nitrogen (NO_3^--N), the sources include the inflowing water as well as nitrification in the water column, while the sinks of nitrate include plant assimilation, denitrification, and outflow from the tank. The equations for the nitrogen sub-model state variables are expressed as Eqs. (10), (11), and (12) in mg L^{-1} d^{-1}:

$$\frac{dOrgN}{dt} = \frac{S_{FTW}}{V_W} \cdot FNO_{PL} \cdot R_{RO} \cdot LPLNM \cdot B_{RO} - NMI \cdot OrgN - KNSED \cdot OrgN + \frac{1}{V_W}(Q_{IN} \cdot OrgN_{IN} - Q_{OUT} \cdot OrgN_{OUT} \cdot OrgN) \quad (10)$$

$$\frac{dNH_4}{dt} = NMI \cdot OrgN + \frac{S_{FTW}}{V_W} FNI_{PL} \cdot R_{RO} \cdot LPLNM \cdot B_{RO} - NMI \cdot NH_4 -$$

$$\frac{S_{FTW}}{V_W} LPLNM \cdot PN_{PL} \cdot P_{SH} \cdot B_{SH} + \frac{1}{V_W}(Q_{IN} \cdot NH_{IN} - Q_{OUT} \cdot NH_{OUT} \cdot NH_4) \quad (11)$$

$$\frac{dNO_3}{dt} = Nit \cdot NH_4 - \frac{S_{FTW}}{V_W} LPLNM(1 - PN_{PL}) \cdot P_{SH} \cdot B_{SH} -$$

$$Denit \cdot NO_3 + \frac{1}{V_W}(Q_{IN} \cdot NO_{IN} - Q_{OUT} \cdot NO_{OUT} \cdot NO_3) \quad (12)$$

For these equations, S_{FTW} is the water surface area (m^{-2}), and V_W is the water volume (m^3). FNO_{PL} and FNI_{PL} are the fractions of nitrogen metabolized by plants as organic nitrogen and ammonium, respectively; *LPLNM* is the ratio of nitrogen to plant biomass. *NMI* and *KNSED* are the mineralization rate and sedimentation rate of organic nitrogen (day^{-1}), respectively; PN_{PL} is the NH_4^+-N uptake preference factor for the plants; Nit and Denit are the nitrification and denitrification rate (day^{-1}), respectively; Q_{IN} and Q_{OUT} are the inflow and outflowing water (m^3 day^{-1}), respectively; and $OrgN_{IN}$, NH_{IN}, and NO_{IN} are the influent concentration of OrgN, NH_4^+-N and NO_3^--N ($mg\ L^{-1}$), respectively.

NMI, *Nit*, and *Denit* are expressed as a function of temperature and are described in Eqs. (13) (14) and (16):

$$NMI = NMIM \cdot e^{KNMI(T-TNMI)} \quad (13)$$

$$Nit = Nitm \frac{NH_4}{KHNit + NH_4} f_{Nit}(T) \quad (14)$$

$$f_{Nit}(T) = \begin{cases} e^{-KNit1(T-TNit)^2} \; if \; T \leq TNit \\ e^{-KNit2(T-TNit)^2} \; if \; T > TNit \end{cases} \quad (15)$$

$$Denit \; = \; Denitm \frac{NO_3}{KHDenit + NO_3} f_{Denit}(T) \quad (16)$$

$$f_{Denit}(T) = \begin{cases} e^{-KDenit1(T-TDenit)^2} \; if \; T \leq TDenit \\ e^{-KDenit2(T-TDenit)^2} \; if \; T > TDenit \end{cases} \quad (17)$$

where *NMIM* is the mineralization rate of OrgN (day^{-1}) at the reference temperature *TNMI* (˚C); *KNMI* is the effect of temperature on OrgN mineralization (˚C); TNit and TDenit are the optimum temperature for nitrification and denitrification, respectively; *Nitm* and *Denitm* are the maximum nitrification and denitrification rates at *TNit* and *TDenit* (day^{-1}), respectively; *KHNit* and *KHDenit* are the nitrification half-saturation constant for NH_4^+-N and the denitrification half-saturation constant for NO_3^--N ($mg\ L^{-1}$), respectively; *KNit1* is the effect of temperatures below TNit on the nitrification rate ($°C^{-2}$); *KNit2* is effect of temperatures above TNit on the nitrification rate ($°C^{-2}$); *KDenit1* is effect of temperatures below *TDenit* on the denitrification rate ($°C^{-2}$); and *KDenit2* is effect of temperatures above *TDenit* on the denitrification rate ($°C^{-2}$).

In this model, we include the preferential uptake of NH_4^+-N over NO_3^--N, and it is described in Eqs. (18)

$$PN_{PL} = \frac{NH_4 \cdot NO_3}{(KHN_{PL}+NH_4)(KHN_{PL}+NO_3)} + \frac{NH_4 \cdot KHN_{PL}}{(NH_4+NO_3)(KHN_{PL}+NO_3)} \quad (18)$$

where KHN_{PL} is the half-saturation coefficient for nitrogen uptake in plants.

To simulate the nitrogen processes occurring within the media matrix, we implemented the same formulations explained above and we added a coefficient to each transformation process in the media model, which we hereby call an "amplifier", which represents the additional surface area for microbial processes afforded by the complex three-dimensional network of the media represented in Eq. 19.

$$kMedia = (\frac{media\ area\ m^2}{media\ volume\ m^3})/surface\ area\ m^2 \quad (19)$$

The media amplifier is a dimensionless factor I could utilize to replicate the magnitude of the nitrogen transformations in the media. So, for example, when representing nitrification happening in the media, the model equation will look like Eq. 20.

$$Nit = \left(Nitm \frac{NH_4}{KHNit + NH_4} f_{Nit}(T)\right) \cdot kMedia \quad (20)$$

Calibration and validation

We used a mesocosm experiment described by Butler Viruet et al. (2025) to set the boundaries and initial conditions and validate the model. These studies measured inflow and outflow rates and concentrations of all state variables, root and shoot biomass, and denitrification rates. For the experiments, water was pumped directly from the lower Patuxent River in Solomons, MD with a salinity range from 5-18. Floating wetlands had a surface area of 2.5m^2 and were initially planted with 20 plant plugs of 5 cm in height. The calibration measurements were made during 90-day mesocosm experiments (triplicate mesocosms) made during the summer months from June until September of 2019 whereas validation data came from similar mesocosm experiments made during the April until June 2021. Initial conditions for calibration and validation simulations can be found in the appendix C (S1).

For the 2019 experiments, we calibrated the model with measurements of outflow rates of organic nitrogen (OrgN), ammonium (NH_4) and nitrate (NO_3) as well as denitrification rates and plant biomass accumulation. We applied the root mean square error (RMSE) and the coefficient of determination (R^2) to evaluate the deviation between the experimental data and simulation data.

$$RMSE = \sqrt{\frac{\Sigma_{i=1}^{N}(M_i - S_i)^2}{N}}$$

$$R^2 = \left[\frac{N\Sigma_{i=1}^{N} M_i S_i - (\Sigma_{i=1}^{N} M_i)(\Sigma_{i=1}^{N} S_i)}{\sqrt{\Sigma_{i=1}^{N} M_i^2 - (\Sigma_{i=1}^{N} M_i)^2}\sqrt{\Sigma_{i=1}^{N} S_i^2 - (\Sigma_{i=1}^{N} S_i)^2}}\right]^2$$

Where M_i and S_i are the experimental data and simulation data, respectively: and N is the number of data sets. We then validated the model with the Spring 2021 conditions using the same variables as in 2019.

Sensitivity Analysis

We applied a sensitivity analysis on three important parameters for plant growth, including the maximal plant growth rate (PM_{SH}), the shoot-to-root translocation ratio ($FSTR_{max}$), and the temperature coefficients for the temperature-growth factor ($KT1_P, KT2_P$). For each variable, we ran 5 simulations with varying parameters by 10% to 50% from their baseline values (appendix C table S1). We also ran model experiments with and without the wetland media amplifier, in order to evaluate the impact of elevated microbial surface area on nitrogen cycling processes.

Results

Calibration

Plant biomass: The modeled above-ground plant biomass at the end of the 2019 experiment was 652 g DW/m^2, which was 59.7 gDW/m^2 lower than the measured values (fig. 2). The modeled below-ground plant biomass at the end of the 2019 experiment was 278 g DW/m^2, which was 69 gDW/m^2 higher than the measured values (fig. 2). In the simulations where the media amplifier was excluded, the model underestimated both above and below ground biomass by 548 and 139 gDW/m^2, respectively.

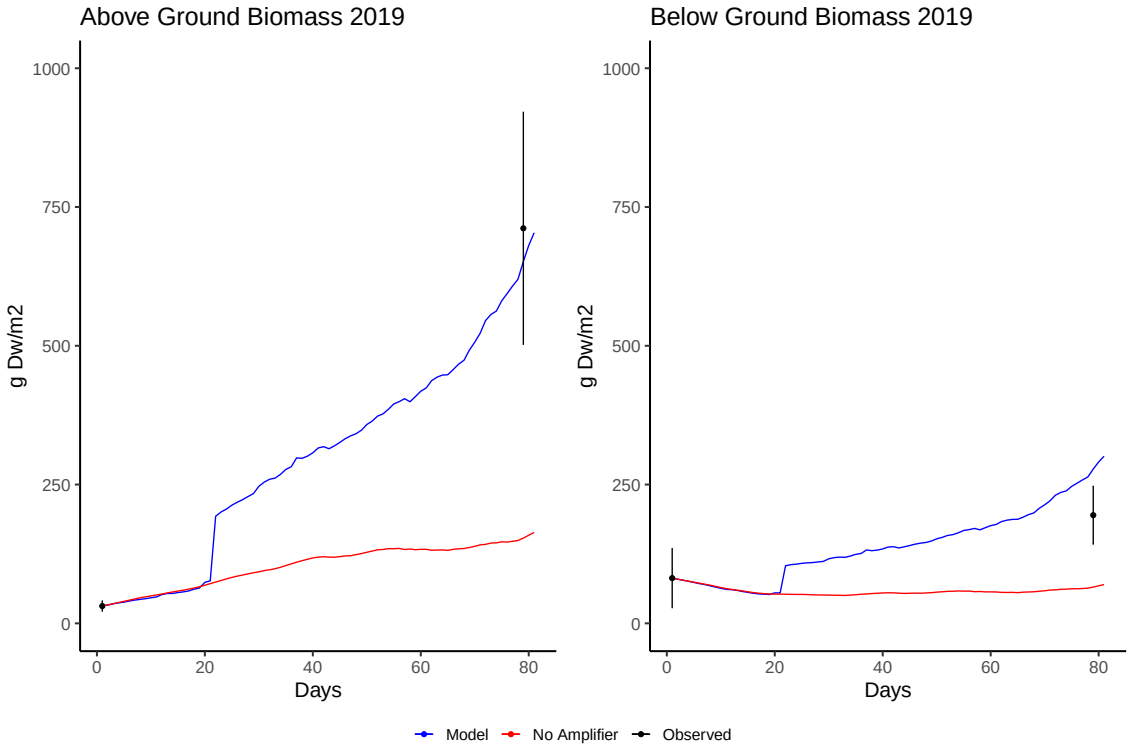

Figure 2. Plant modeled biomass and measured initial and final values. Red line indicates modeled values without using the media amplifier. Blue line indicates modeled values with the media amplifier. Black dots indicate the measured values at the beginning and at the end of the experiment with the standard deviation of the mean.

Nutrient outflow rates: The 2019 model simulation with the amplifier tended to underestimate nitrate outflow (figure 3, top) while overestimating ammonium outflow (figure 3,

middle). The calibrated model performed relatively well without the amplifier when it came to organic nitrogen, however, when the amplifier was implemented, the model underestimated organic nitrogen outflow (figure 3, bottom). The root mean squared values of the nutrient outflows reveal that the model including the media tended to overestimate the outflows (NO_{2+3} $RMSE = 148$, $R^2 = 0.34$; NH_4^+ $RMSE = 41$, $R^2 = 0.003$; OrgN $RMSE = 130$, $R^2 = 0.001$).

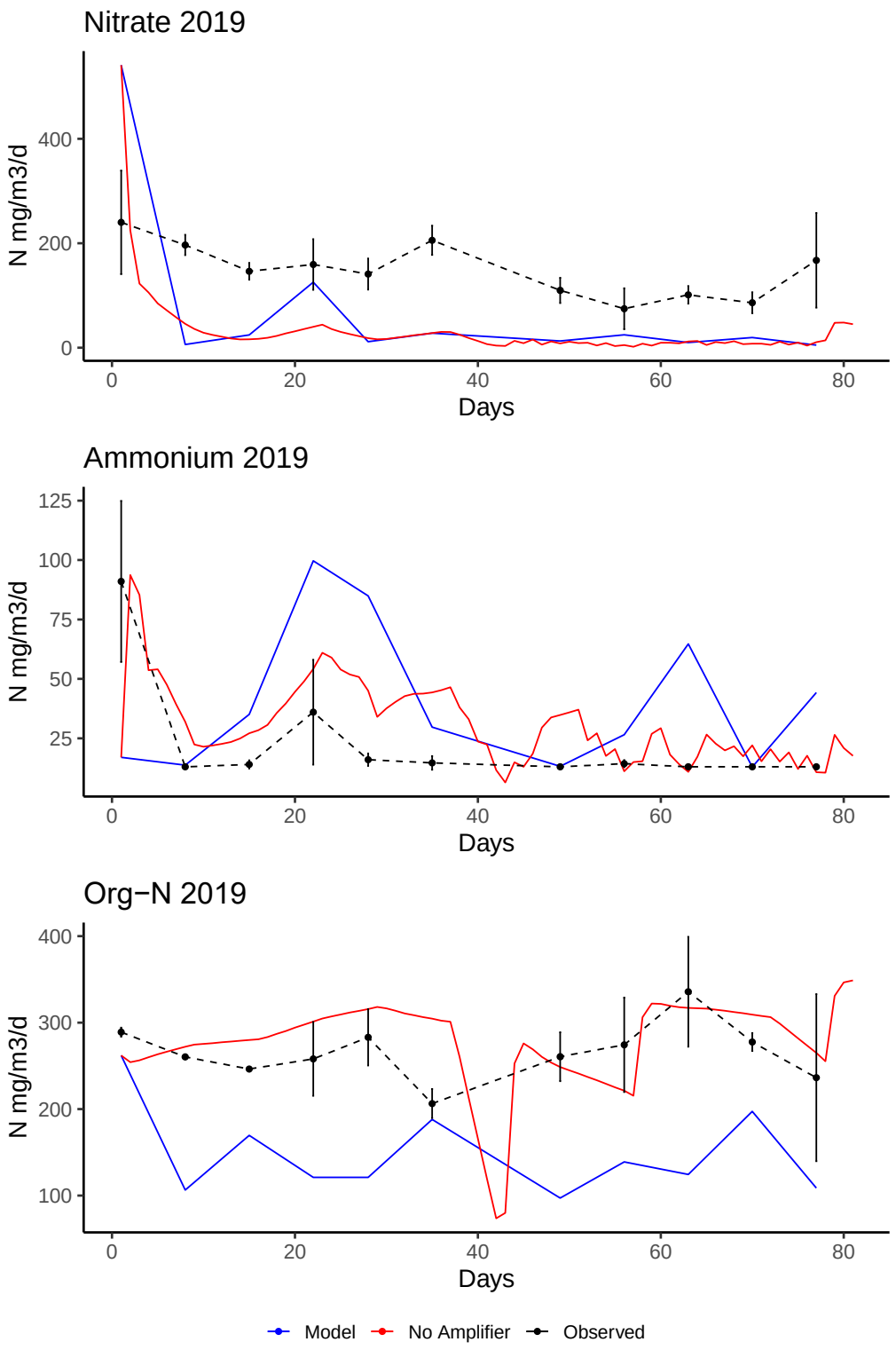

Figure 3. Modeled time-series of nitrogen outflow rates in simulations that include the amplifier (blue) and those that exclude the amplifier (red). The black dashed line represents the weekly measured values with the standard deviation of the mean.

Denitrification: The model without the amplifier underestimated the magnitude of denitrification throughout the experiment by 60 mg m^{-2} d^{-1} on the low range and up to 200 mg m^{-2} d^{-1}.Once the amplifier was implemented in the model, the magnitude of denitrification increased to represent the mean measured values, but did not follow the temporal pattern that the measured data followed, (N_2-N R^2 = 0.595, figure 4).

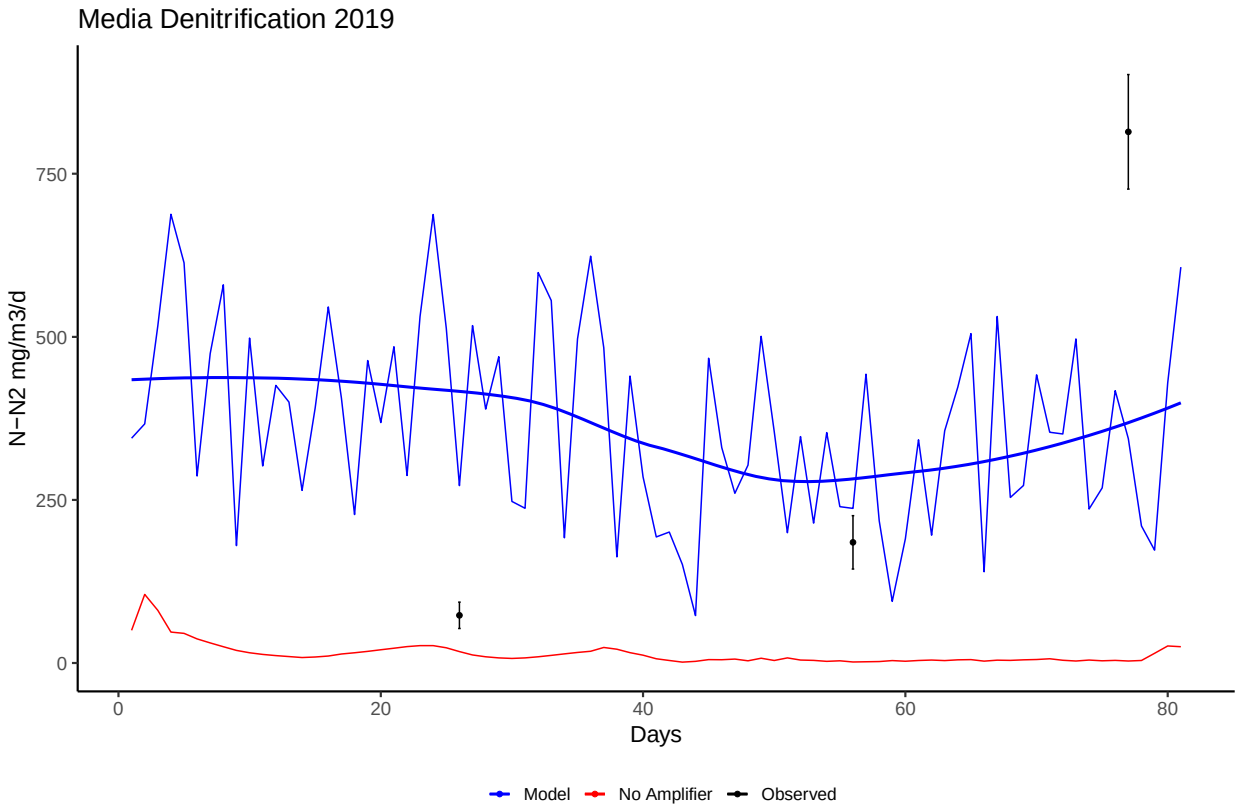

Figure 4. Time-series of modeled and measured denitrification. Red line represents the modeled values without using the media amplifier while the blue line represents the modeled values with the media amplifier. Black dots represent the monthly measured media denitrification with the standard deviation of the mean.

Validation

Plants: Validation of the model using the Spring 2021 data indicates the model tends to overestimate above ground biomass when modeled both with and without the amplifier.

However, when modeling below ground biomass the model with the amplifier performs relatively well with a difference of 4 g DW/m^2 between the modeled and the measured data (figure 5).

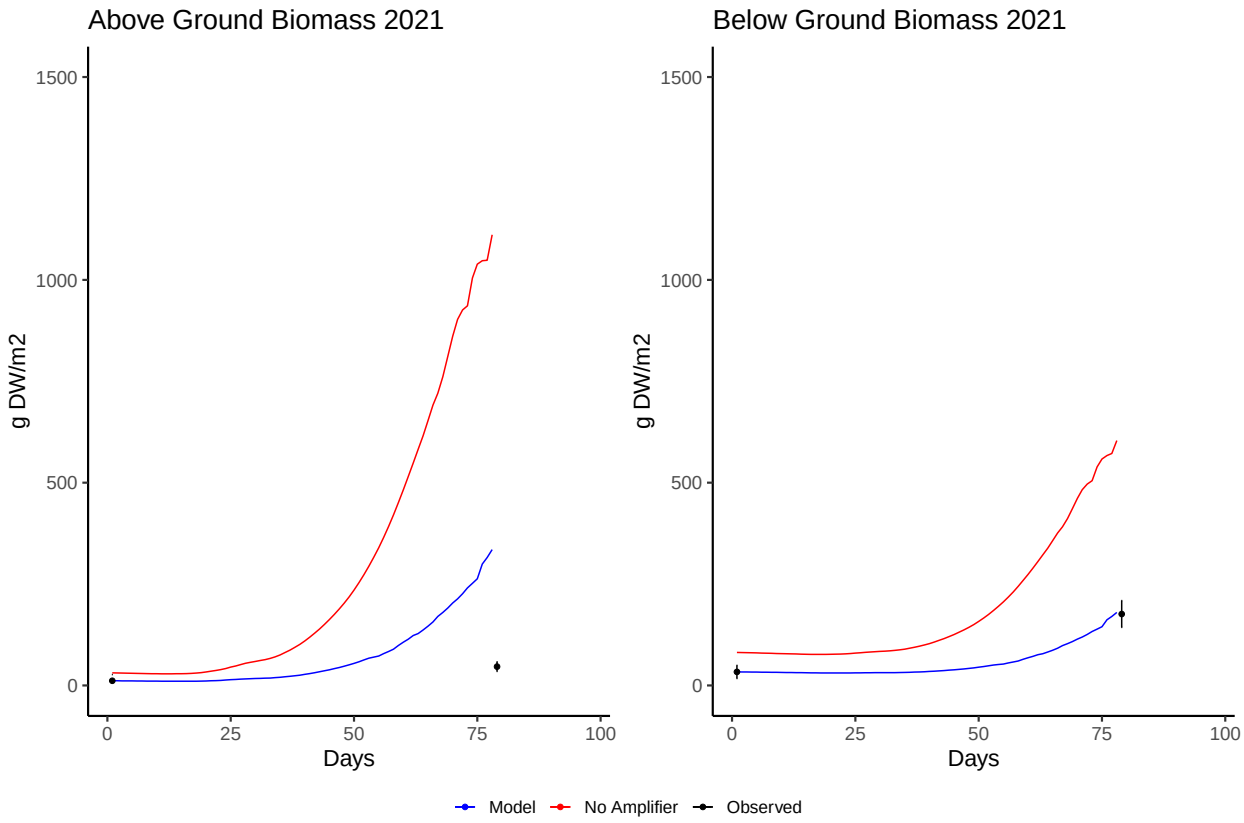

Figure 5. Time/series of root and shoot biomass in the 2021 validation simulations. Red line indicates the modeled values without the media amplifier while the blue line represents the modeled values with the media amplifier. The black dots indicate the measured initial and final plant biomass with the standard deviation of the mean.

Nutrient outflow: The nutrient outflow simulations show that the model underestimated nutrient outflows with and without the amplifier (figure 6). RMSE and R^2 indicate the poor prediction of the model with the amplifier (NH_4^+ *RMSE* = 65, R^2 = 0.038; NO_{2+3}^- *RMSE* = 209, R^2 = 0.401; Org-N *RMSE* = 282, R^2 = 0.032).

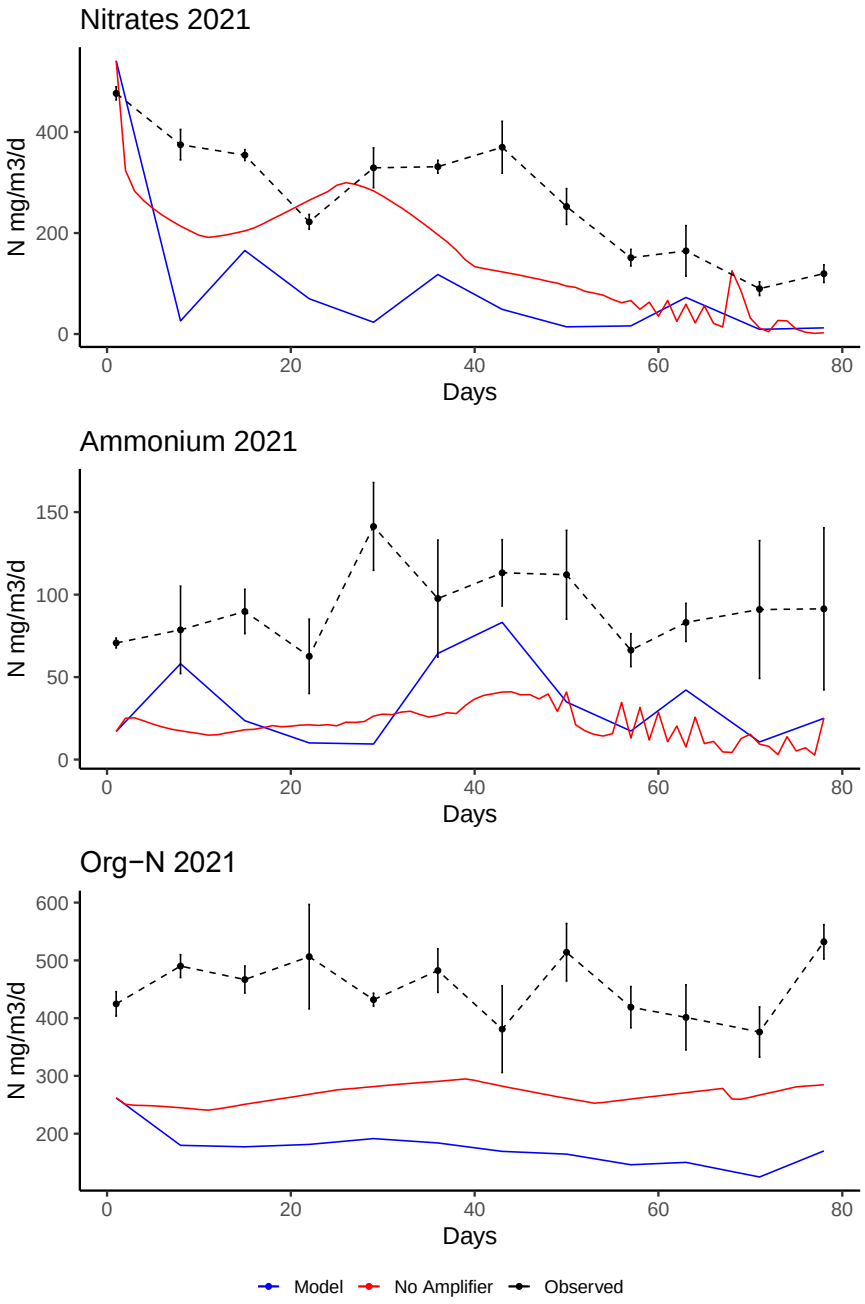

Figure 6. Time-series of modeled values and measured values of nitrogen outflows during the 2021 validation experiment. Red line represents modeled values without amplifier while the blue line represents the modeled values with the media amplifier. Black dashed line represents the measured values with the standard deviation of the mean.

Denitrification: The model without the amplifier underestimated media denitrification rates (figure 9). After implementing the amplifier, the magnitude of the rates increased and had similar temporal variability as the measured rates, even as short-term variability increased ($R^2 = 0.236$). The denitrification rates were comparable in the 2019 and 2021 experiments, but denitrification increased over time in summer 2019 but decreased over time in Spring 2021 (figure 4,8).

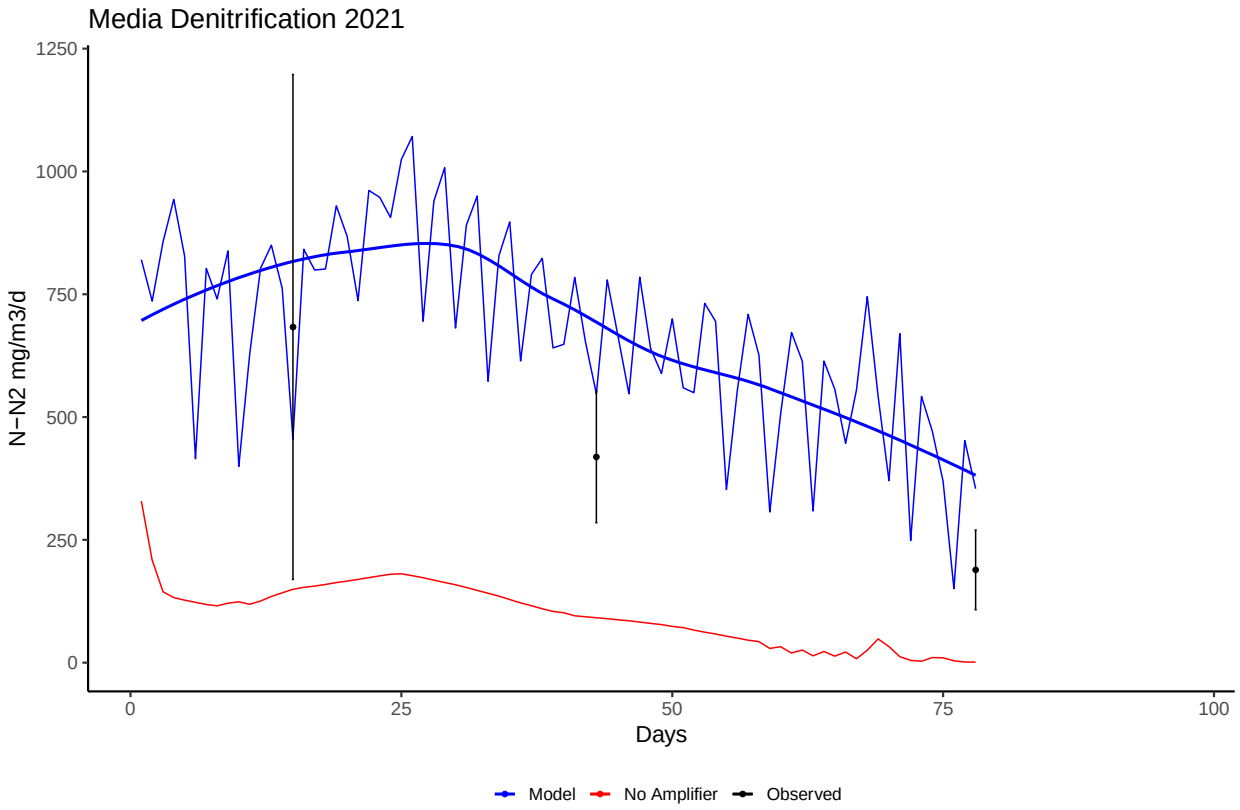

Figure 8. Time/series of denitrification in the 2021 validation experiment. Red line represents the modeled values without using the media amplifier while the blue line represents the modeled values with the media amplifier. Black dots represent the measured media denitrification with the standard deviation of the mean.

Discussion

Model-simulated plant tissue growth during the experiments was within the range of measured values during the calibration (2019), but deviated from the measured final biomass

values measured in the 2021 experiments during validation. There are multiple limitations of the model that may have led to this discrepancy. Sensitivity analysis indicates that when maximum allocation of biomass from shoots to roots is at its highest (*FSTRmax* = 0.5, table S2, figure S1) it replicates an above ground biomass closest to the measured final values in 2021. However, it fails to do the same for below ground biomass where a lower value (*FSTRmax* = 0.28, table S2, figure S1) seems to produce the closest values to the measured final below ground biomass. Partitioning of N between above and below ground biomass was set to a fixed value in the model (Wang et al. 2019), but changes in nitrogen availability can alter the nitrogen allocation between roots and shoots (Hester et al., 1994). Meanwhile sensitivity simulations involving altered maximum growth rates, suggested that increasing this rate beyond that in the calibration would lead to an overestimation of biomass (table S2, figure S10). However, a higher growth rates seems to replicate best the measured below ground biomass (*PMsh* = 0.16, table S2, figure S10). When evaluating sensitivity of the minimum temperature needed for plant growth, the higher the temperature the better it predicts above ground biomass (*TP1p* = 25, table S2, figure S7) while the lowest temperature seems to replicate below ground biomass better (*TP1p* = 22, table S2 figure S7). When comparing modeled nutrient outflows and denitrification in all of these sensitivity simulations, there were no substantial changes between any of the values used in the sensitivity analysis.

Another factor that influenced plant growth was the incorporation of the "amplifier" that represented the extensive microbial community within the wetland media. The amplifier was intended to represent the presence of a microbial biofilm in the media, which could encourage denitrification but also provide elevated rates of decomposition of organic nitrogen to generate nutrients for the plants to grow (Mazur et al. 2021). Although the amplifier appeared to lead to a

more realistic plant growth outcome in the calibration, the model over predicted above ground biomass during validation in spring 2021, suggesting that there were other factors influencing the plant biomass in the spring 2021. It is possible that the presence of the media amplified the rates of remineralization in the, releasing nutrients to stimulate growth during summer (2019). This may have also led to elevated nutrient recycling which stimulated excessive growth in spring (2021). Prior research has shown that low water column TN can limit plant biomass and microbial metabolism (Chapra 2008). Another factor which may have influenced this behavior in the model is temperature. Other research has shown that temperatures between 5 and 15^{o}C were shown to have the highest removal rates of N and P, while above and below this range led to reduced efficiency (Van De Moortel et al. 2010). The spring 2021 experiment had temperatures comparable to the range reported in (Van De Moortel et al. (2010), however, a direct comparison is not possible since they attempted to estimate removal efficiency of N and P in floating wetlands deployed in retention ponds.

Simulations of nitrogen outflows revealed that the 2021 model experiment tended to underestimate all the nitrogen outflows with and without the amplifier. Other factors that could be affecting the outflow are water column nutrient availability in addition to plant density, as higher plant density contributed to a higher TN removal (Marimon et al. 2013). We also hypothesize a source of "missing N' could be attributed to omitting a portion of experimental N from model inputs. A starter application of nitrogen fertilizer as well as both peatmoss and topsoil were added to the media at the beginning of the experiments. A common practice used to stimulate initial plant growth, this likely introduced an additional source of nitrogen into the media and water column. The result of this would likely have been increased nitrogen concentrations measured in the mesocosms and thus higher outflows. Budget analyses of our

experiments indicated that topsoil contributed 4% of the TN sources in our nitrogen budget while peatmoss contributed 30% in the summer 2019 experiments, and 6% and 42%, respectively for the spring 2021 experiments. Thus, a refined version of this model would explicitly include these nitrogen sources. Additionally, the model does not consider above ground biomass decay which indicates how a potential source of organic and dissolved nitrogen is not considered and implemented in the model. However, there was no visual presence of decaying above ground biomass on top of the floating wetland in our experiments, so this may be a minor effect. Future experiments should evaluate the floating wetland design and avoid the addition of topsoil and peatmoss at the beginning.

With the amplifier, the model, performed relatively well by replicating the magnitude and trend observed in the measured rates, especially in 2019. This indicates that the media and its high surface area play a significant role in generating and sustaining these high rates of denitrification measured in the floating wetlands. Oxygen concentrations measured in the mesocosms were nearly always above 2-3 mg $L^{-1,}$ which would inhibit denitrification. Despite this general observation it is possible that anoxic microenvironments were present within the media complex. These potential microzones, although difficult to measure directly, have been suggested to occur in aerobic marine sediments (Testa et al. 2013), the pore spaces of oyster shells (Caffrey et al. 2016) , and restored oyster reefs (Kellogg et al. 2013). If they exist, these micro-zones would be in close proximity to oxic environments where nitrification can occur. Within the pore waters of the media in summer 2021 experiments, we measured a gradual accumulation of NO_{23}^- and reduction in NH_4^+ relative to the outside water column (Butler-Viruet et al. 2024). These measurements support the notion of nitrification occurring alongside denitrification in distinctive microzones. Future studies should more explicitly quantify the

potential for these N transformation rates. This should be accompanied by an identification of relevant organisms, and the extent of potential anoxic micro-zones. The current model is also limited by the current algorithm simulating nitrification and denitrification. Currently this process is based on the available concentration of ammonium and nitrate and temperature, while not taking oxygen or bacterial biomass into consideration.

An unexpected observation in our experiments was the growth of a green algal mat on the surface of the floating media in the mesocosoms. These mats were likely photosynthetic, and thus the amplifier used in the model may not fully represent the microbial community in the media. Given that these additional algae would have sequestered nitrogen we would likely have even less modeled outflow of nitrogen from the media. In an attempt to experimentally estimate the N uptake of the biofilm growing in the media, we performed diagenesis experiments in 2022 (see Appendix B for details). Results from these experiments showed that after 12 days, the media with biofilm released an average of 4 g ± 1.2 g of N. It is noteworthy that this duration was not long enough to decompose all the biofilm. To account for this fact, we developed a simple model that predicted the total amount of nitrogen released from the biofilm after a year and it ranged from 6 g to 16 g of highly reactive N (see chapter 2). These numbers would account for 6% to 19% of additional N uptake and storage. This simple model could indicate the importance of adequately modeling the biofilm and a potential sink (and eventually a source) of nitrogen that should be included in future models. To more accurately represent the accumulation, turnover, and contribution of algal mats that can develop on floating wetlands a more thorough modeling approach could prove beneficial.

Our model simulations would suggest that over the course of a growing season (April to September), the floating wetland would take up 27 kg TN m^{-2} (11 kg TN m^{-2}) via denitrification

and 9 kg TN (3.6 kg TN m^{-2}) from plant assimilation. This is consistent with a growing number of studies that indicate that plant N uptake can be small relative to denitrification (Butler Viruet et al., 2025; C. Y. Wang & Sample, 2014). A hypothetical application of the model simulations shows the potential for floating wetland nitrogen removal in the Patapsco estuary, we simulate the experimental additions of various areas of floating wetlands. The annual N load to the Patapsco River estuary is 2 x 10^6 kg/yr. If 1000 m^2 of floating wetland could be deployed, roughly 500 of the floating wetlands we measured in the mesocosm, the N loss from these wetlands would be 3.6 x 10^4 kg/yr. This would equate to a 1.8% reduction of the annual load. Recent wastewater treatment upgrades in the Patapsco estuary have resulted in a 1 x 10^6 kg/yr decline in N loads. To accomplish this same reduction would require 70,000 m^2 of floating wetlands, considering our 2.5 m^2 floating wetlands consumed 36 kg N. Given that the Patapsco tidal water surface area is 68,400,717 m^2, this would cover approximately 0.1% of the tidal surface area. Thus, there is a potential to perform large-scale wetland additions in-situ in an estuary like the Patapsco, but the costs of such a venture relative to other BMPs needs to be quantified.

This model analysis adds to a growing number of floating wetland models and experiments that have been developed in recent years. We took the approach of adapting a process-based model to our experiments. This type of modeling approach fosters a more quantitative and mechanistic understanding of system performance (Defo et al. 2017). In contrast to Wang et al., 2019 our process-based model contains several significant differences. First, an amplifier to represent the media component of the floating wetland was added, given how extensive the surface area of the media is to host microbial communities. Second, a photosynthetic function to influence the plant biomass accumulation depending on sunlight

availability and intensity was added so that a seasonal analysis could be done, which is necessary to discern N removal rates during periods of varying temperature, nutrient availability, and sunlight. The sunlight-dependence could be further developed to represent oxygen transport to wetland plant roots, which may influence nitrification and denitrification. Third, a function for allocating biomass from the shoots to the root dependent on inorganic nitrogen availability was added to represent the fact that wetland plants may partition more biomass to above-ground tissues under conditions of high nutrient availability. Lastly, our model incorporates a flow through parameter to simulate an estuarine environment with constant water flow. This final piece allows for the estimation of N removal rates relative to inputs. Other process-based models have been developed to measure floating wetland performance in a retention pond or retention pond simulated environment. McAndrew & Ahn, (2017b) developed a process-based model composed of three sub models (hydrology, plant growth, and nitrogen) and showed an increase in nitrogen removal when hydrologic retention time and surface area increase. Wang et al., (2019), developed a model with three sub models (plant, nitrogen and phosphorus) which indicates that floating wetlands nutrient removal performance is sensitive to plant characteristics and microbial activities. Both models are sensitive to plant characteristics and productivity. Each indicates that plant nitrogen removal increases in effectiveness when the hydraulic retention time increases.

Future Improvements and Applications

The model developed here was intended for two purposes: first, to better represent the dynamics of nitrogen cycling in floating wetlands and second, as a tool to predict the effects of floating wetlands on whole estuarine ecosystems based on surface area coverage. A significant improvement for future versions of the model should include the addition of oxygen concentration as a state variable. We hypothesize the addition of oxygen to the model will help

increase the predictive capabilities of oxygen dependent processes in the model. Although based on the oxygen concentrations in our tanks these systems were relative well oxygenated (table S1). These include processes such as mineralization, nitrification and denitrification. Another area where improvements could be gained is in the implementation of algal mat and biofilm sub-models. Such an addition could better account for the micro bacterial communities and algal mats encountered in our experiments. Finally, the addition of nitrogen sources like peatmoss and topsoil to the model could also help increase the accuracy of the model with respect to the specific experiments we simulated here.

Chapter 5: Floating wetlands in estuarine systems: Implications, gaps in our understanding, and future steps

Implications

Floating wetlands have been utilized as a tool to overcome limitations of retention ponds when it comes to treating stormwater runoff. Recently, there has been a desire to research and expand floating wetland performance and implementation beyond retention ponds and into coastal and riverine systems in an attempt to further aid natural system buffering against eutrophication (Karstens et al. 2021). This desire stems from the fact that retention ponds may treat only a small portion of a given watershed, thus even if effective, they can only make a small reduction in the overall nutrient input to an estuary. Floating wetlands deployed directly into estuarine waters may able to remove a more substantial fraction of the total nutrient load to an estuary, and more directly mitigate eutrophication. Research as performed in this dissertation helps inform the effectiveness and scope for application of floating wetlands outside retention ponds.

Floating wetlands when deployed in mesohaline environments are capable of transforming and permanently removing nitrogen from the system. This research helps inform future implementation of floating wetland technology, including identifying the potential benefit of nutrient removal in systems where other forms of restoration are either not an option or have limited success. This dissertation aimed to shed light at how floating wetlands in estuarine systems performed and transformed nitrogen. From our experiments, we found that floating wetlands have N removal processes in addition to plant assimilation creating an environment that supports ultimate removal of nitrogen. In other words, the wetlands create environments favorable to producing inorganic forms of nitrogen that in turn support high rates of denitrification. In the experiments, the complex floating media removed up to 40% of the

nitrogen entering the floating wetland. Although plant nitrogen assimilation only accounted for no more than 10% of the nitrogen removed, it identified at least one species of plant that can remove nitrogen effectively in mesohaline environments. These results are promising as there is data indicating the effective removal and transformations of nitrogen in floating wetlands deployed in estuarine-like environments.

Research Gaps

Research beyond mesocosms: new vs. established, in isolation vs. in-situ – Although our research indicates that floating wetlands performed relatively well and removed a significant amount of nitrogen from our mesocosm experiments, these experiments were limited to one type of environment. To further understand floating wetlands across a broader range of coastal systems, it is important to understand how these work under different salinity gradients and coastal conditions. Landaverde et al., (2024) shed light on how different pants species perform under different salinity gradients showcasing how *Spartina patens* and *Spartina alterniflora* performed the best in saline environments in the east coast of the US. While Sanicola et al. (2019) showcased how *Phragmitis australis* and *Sarcocornia quinqueflora* performed the best in saline conditions off the coast of Australia. (Karstens et al. 2018; Karstens et al. 2021) researched floating wetlands in Baltic Sea lagoons in an attempt to understand floating wetland performance and its interactions with their environments. The floating wetlands they studied not only removed nitrogen but also served as a nursery ground for juvenile eels (*Anguilla anguilla*) and foraging ground for the grey heron *Ardea cinerea*. In experimental settings in Oklahoma, US, Strosnider et al. (2017) indicated that their floating wetlands were utilized as sheltering habitat by birds, amphibians, snails, and spiders. Thus there is a potential to better quantify the food and habitat effects of floating wetlands.

There are also considerations of experimental methods and their impacts on nitrogen cycling. We allowed our floating wetlands to settle and plants to establish for a short period of time before experimental measurements began. However, accumulation of organic matter occurs for relatively long periods in a floating wetland as well as the degradation of the floating media due to biotic and abiotic factors. It is important to understand how the performance and the ability of floating wetlands to remove nitrogen changes overtime with organic matter accumulation and natural decay of the media. For example, naturally occurring floating wetlands can cause low oxygen zones directly underneath the floating wetland (Swarzenski et al. 1991; Alam et al. 1996) as well as organic-rich zones due to decay plant and root material (Scheffer et al. 2003) and this is just to name a few of the effects of naturally occurring floating wetlands. These factors, over time, can influence the performance of the floating wetland. Researching them can provide implementers enough information to better estimate the overall nitrogen removal potential, the possibility that this potential could decline over time, and the effects of floating wetlands on their surroundings. Research on artificial floating wetlands and their effects in their surroundings have indicated that floating wetlands do have the capability to minimize oxygen concentrations directly underneath providing an overall less aerobic, highly organic, and cooler conditions directly underneath the floating wetland (Strosnider et al. 2017).

Floating wetland implementation practices – Floating wetlands do not typically follow specific implementation practices. Plants often come from plant nurseries where fertilizer is applied to aid the pant with growth at the early stages and through the time while these are in the nursery pots. Utilizing plants with fertilizer can be detrimental for the area of interest as these can add substantial amounts of nitrogen and phosphorus to the system and can hamper or delay the treatment effects. More research understanding the performance of a floating wetland or

plants without fertilizer in floating wetlands can aid in new designs optimized to aid establish the plants without the need of fertilizer. We also added peatmoss and topsoil to floating wetlands to be consistent with industry practices, but these materials also bring nitrogen and phosphorus to the system from outside. Our nitrogen budgets indicate that although fertilizer only accounted for 0.004% of the sources of nitrogen, topsoil accounted for up to 6% of the TN sources while peatmoss accounted for up to 42% of the TN sources on the floating wetland, thus it would be best to avoid their use in in-situ plantings.

Floating wetlands can have multiple designs – Floating wetlands can come in many different shapes and forms. It is important to understand how other designs perform to find the most appropriate design for the area of interest. Different designs could enhance different nitrogen processes and the understanding of how this design will affect the internal nitrogen process can she light into design improvement based on what the implementer is interested in doing. Our experiments used a traditional floating wetland design. A floating media made of recycled PET fibers, placed 50% submerged with plants, peatmoss and topsoil to aid in the establishment of the plants at the beginning of the growing season. Although it is the most common, it is not the only design. Strosnider et al. (2017) and Borne et al. (2013) used the same PET design to research the effects of floating wetlands on the underlying water column and overall nutrient removal, while Wang and Sample (2014) used PVC pipes, plastic mesh, and potholders to construct their floating wetlands in mesocosm batch experiments. These experiments all produced different rates of removal due to the use of different plants and different experimental settings. Other approaches have included the use of burlap fabric, wood, inorganic matting, or fiber glass (Lucke et al. 2019). Understanding how all of these perform in estuarine systems can help inform implementer and choose the design that best fits their nutrient reduction targets.

Floating wetland model missing formulations and additional interacting factors – Our floating wetland model is a process-based model composed of three sub-models: a plant sub-model, a water column nitrogen sub-model, and a media nitrogen sub-model. These formulations do not include the effects of oxygen in any of the nitrogen processes known to rely on oxygen presence or absence for optimal performance. *Spartina patens* research indicates that these carry oxygen from the shoots to the roots to create oxic zones at the rhizosphere providing an environment ideal for mineralization and nitrification by microbial communities associated to the roots of these plants (Welsh et al. 2010). Additionally, the high porosity of the media, as described in chapter 2 and 3 make the case for the importance of a biofilm model and the inclusion of oxygen model that can represent the oxic zones that can be potentially supporting mineralization and nitrification in the media and subsequently high denitrification rates. Beyond the addition of oxygen, the model can benefit from the addition of a biofilm model that can represent the net storage of nitrogen in the biofilm as well as the constant turnover and release of nitrogen back into the system.

Future Steps

Research biofilm composition in the floating media – Our experiments indicated that the media alone is responsible for sustaining high rates of denitrification. This type of behavior is not uncommon as previous research has demonstrated the media's ability to sustain microbial communities capable of transforming nitrogen from mineralization to nitrification (Stewart 2008) and subsequent denitrification (Butler Viruet et al. 2025). More experiments are needed to further understand the microbial composition of the media and how different media designs shape the microbial composition and thus its ability to support and transform the nitrogen in the system.

In-situ experiments in different environments – As mentioned above, our experiments were performed in a highly controlled environment. Although great for isolating floating wetlands effects, these idealized experiments introduce artifacts that are not present, such as periphyton in the tank walls, while excluding important variables that interact with the floating wetland and influence their performance. For example, fish larvae, mussels, oysters, eels, turtles and migratory birds may both benefit from floating wetlands, but also use them for habitat, which may lead to modification of the wetland itself. For example, migratory birds utilizing the floating wetland as a temporary foraging or nursing ground can become a source of nitrogen and phosphorus because of their feces. Meanwhile, although mussels can aid with filtration and removal of nutrient, their oxygen consumption can cause even lower concentration directly underneath the floating wetland negatively impacting other organisms and the nitrogen transformations dependent on oxygen availability. Research should be conducted on floating wetlands under in-situ conditions to understand overall performance under the influence of all other biotic and abiotic factors.

Conclusions

Floating wetlands can transform and permanently remove nitrogen from estuarine-like environments through both denitrification and assimilation into plant tissue. Nonetheless more research is needed to better guide design, performance, and implementation. This dissertation provides the foundation needed to understand how this technology transforms nitrogen in the system and what are the next steps needed to further develop and implement this technology to tackle eutrophication in coastal systems.

Appendix A

Supplemental Material for Chapter 2: Floating wetlands beyond retention ponds: estimating nitrogen cycling and removal in tidal waters

Section 1: Methods

Plant Biomass Calculations

Plant biomass was estimated by comparing the difference between initial plant nitrogen concentration and final plant nitrogen concentration combined with the dry weights of the plant tissue extrapolated to each tank. To estimate initial plant biomass (above and below ground) and N mg we used the following equation:

$$B_i = \frac{P_B * N_P}{A_M}$$

where B_i is the initial estimated plant biomass (mg DW m^{-2}), P_B is the plant biomass average from three plant samples (mg DW) and N_P is the number of plants that were planted in each tank and A_M is the surface area of the floating media (m^{-2}). We assumed all plants to contain the same amount of initial N content. The same equation was used to estimate below ground biomass. To estimate the final plant biomass accumulation, we used the following equation:

$$B_f = B_i - T_F$$

where B_f is the final estimated plant biomass accumulation (mg DW m^{-2}), B_i is the initial estimated biomass (mg DW m^{-2}) and T_F total plant biomass collected in (mg DW m^{-2}). This was done individually for all tanks. The same equation was used to estimate below ground biomass.

B. Experimental Calculations for nutrient, oxygen and denitrification fluxes

(1) The equations below describe the approach for computing a net sediment-water flux from a time-series of a constituent measured in the water overlying the sediment in the incubation of an intact core. First, the height of water above the sediment surface in the sediment core chamber (Core Water Depth; m) is computed from the core area and volume of water measured after the incubation.

Core H_2O Depth = (CORE VOL^a/CORE SURFACE AREA^b)/100^c

where

- *a* is the measured volume of water in the sediment core (cm^3)
- *b* is the surface area measurement of the core cylinder (cm^2)
- *c* converts measurement units to m

The slope of the linear regression fit of the constituent time-series during the incubation (concentration versus time) is then used to estimate an hourly net sediment-water flux per unit area, expressed by the general equation below:

NET SEDIMENT-WATER FLUX ($\mu mol\ m^{-2}\ h^{-1}$) = [(SLOPE^a) x (Core H_2O DEPTH^b) x (60^c)]

where

a variable-specific slope of linear fit (NH_4^+, NO_{2+3}^-, O_2, N_2)

b converts measurements from volumetric to areal basis

c converts time units from minutes to hours

Blank corrections were made by simply subtracting the slope (slope of oxygen or nutrient concentration versus time plot) of the blank core from the slope of the oxygen or nutrient concentration versus time plot for the full sediment core. These corrections were generally either zero or quite small.

C. Criteria for accepting, rejecting, and modifying variable slopes used in calculating net sediment water fluxes: Constituent concentrations were plotted against time of sampling and the slope of this curve is used to calculate net sediment-water exchanges. The following steps assume that all data have been previously verified following normal protocols.

1. If the slope of the nutrient concentrations vs. time plot was statistically significant ($p<0.05$), the slope was used in calculating fluxes without modification.
2. Occasionally, there were plots which indicated a clear increasing or decreasing trend in concentrations over time but had one observation which diverged strongly (either higher or lower concentration) from the trend. We consider these divergent data to represent contaminated samples (either by addition of the compound or addition of water having a much lower concentration of the compound) and they were not used. The slope was recalculated using lower degrees of freedom and a higher "r" value as a criteria for significance. If the slope is statistically significant, it was used in calculating fluxes.
3. If the concentration vs. time plots were erratic (i.e. no statistically significant increasing or decreasing trend in concentration over time), and if the difference in concentration among variables was greater than twice the detection limit for that variable, the data for that variable were considered to be non-interpretable. The slope was not calculated and the entry for that variable was recorded as "NI".
4. If the concentration vs. time plots were erratic (i.e. no statistically significant increasing or decreasing trend in concentration over time), and if the difference in concentration among variables was less than twice the detection limit for that variable, then the slope was taken to be zero and the net sediment-water flux was reported as zero. Occasionally, statistically significant slopes have been found for some variables (mostly nitrite and dissolved inorganic phosphorus) where concentration differences over the incubation period do not exceed twice the reported detection limit. These slopes were used to calculate net sediment-water exchanges.

D. Indices of N transformation

To quantify metrics of nitrogen cycling associated with the media, we derived a series of indices of nitrogen transformations. First, we computed the nitrification needed to support denitrification using the following equation:

$$Apparent\ Nitrification = N_2 + NO_{2+3}$$

where N_2 is the net N_2 fluxes and NO_{2+3} is the nitrate fluxes. This metric assumes that any N that was denitrified in excess of the NO_{2+3} influx was generated through nitrification. We also calculated the denitrification efficiency using the following equation:

$$Denitrification\ Efficiency\ (\%) = \frac{N_2 - N}{\sum N} x100$$

where N_2 is the denitrification rate and $\sum N$ is the summation of the NH_4, N_2, and NO_{2+3} fluxes multiplied by 100 to obtain a percentage. Lastly, we calculated the ammonium recycling index using the following equation:

$$Ammonium\ recycling\ index = \frac{NH_{4^+}}{\sum N} x100$$

where NH_4 is the ammonium flux and $\sum N$ is the summation of N_2, NH_4 and NO_{2+3} fluxes, multiplied by 100 to obtain a percentage.

Section 2: Results

Environmental characteristics of the mesocosms

Temperature, dissolved oxygen, chlorophyll-a, and salinity variation for 2019 and 2021 mesocosm experiments are shown in Table S1. The 2019 experiments were conducted in the summer months while the 2021 experiments were conducted in the spring months.

Table S1. Environmental characteristics for the mesocosm tanks in summer 2019, and spring 2021. These values represent the minimum, maximum and average values for the length of the experiments. pH data not shown due to the sensor experiencing a malfunction halfway through the experiment.

Parameter	2019 Control			2019 Experimental			2021 Control			2021 Experimental		
	Min	**Mean**	**Max**	**Min**	**Mean**	**Max**	**Min**	**Mean**	**Max**	**Min**	**Mean**	**Max**
Dissolved Oxygen (mg L^{-1})	1.4	4.1	7.43	1.5	4.1	6.7	2.6	6.8	10.2	3.3	6.9	10.1
Oxygen Saturation (%)	18.3	54.5	103.8	20.5	54.4	89.1	34.8	77.8	107.4	44.9	78.4	105.1
Salinity (PSU)	8.0	10.5	10.5	7.9	12.7	10.5	10.3	11.8	13.2	10.4	11.8	13.2
Temperature (C°)	13.9	17.8	21.4	13.9	17.9	21.3	17.5	21.7	27.0	16.5	21.6	26.5
Active Chlorophyll-a (µg L^{-1})	0.4	3.1	9.5	0.2	2.2	9.3	0.7	6.8	20.6	0.68	6.6	20.1

The inflowing waters contained a higher concentration in chlorophyll-a than in the tanks (fig. S1), suggesting that algal cells in the inflowing water settled within the mesocosms.

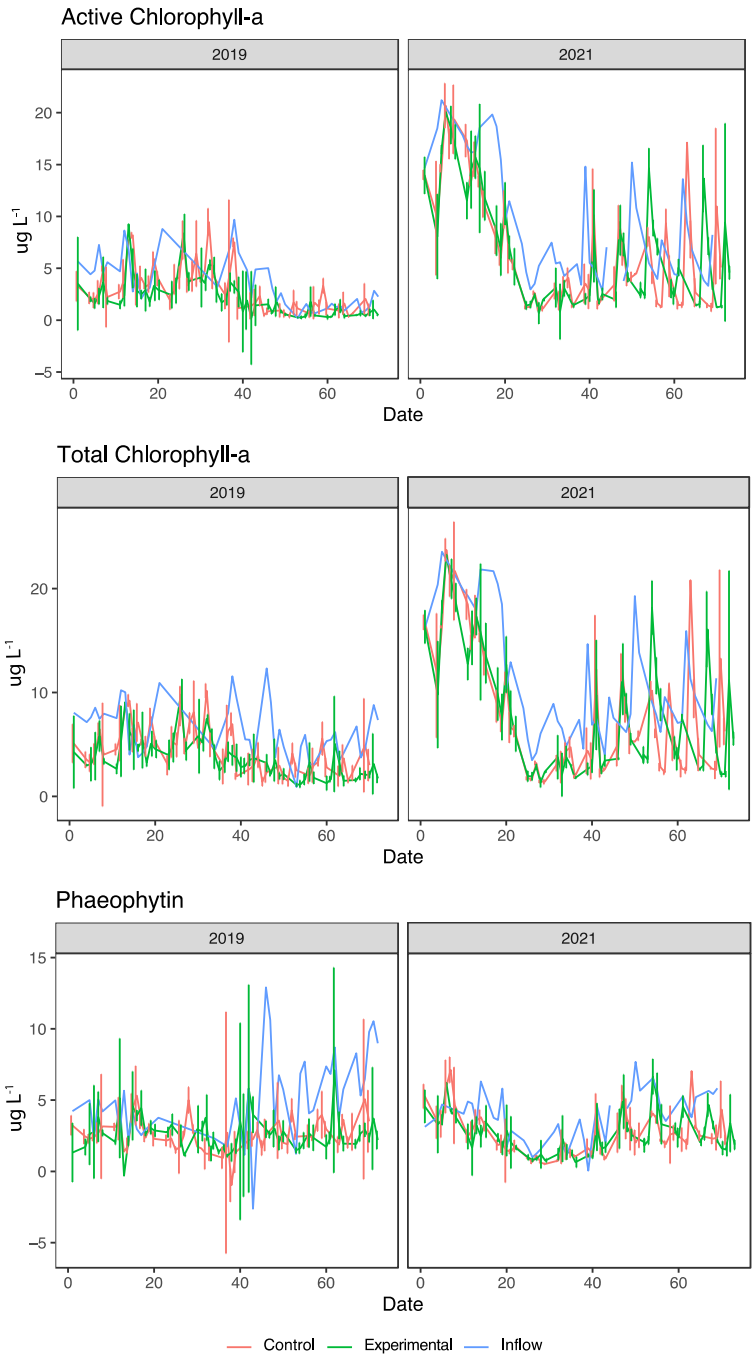

Figure S1. Active chlorophyll-a, total chlorophyll-a, and phaeophytin collected from the inflow and treatment tanks. Experimental and control data represent the average of the three tanks for each treatment. The error bars represent the standard deviation from the mean. Spikes observed in the active and total chlorophyll-a plots indicate that the sample was collected shortly after tanks were cleaned.

The inflowing waters contained a higher PN concentration than in the tanks and outflow (fig. S2), suggesting that PN in the inflowing water settled within the mesocosms. NO_{2+3}^- was elevated in the outflowing water relative to the inflow, while NH_4^+ and DON differences were less clear.

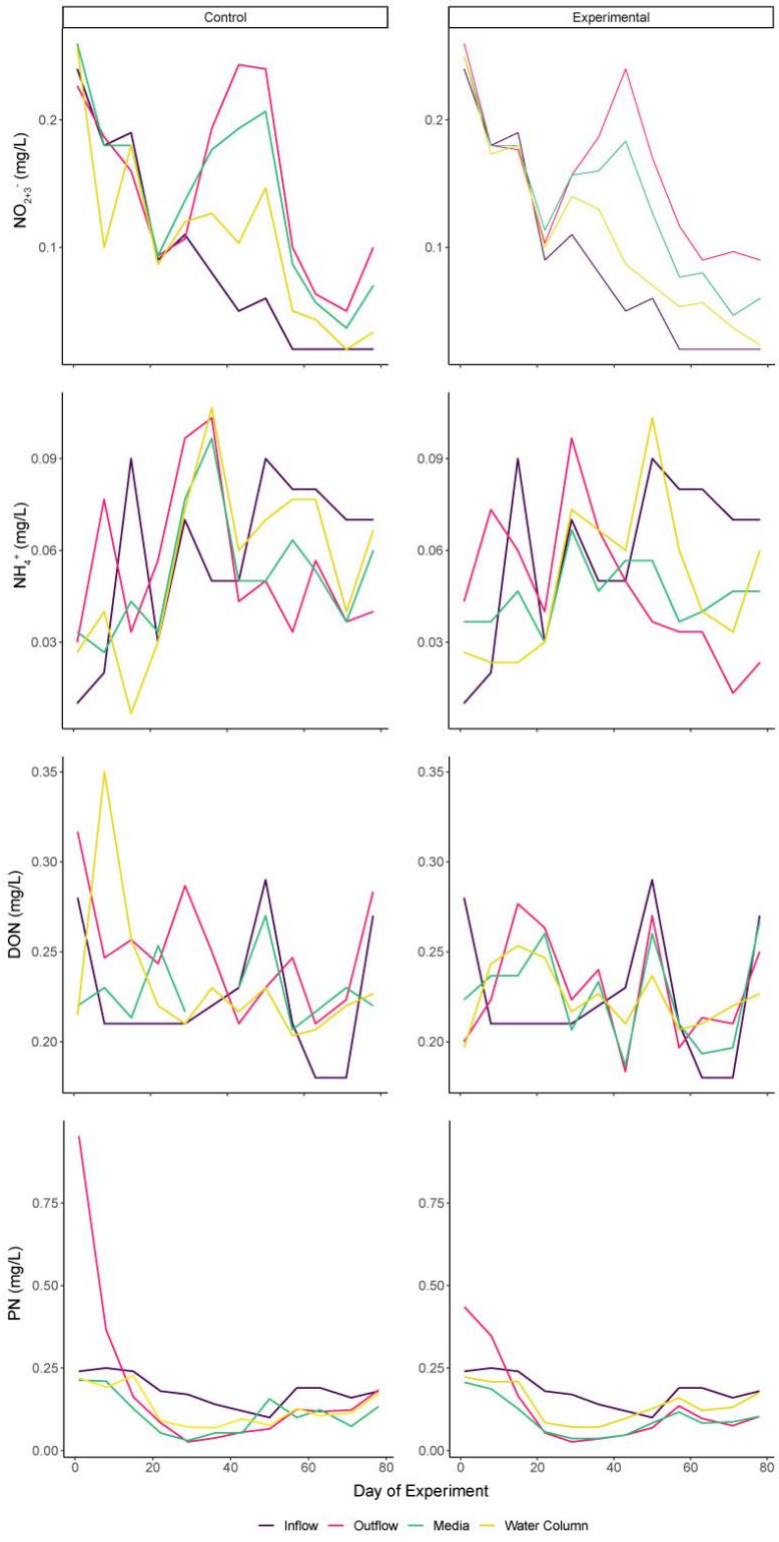

Figure S2. (from the top) NO_2 + NO_3, NH_4^+, DON and PN concentrations within different environments in the mesocosm experiments in 2021 (Day 0 is April 16, 2021).

B. Periphyton

Periphyton was collected on a weekly basis and analyzed for total mass and nitrogen content. The control tanks accumulated less periphyton when compared to the experimental tanks (fig. S3). Interestingly, when plotting the periphyton biomass (fig. S3) and the periphyton nitrogen content (fig. S3) for the control and experimental tanks, it is clear that although the control tanks accumulated less periphyton, the nitrogen percent contained in that periphyton is actually 0.8 percent N higher than in the experimental tanks, although not statistically significant (p>0.05) (fig. S3). The weight of periphyton also declined over time in the experimental tanks, but not in the control tanks (fig S3). This behavior can be observed on both experiments in 2019 and 2021.

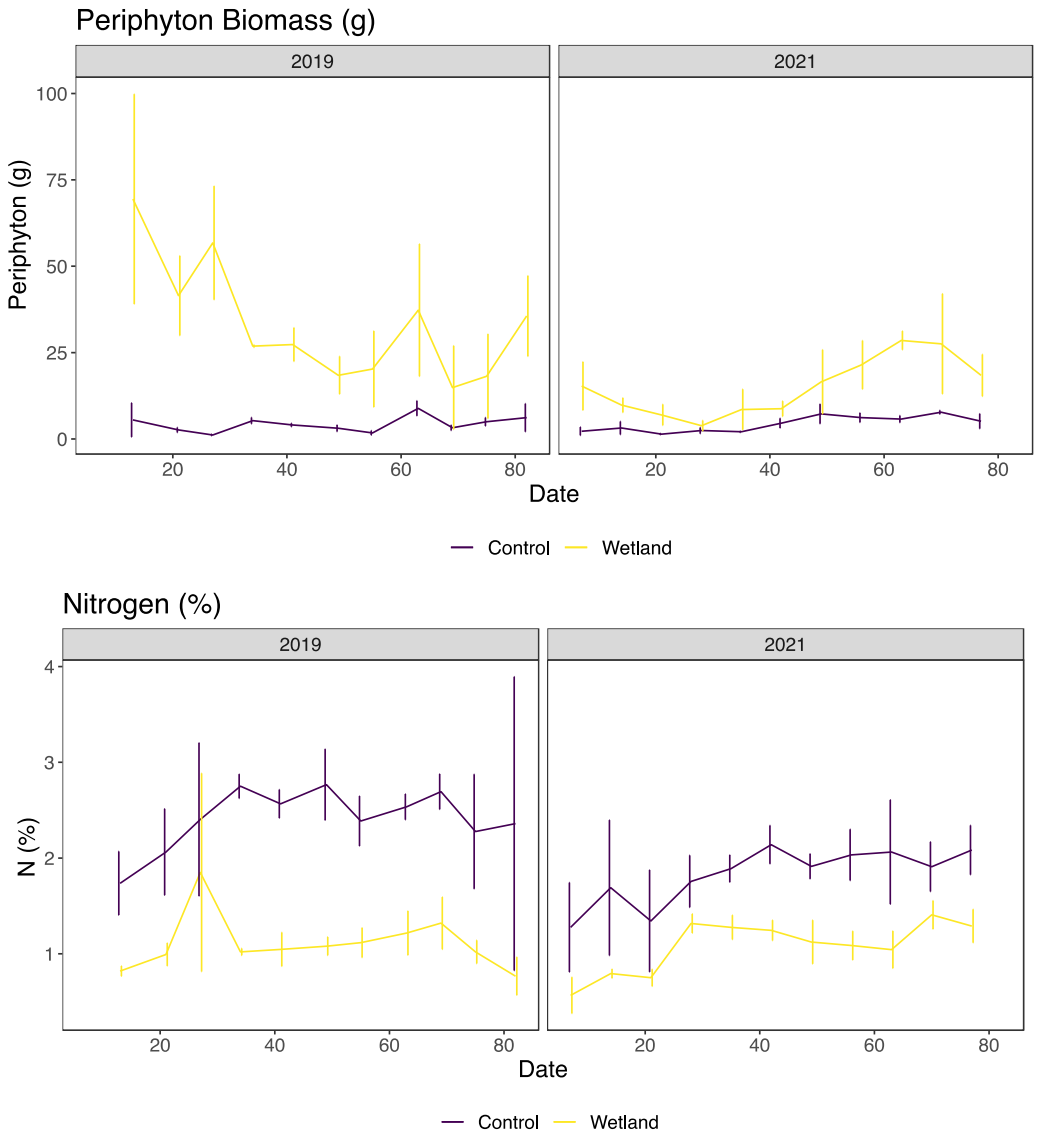

Figure S3. Periphyton weekly accumulation in the control and experimental tanks, including total weight (top panels) and % N (by weight) of collected tissue (bottom panels). Periphyton was collected during weekly cleaning utilizing a plankton net. Error bars indicate the standard deviation from the mean of the three tanks.

Appendix B

Supplemental Material for Chapter 3: Partitioning nitrogen removal potential in floating wetlands using mass balance budgets

Estimating Error Propagation

To estimate the error propagation of the budget we estimated the weekly uncertainty for each of the individual analytes that compose TN (NO_{2+3}^-, NH_4^+, DON and PN), as well denitrification and periphyton using the following equations:

$$\delta\overline{x} = \frac{SD}{\sqrt{N}} \quad (1)$$

where SD is the standard deviation of the N measurements. This quantity, SD/√N, is called the standard error of the mean or just the standard error (SE). The we estimate the fractional uncertainty using equation 2:

$$fractional\ uncertaity = \frac{\delta x}{|x|} \quad (2)$$

Where fractional uncertainty, defined as the uncertainty divided by (the best-guess value of) the quantity x itself. Then we estimated the error propagation of the budget by using the standard error and the fractional uncertainty using the following equation:

$$\delta Q = \sqrt{(\delta a)^2 + (\delta b)^2 + \cdots (\delta x)^2 + (\delta y)^2} \quad (3)$$

We used this equation since the estimation of the nitrogen budget was a summation of all the weekly rates of from all the nitrogen forms. I estimated the weekly uncertainty of the flow rates for each of the tanks and then estimated the overall error propagation for weekly TN rates (g/week) using eq 3. All weekly errors were added together to indicate the overall uncertainty of the weekly rates. To estimate the error propagation of denitrification we estimated the uncertainty of monthly denitrification rates then added them together to represent the uncertainty of all the measurements added together.

Diagenesis Results

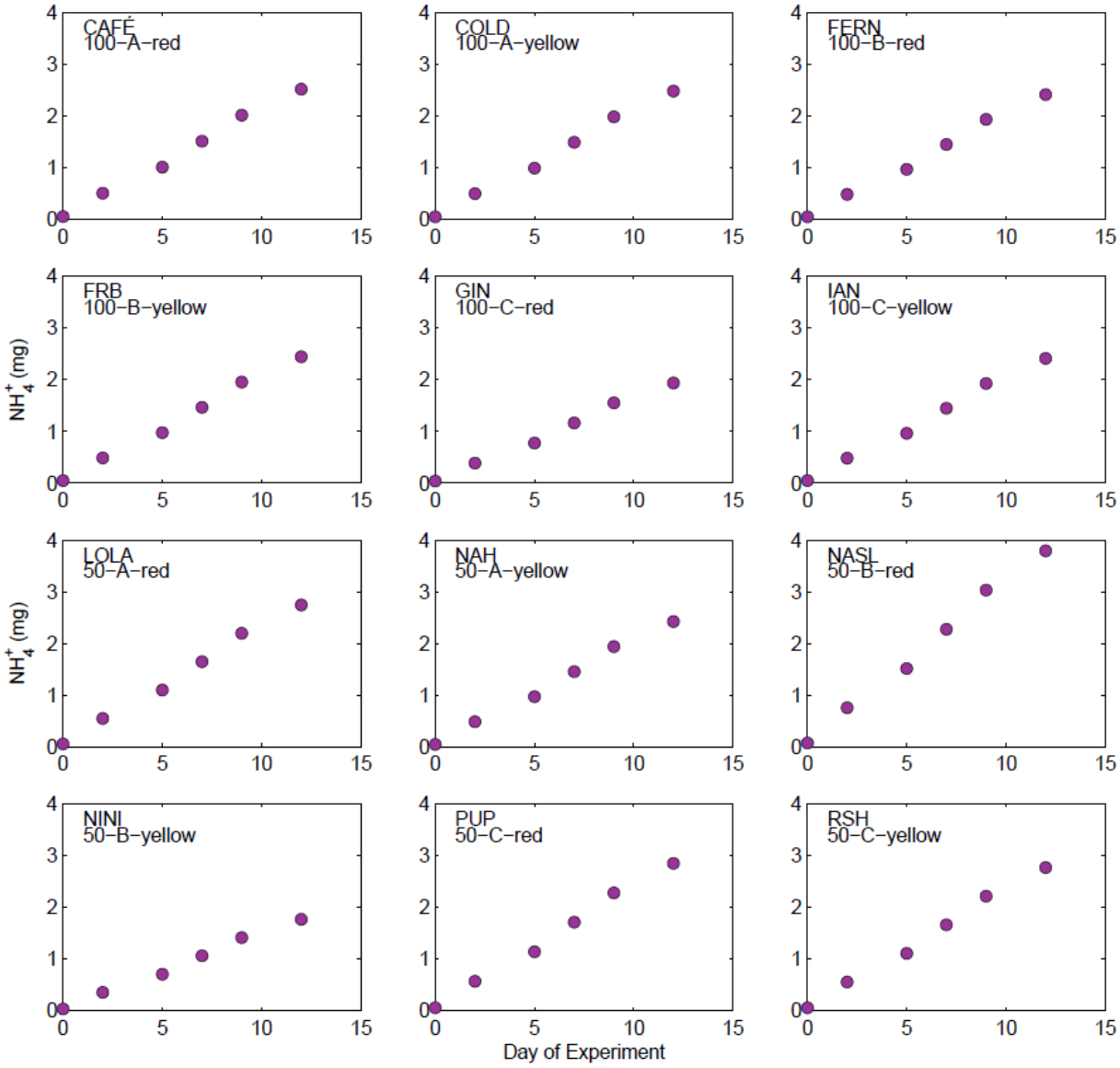

Figure S1. Time-series of NH4 accumulation rates in 12-day diagenesis experiments. 50 represents 50% submerged and 100 is 100% submerged.

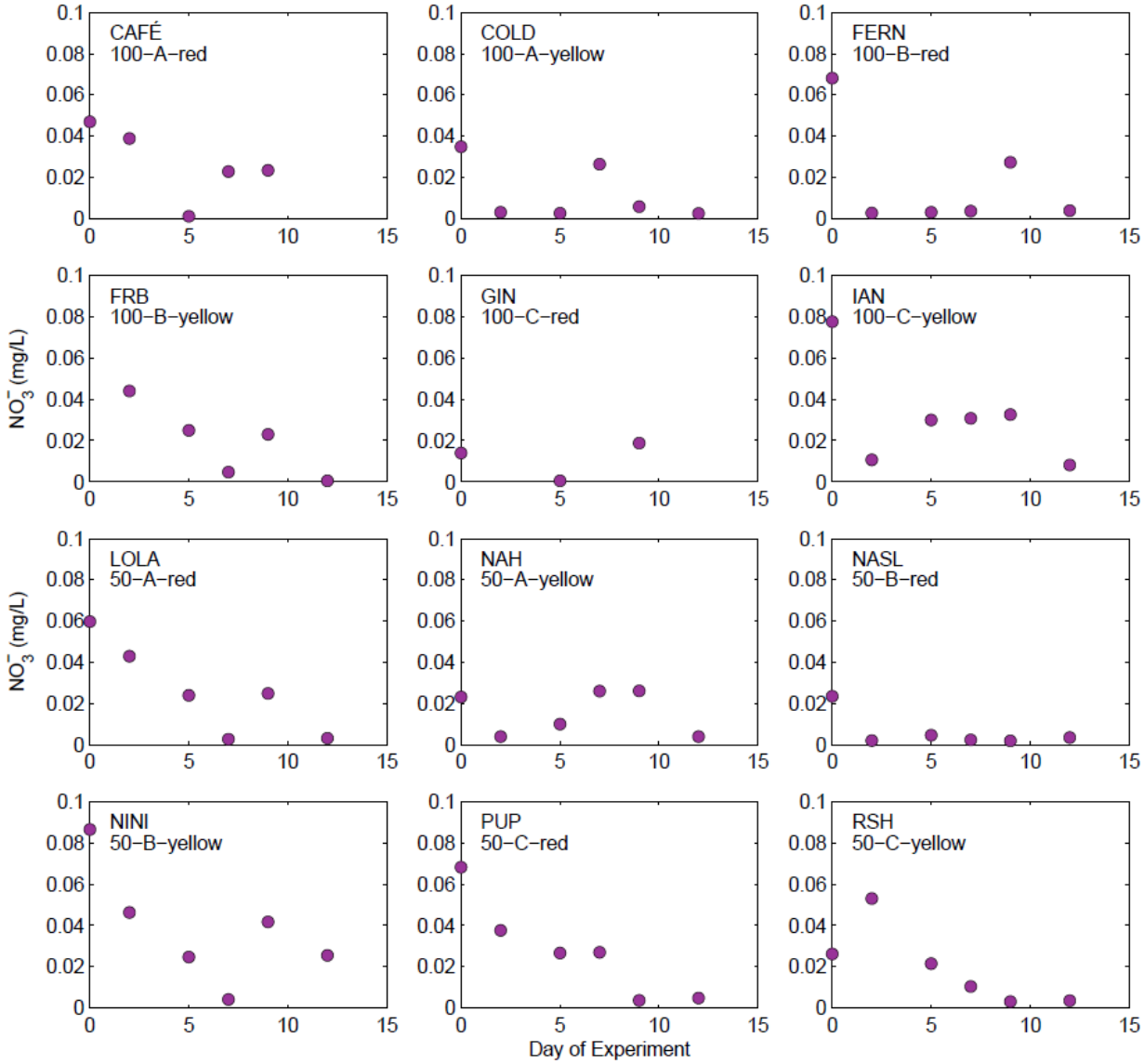

Figure S2. Time-series of NO_{23} concentration in 12-day diagenesis experiments. 50 represents 50% submerged and 100 is 100% submerged. The declines in these concentrations confirm that oxygen levels were maintained at anoxia during the experiment, and concentrations were extremely low.

Appendix C

Supplemental material for Chapter 4: Modeling nitrogen cycling and removal pathways in a temperate *Spartina patens* floating wetland

Model Variables

Table 1. Model variables

Parameter	Description	Units
B_{SH}	Above ground biomass	g DW m^{-2}
P_{SH}	Plant growth rate	day^{-1}
R_{SH}	Decay rate of shoots	day^{-1}
B_{RO}	Below ground biomass	g DW m^{-2}
R_{RO}	Decay rates of roots	day^{-1}
PAR	Photosynthetic Active Radiation	-
PARmax	Maximum photosynthetic active radiation	-
KTR_{SH} and KTR_{RO}	Effects of temperature on the shoots and root decay rates	$°C^{-1}$
RM_{SH}	Shoot death rate at reference temperature	day^{-1}
RM_{RO}	Root death rate at reference temperature	day^{-1}
TR_{SH} and TR_{RO}	Reference temperatures for shoots and roots	°C
PM_{SH}	Maximum growth rate of plant shoot	day^{-1}
T	Temperature	˚C
$KT1_P$	Effect of temperature below TP1P on shoot growth rate	$°C^{-2}$
$KT2_P$	Effect of temperature above TP2P on shoot growth rate	$°C^{-2}$
$TP1_P$	Minimal range of growth temperature	°C
$TP2_P$	Maximum range of growth temperature	°C
KTR_{SH}	Effect of temperature on shoot respiration rate	$°C^{-1}$
KTR_{RO}	Effect of temperature on root respiration rate	$°C^{-1}$
kFSTR	Reaction coefficient of the fraction of shoot photosynthetic products directly transferred to root	-

FSTRmax	Maximum fraction of shoot photosynthetic products directly transferred to root	-
KHN_{PL}	Half-saturation constant for nitrogen uptake	mg L^{-1}
LPLNM	Ratio of nitrogen to plant biomass	mg N g^{-1}
KNSED	Sedimentation rate of OrgN	day^{-1}
NMIM	Mineralization rate of OrgN in reference temperature	day^{-1}
KNMI	Effect of temperature on mineralization rate of OrgN	$°C^{-1}$
Nitm	Maximum nitrification rate	day^{-1}
Denm	Maximum denitrification rate	day^{-1}
KNit	Effect of temperature on nitrification rate	$°C^{-2}$
KDenit	Effect of temperature on denitrification rate	$°C^{-2}$
KHNit	Nitrification half-saturation constant for ammonium	mg L^{-1}
KHDenit	Denitrification half-saturation constant for nitrate	mg L^{-1}
Kmedia	Media amplifier	m^{-2} m^{-2}
OrgN	Organic Nitrogen	mg m^{-3}
S_{FTW}	Water surface area	m^2
V_W	Water volume	m3 day^{-1}
FNO_{PL}	Fractions of nitrogen metabolized by plants as organic nitrogen	-
NMI	Mineralization rate of organic nitrogen	day^{-1}
Q_{IN} and Q_{OUT}	Inflow and outflow of water	m^3 day
xN_{IN} and xN_{OUT}	Nitrogen concentration inflowing and outflowing	mg m^{-3}
NH_4	Ammonium	mg m^{-3}
FNI_{PL}	Fractions of nitrogen metabolized by plants as ammonium	-
PN_{PL}	Ammonium uptake preference factor for plants	-
NMIM	Mineralization rate of OrgN at reference temperature	day^{-1}
KNMI	Effect of temperature on OrgN mineralization	˚C
Nit	Nitrification	Mg m^3 d^{-1}

Denit	Denitrification	
KNit1	effect of temperatures below TNit	($°C^{-2}$)
KNit2	effect of temperatures above TNit on the nitrification rate	$°C^{-2}$
KDenit1	Effect of temperature	
KDenit2	Effect of temperature	
TNit	Optimum temperature for Nitrification	˚C
TDenit	Optimum temperature for denitrification	˚C
KHN_{PL}	Half-saturation coefficient for nitrogen uptake in plants	-

Forcing Data

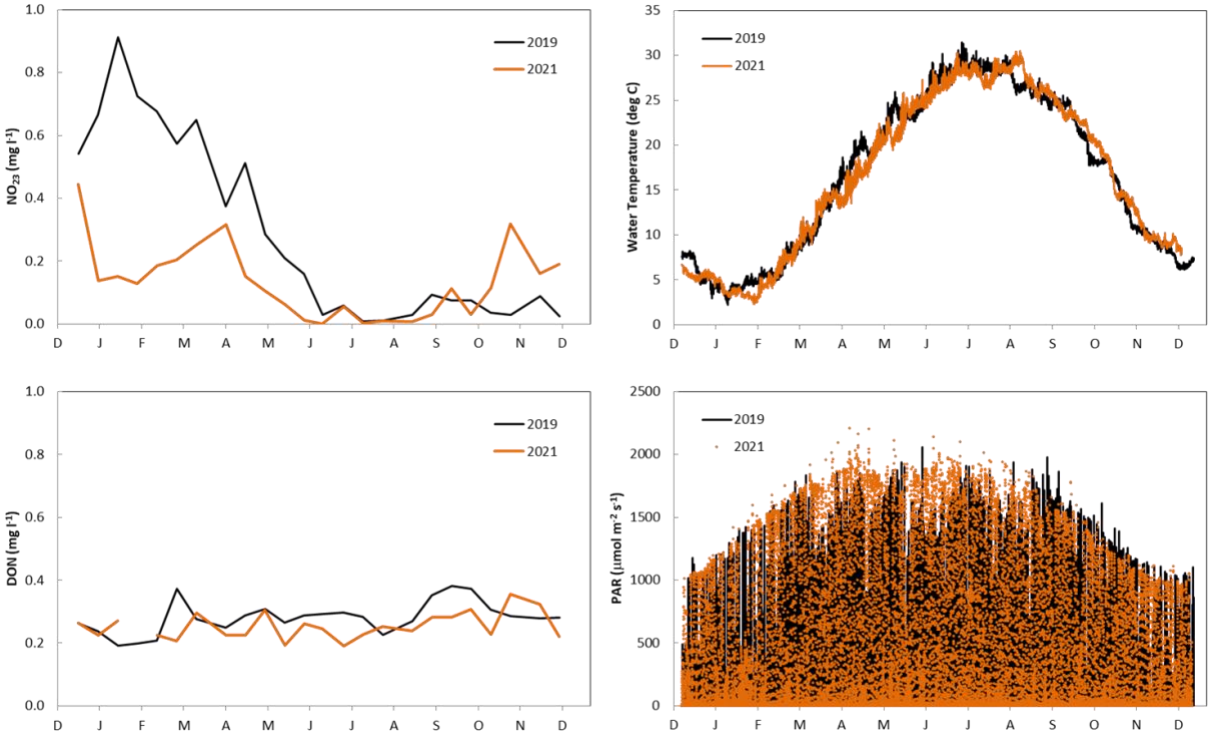

Figure S1. Forcing data for NO_{23}^{+} and DON, water temperature (˚C) and Photosynthetic active Radiation (PAR). NH_4^{+} values are not included as they are close to 10% of the NO_{23} values.

Sensitivity Analysis

Table S2. Sensitivity values used for all the parameters tested in the model. **TP1p** is the minimum temperature plant growth, **kFSTR** is the reaction coefficient for the allocation of biomass from the shoots to the roots, **FSTRmax** is the maximum allocation of biomass from the shoots to the roots, and **PMsh** is the maximum plant growth rate of the plant shoots. Each run represents the model run using each parameter value. Values used in initial run (Run 1) represent the baseline values for each parameter.

Simulation	**TP1p**	**kFSTR**	**FSTRmax**	**PMsh**
Run 1	22	0.1	0.05	0.16
Run 2	22.75	0.2	0.1625	0.1725
Run 3	23.5	0.3	0.275	0.185
Run 4	24.25	0.4	0.3875	0.1975
Run 5	25	0.5	0.5	0.21
Final % change from baseline value	13	5	10	31

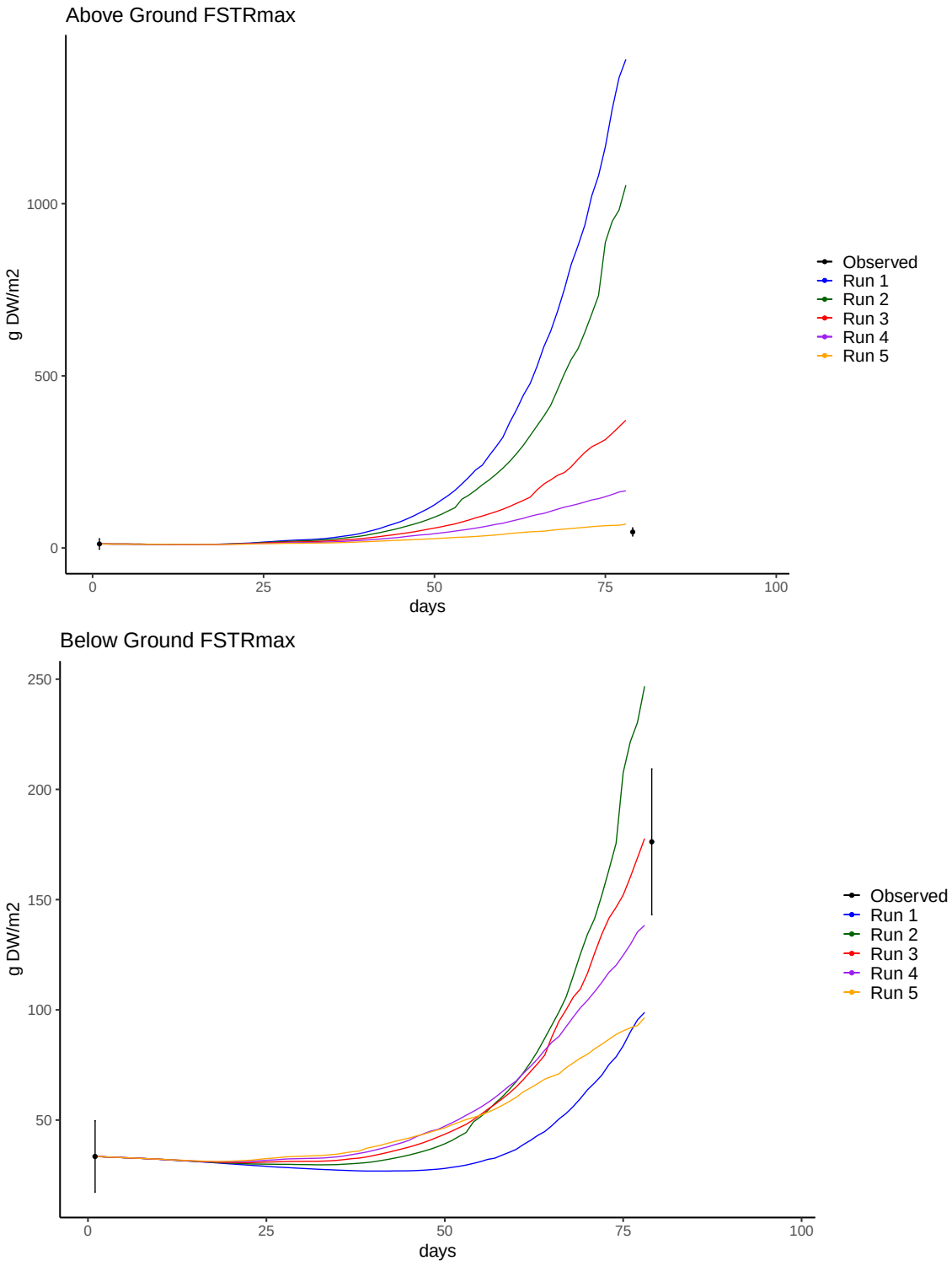

Figure S2. Sensitivity Analysis for FSTRmax on above and below ground biomass. (Top) above ground biomass (bottom) below ground biomass.

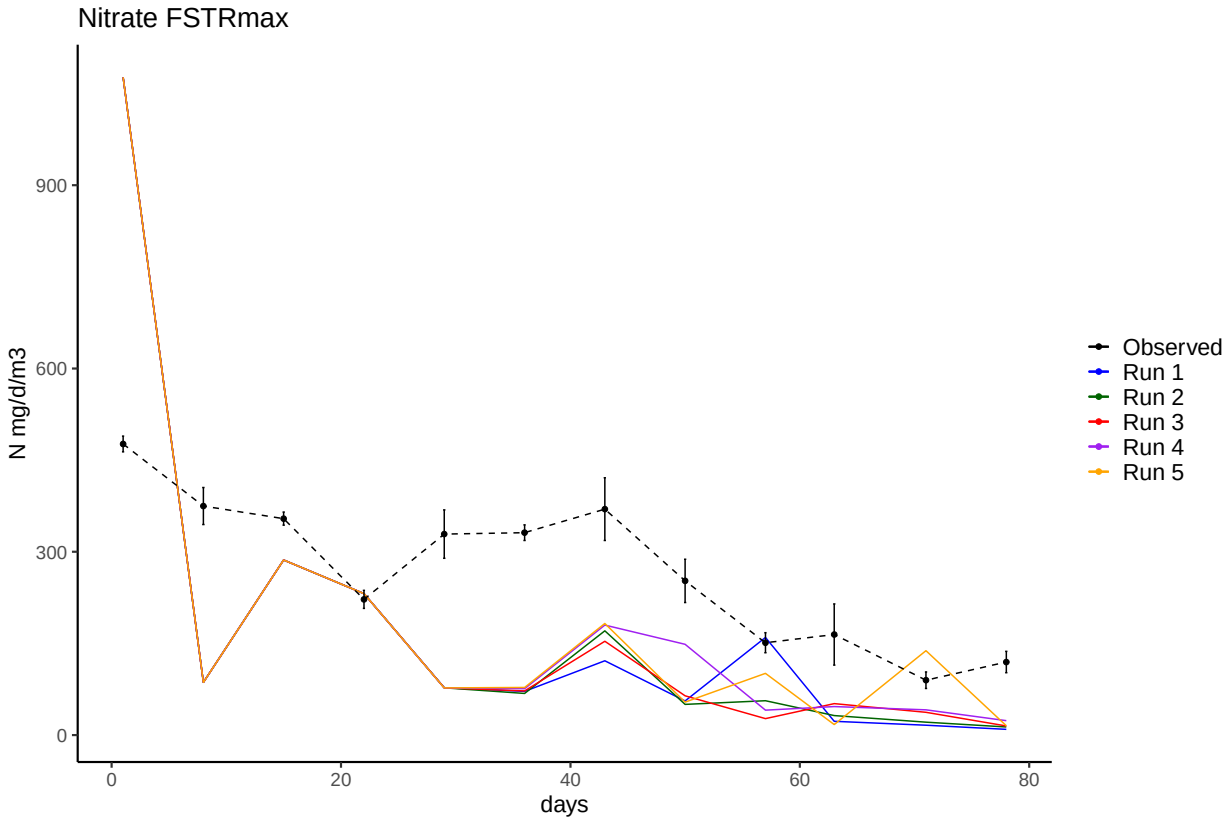
Nitrate FSTRmax
N mg/d/m3
900
600
300
0
0
20
40
60
80
days
Observed
Run 1
Run 2
Run 3
Run 4
Run 5

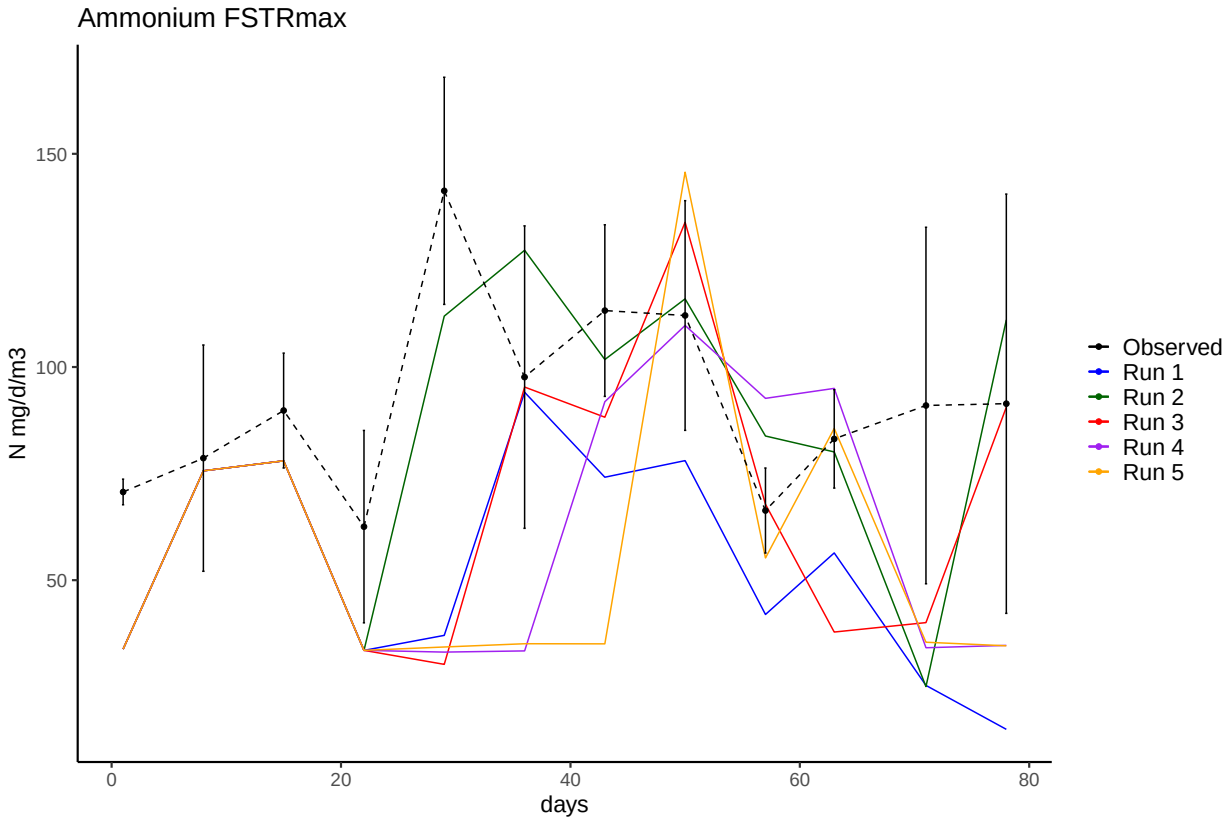
Ammonium FSTRmax
N mg/d/m3
150
100
50
0
20
40
60
80
days
Observed
Run 1
Run 2
Run 3
Run 4
Run 5

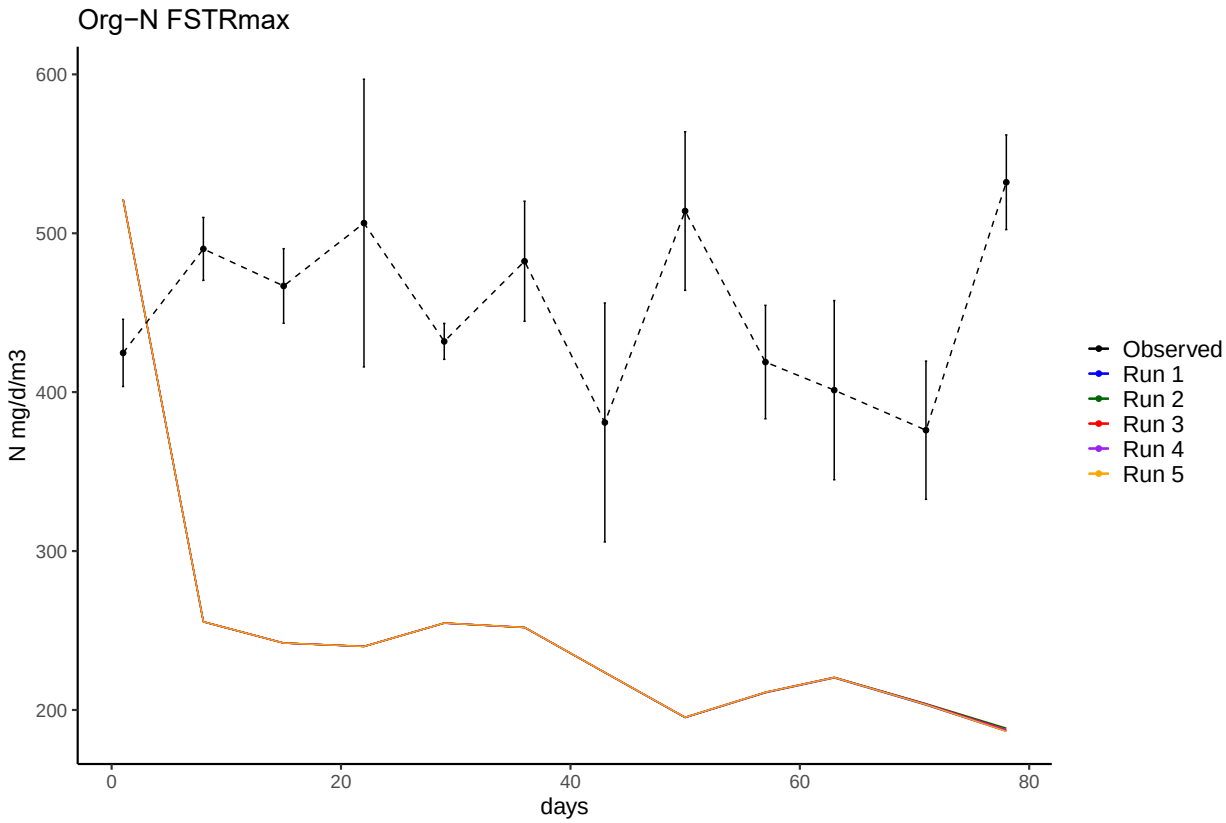

Figure S3. Sensitivity plots for FSTRmax on nutrient outflow.

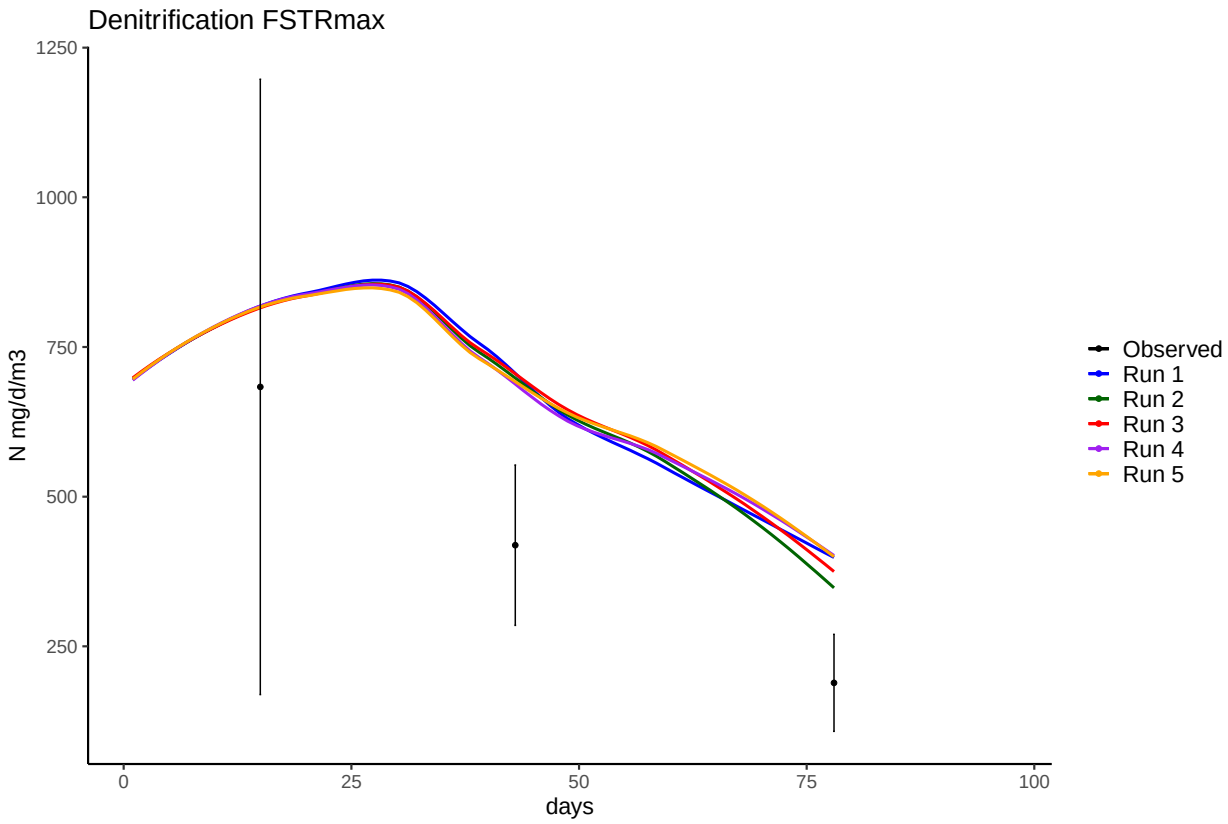

Figure S4. Sensitivity plot for FSTRmax on denitrification. Lines represent the average modeled value the grey area represent the deviation from the mean for each of the sensitivities tested.

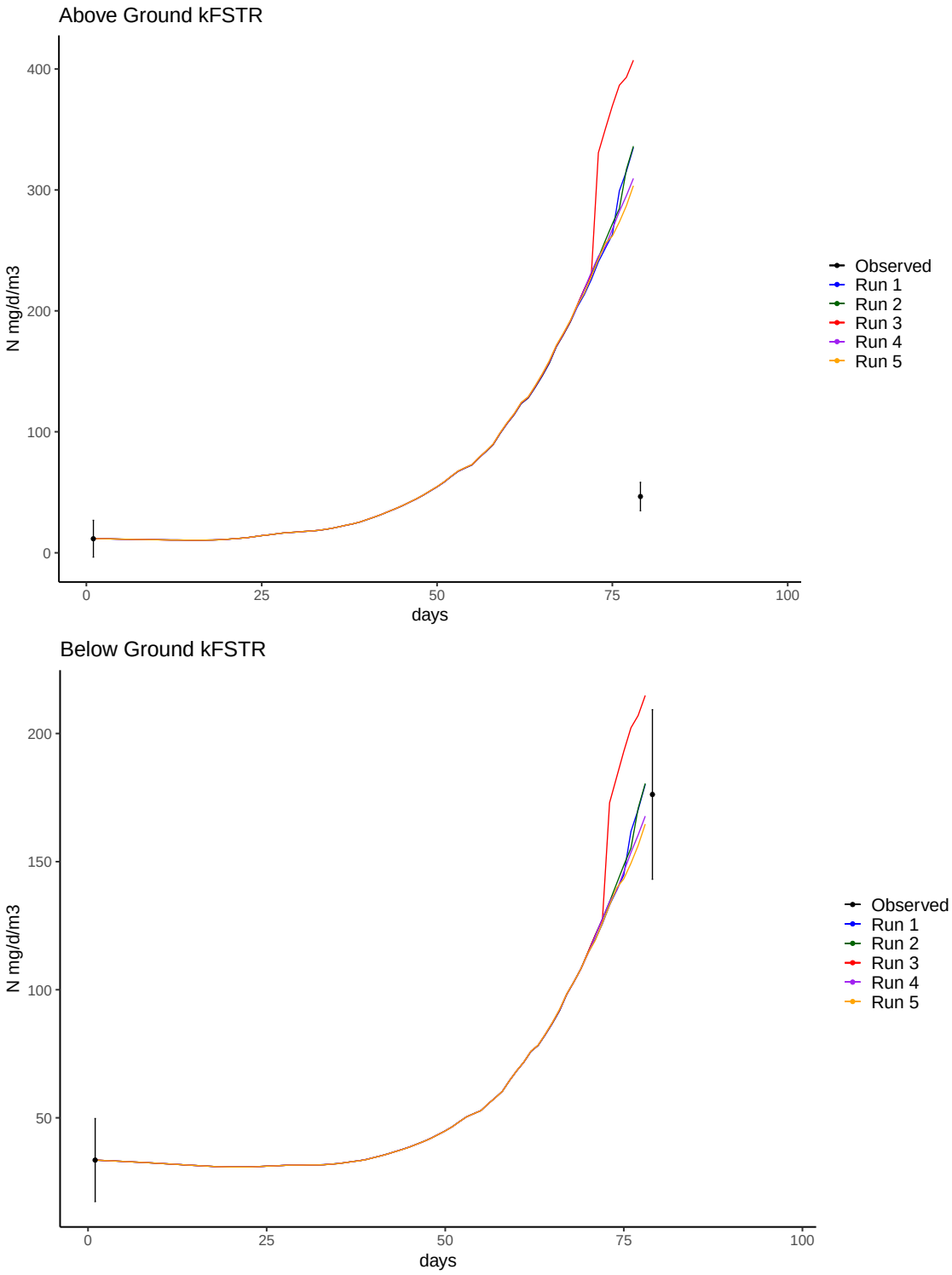

Figure S5. Sensitivity plot for kFSTR on above and below ground biomass. (Top) above ground biomass (bottom) below ground biomass.

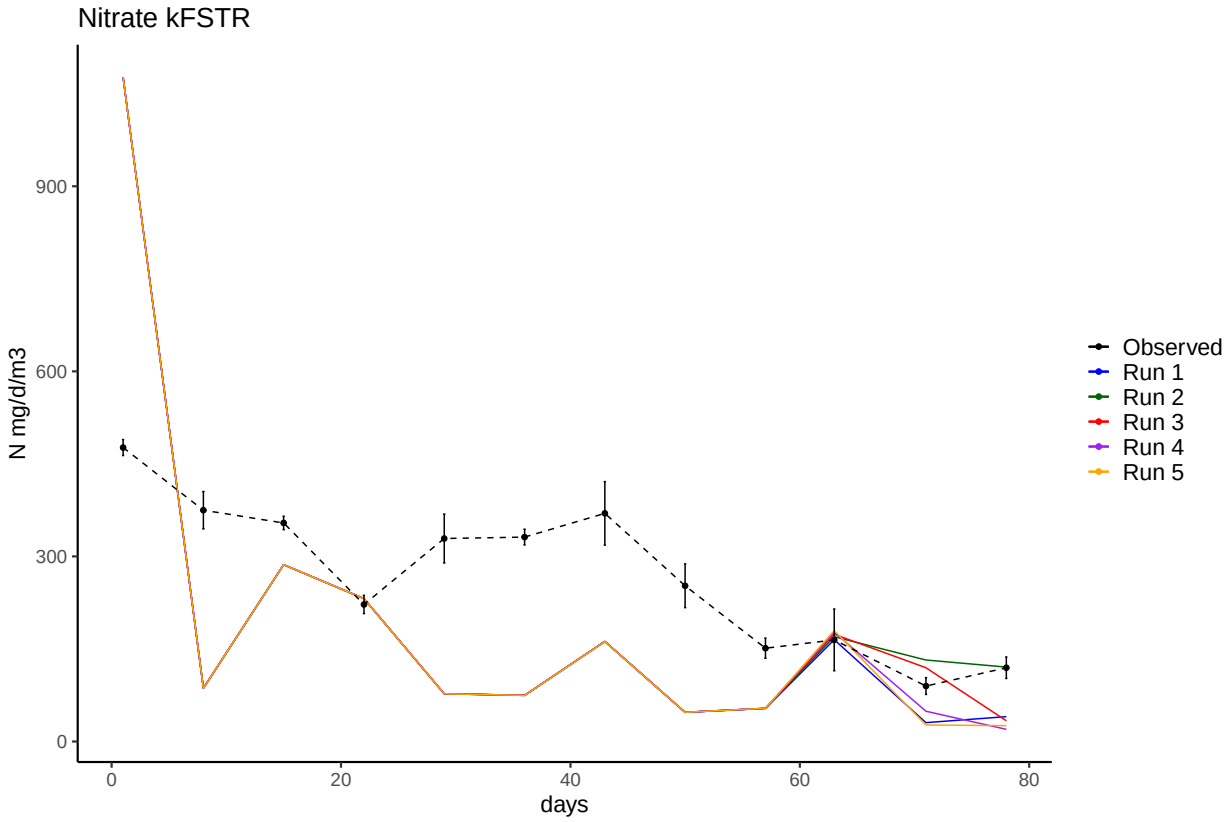
Nitrate kFSTR
N mg/d/m3
900
600
300
0
0
20
40
60
80
days
Observed
Run 1
Run 2
Run 3
Run 4
Run 5

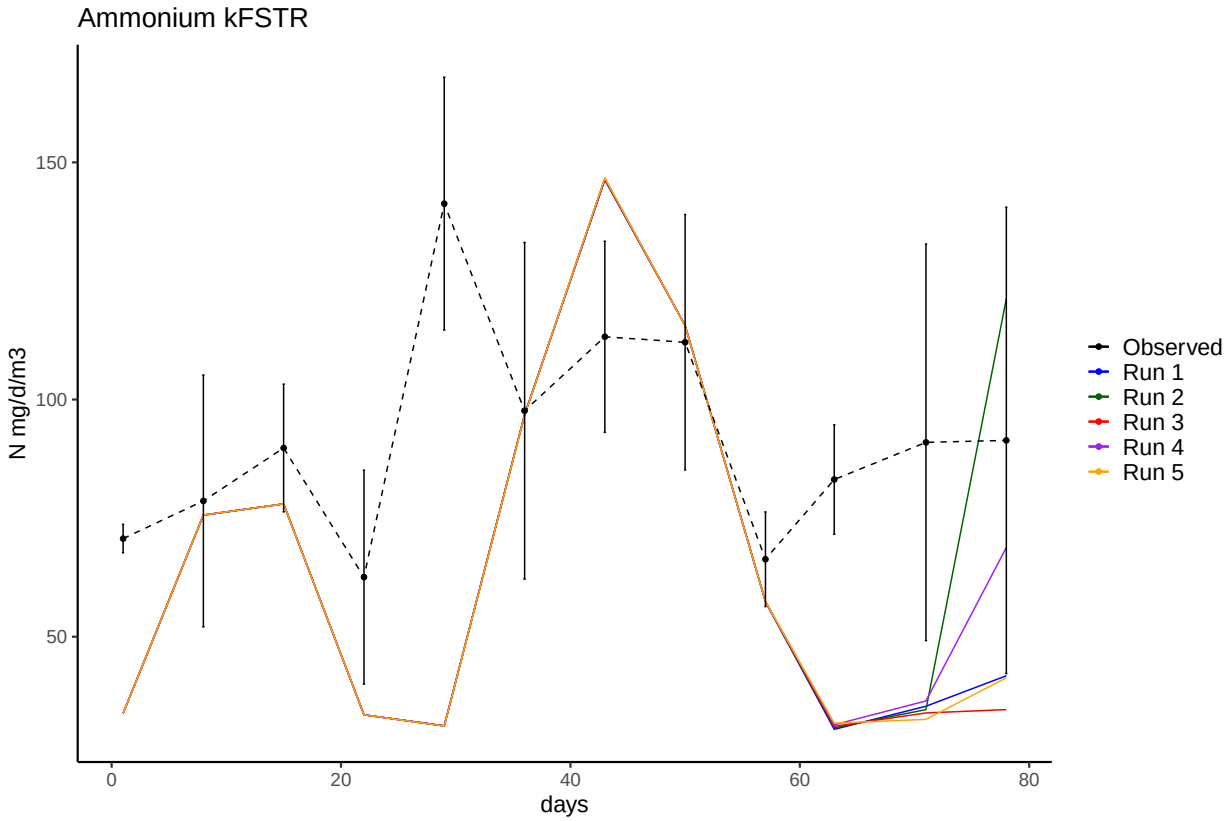
Ammonium kFSTR
N mg/d/m3
150
100
50
0
20
40
60
80
days
Observed
Run 1
Run 2
Run 3
Run 4
Run 5

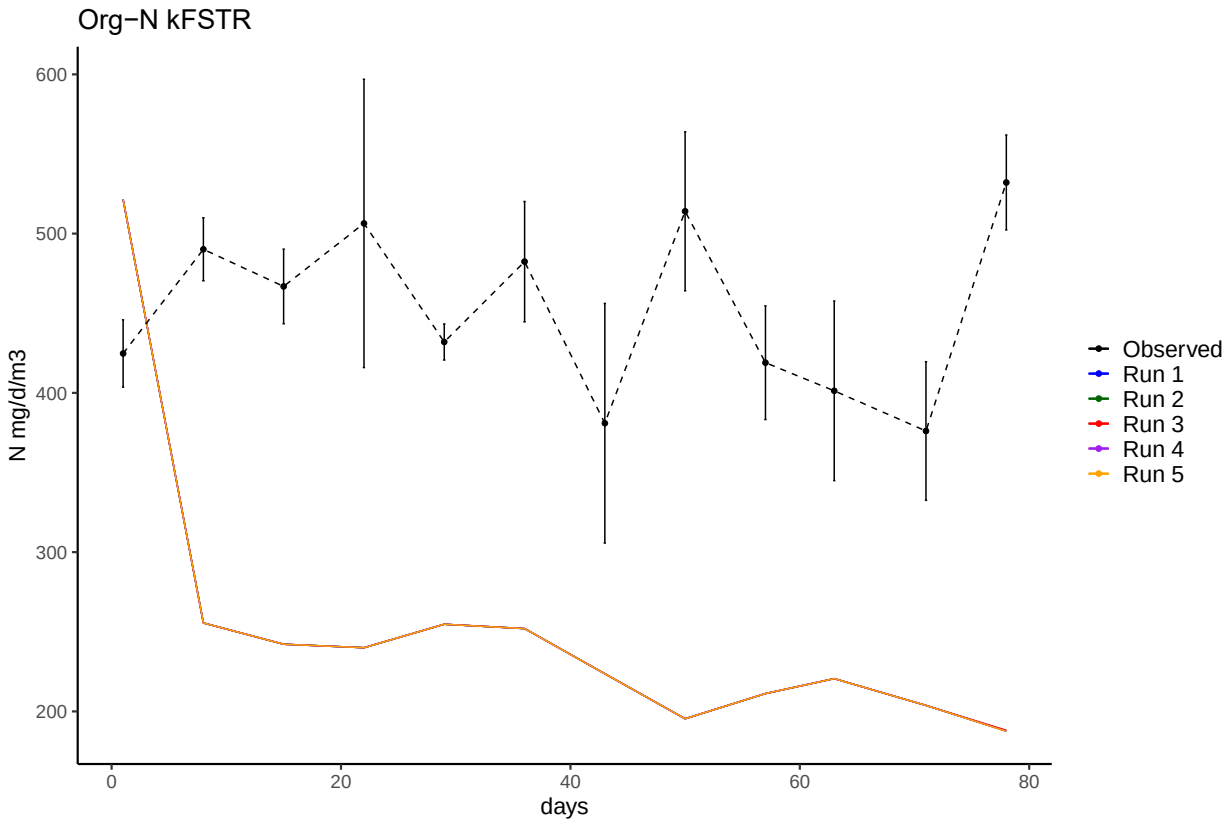

Figure S6. Sensitivity plot for kFSTR on nitrogen outflows

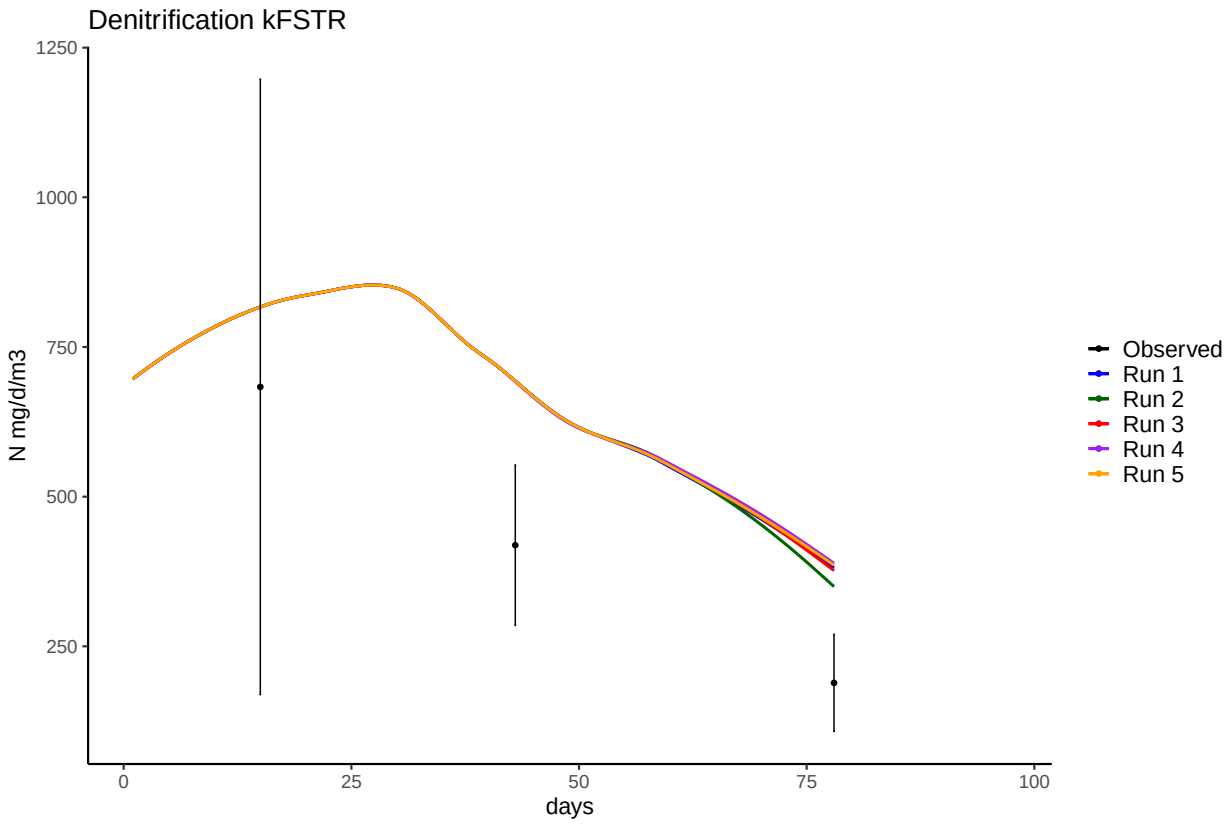

Figure S7. Sensitivity plot for kFSTR on denitrification. Lines represent the average modeled value the grey area represent the deviation from the mean for each of the sensitivities tested.

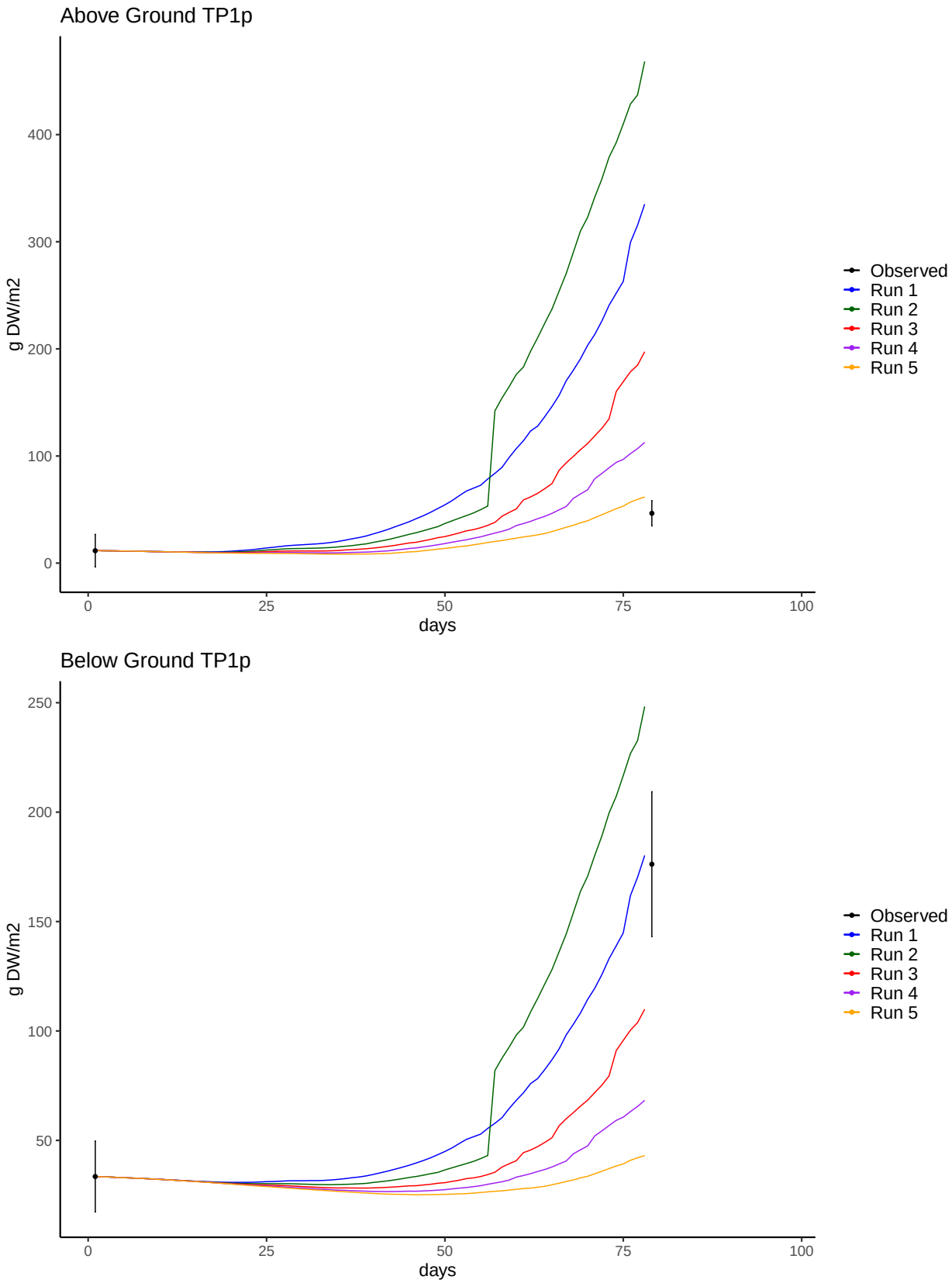

Figure S8. Sensitivity plot for TP1p on above and below ground biomass

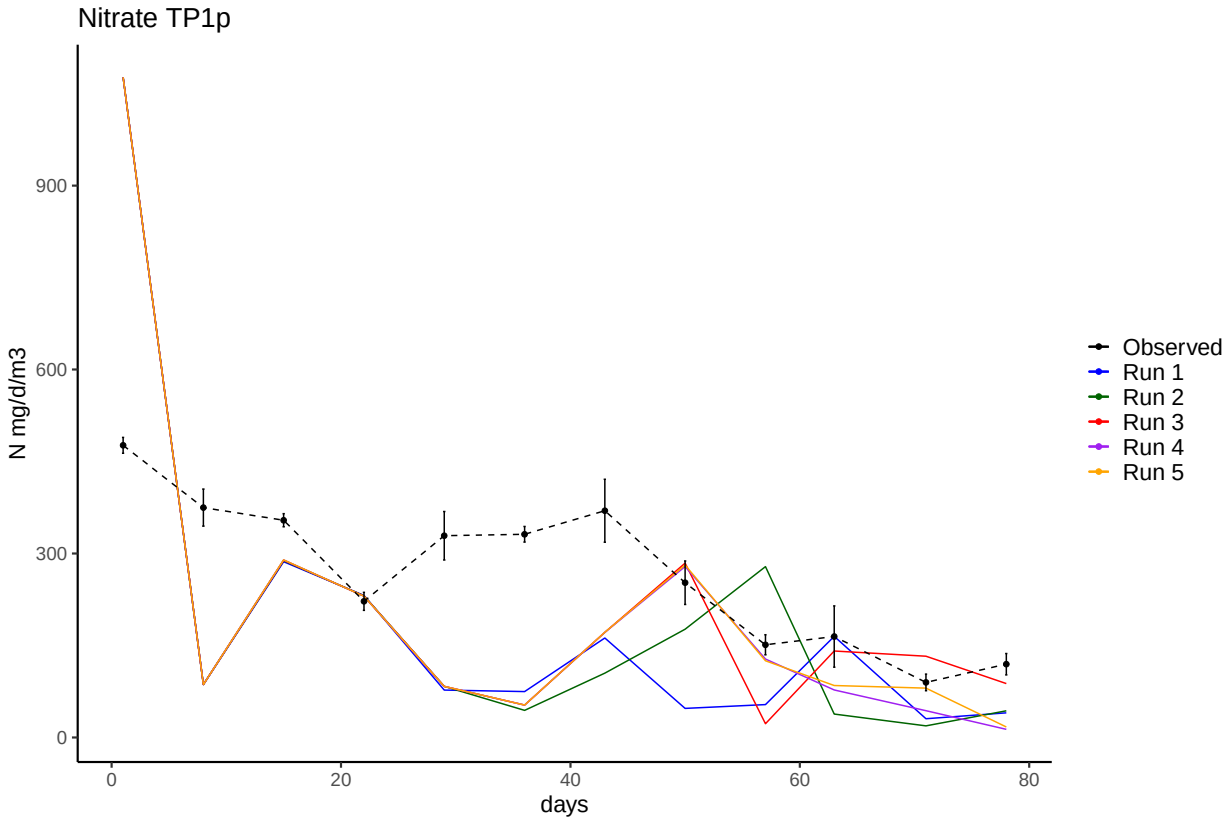
Nitrate TP1p
N mg/d/m3
900
600
300
0
0
20
40
60
80
days
Observed
Run 1
Run 2
Run 3
Run 4
Run 5

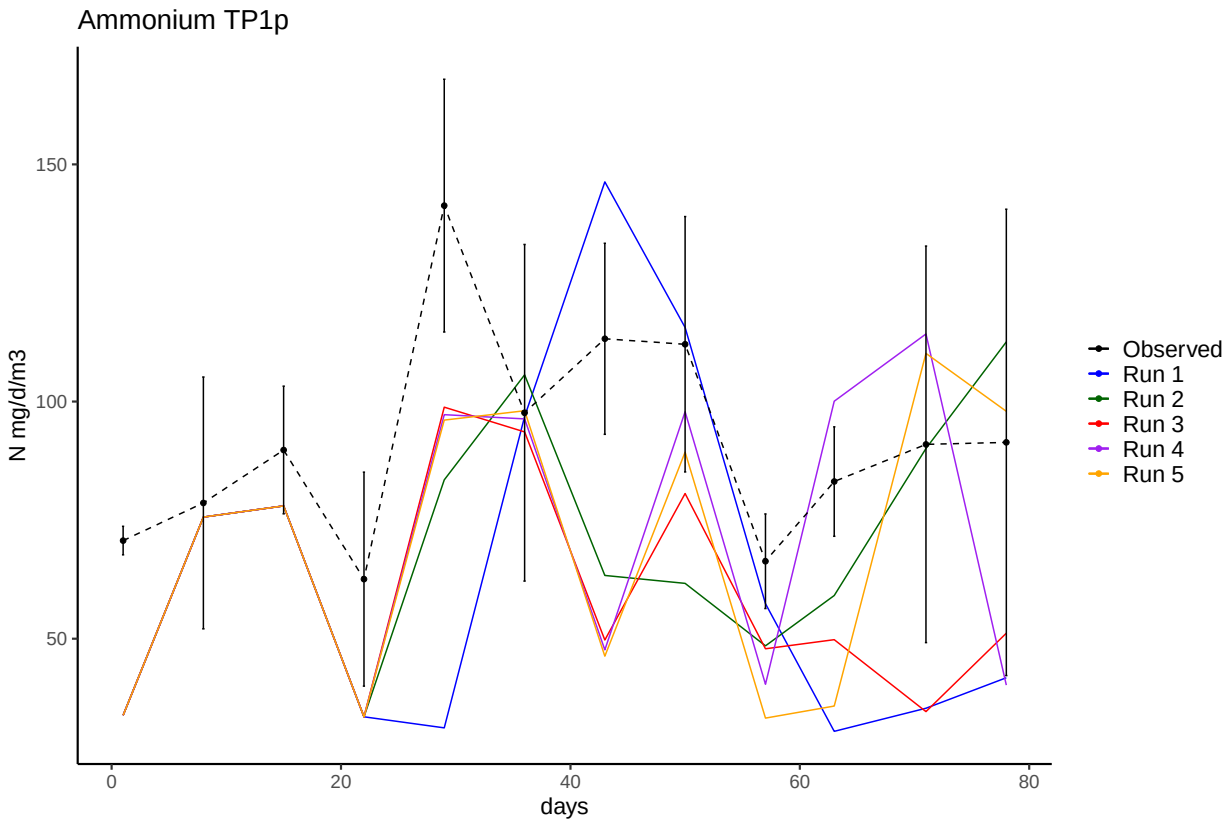
Ammonium TP1p
N mg/d/m3
150
100
50
0
20
40
60
80
days
Observed
Run 1
Run 2
Run 3
Run 4
Run 5

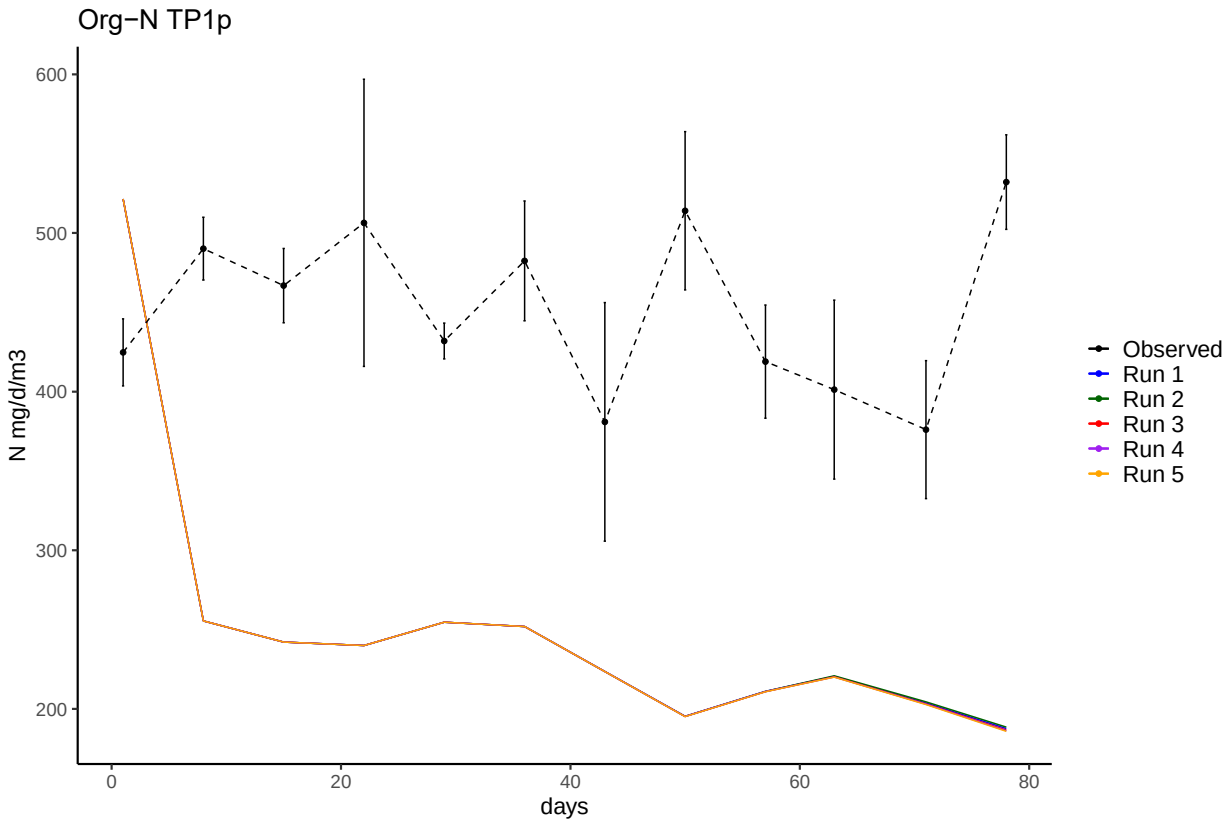

Figure S9. Sensitivity plot for TP1p on nitrogen outflows

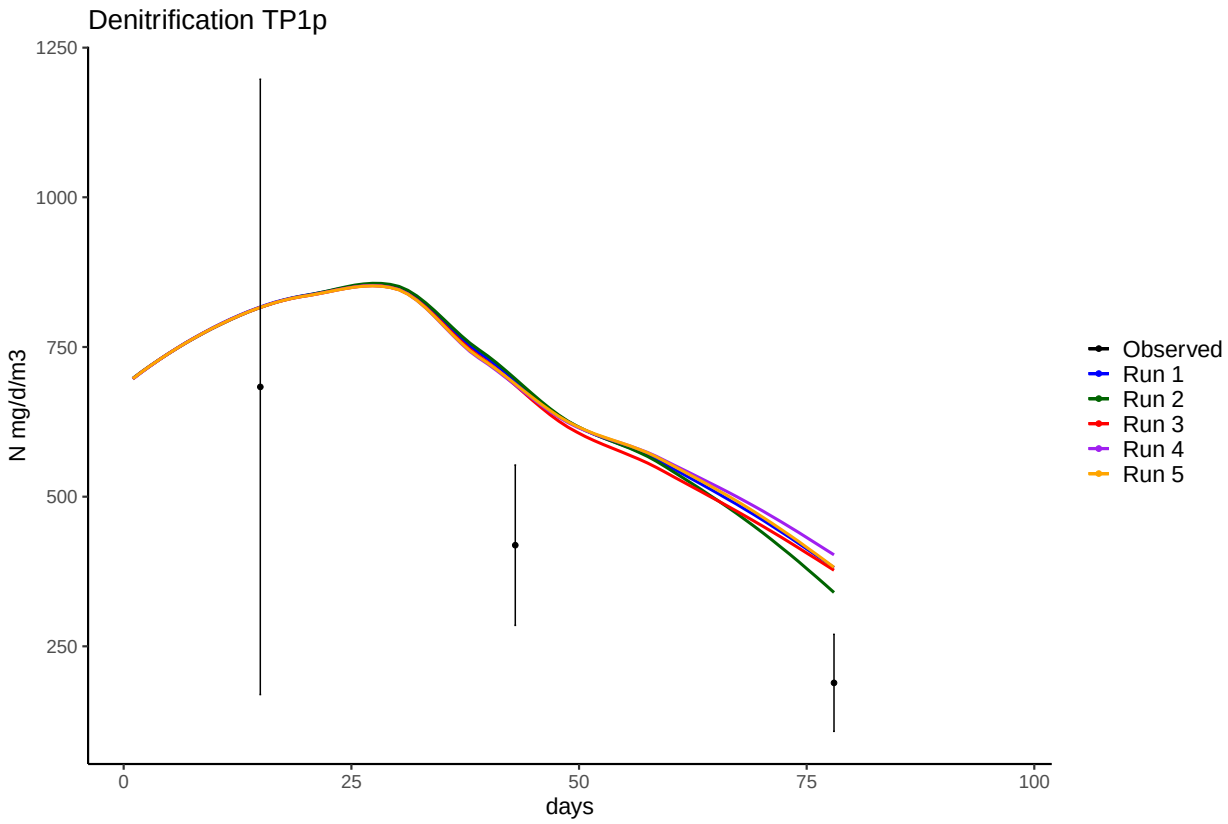

Figure S10. Sensitivity plot for TP1p on denitrification. Lines represent the average modeled value the grey area represent the deviation from the mean for each of the sensitivities tested.

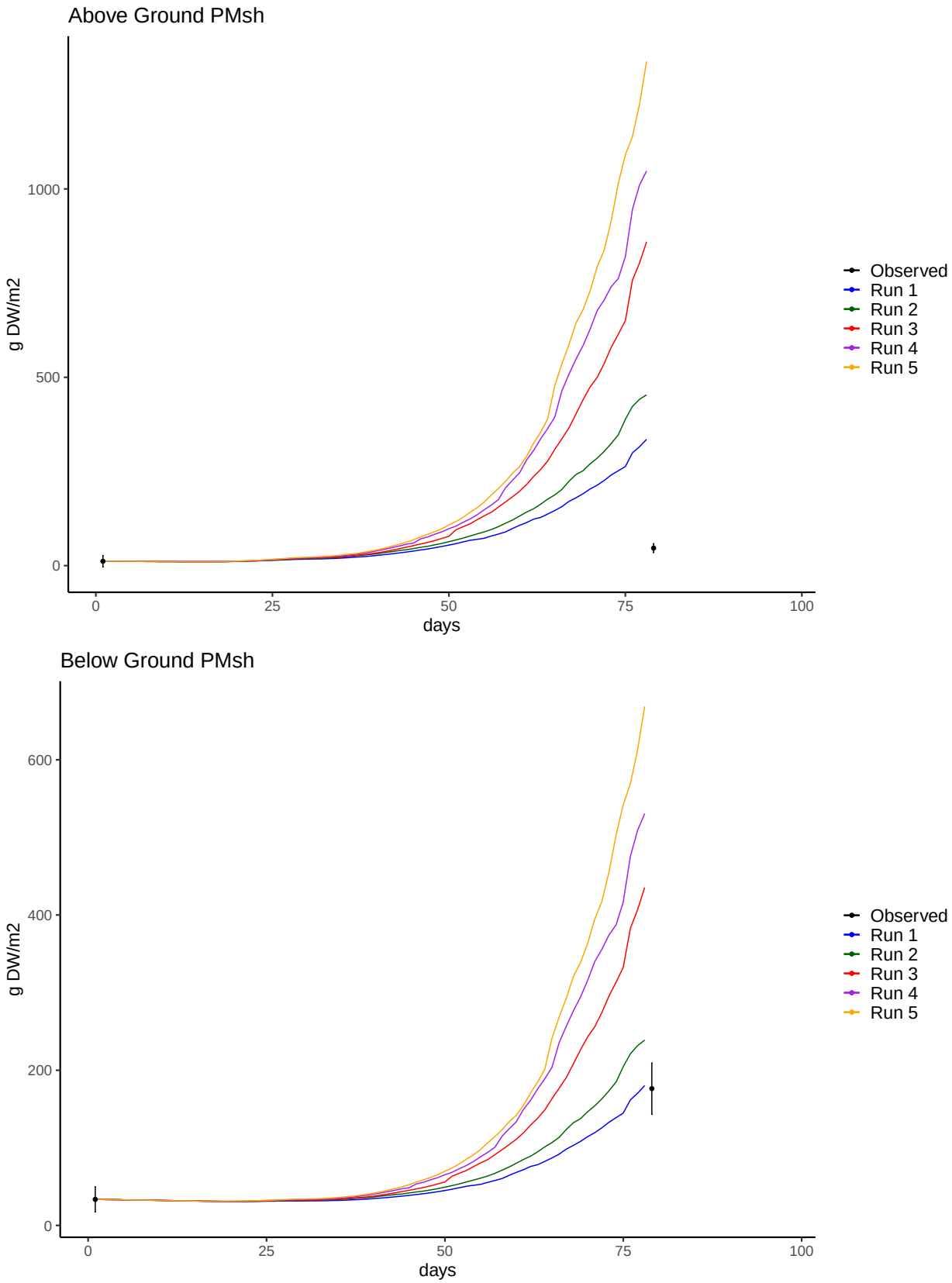

Figure S11. Sensitivity plot for PMsh on above and below ground biomass

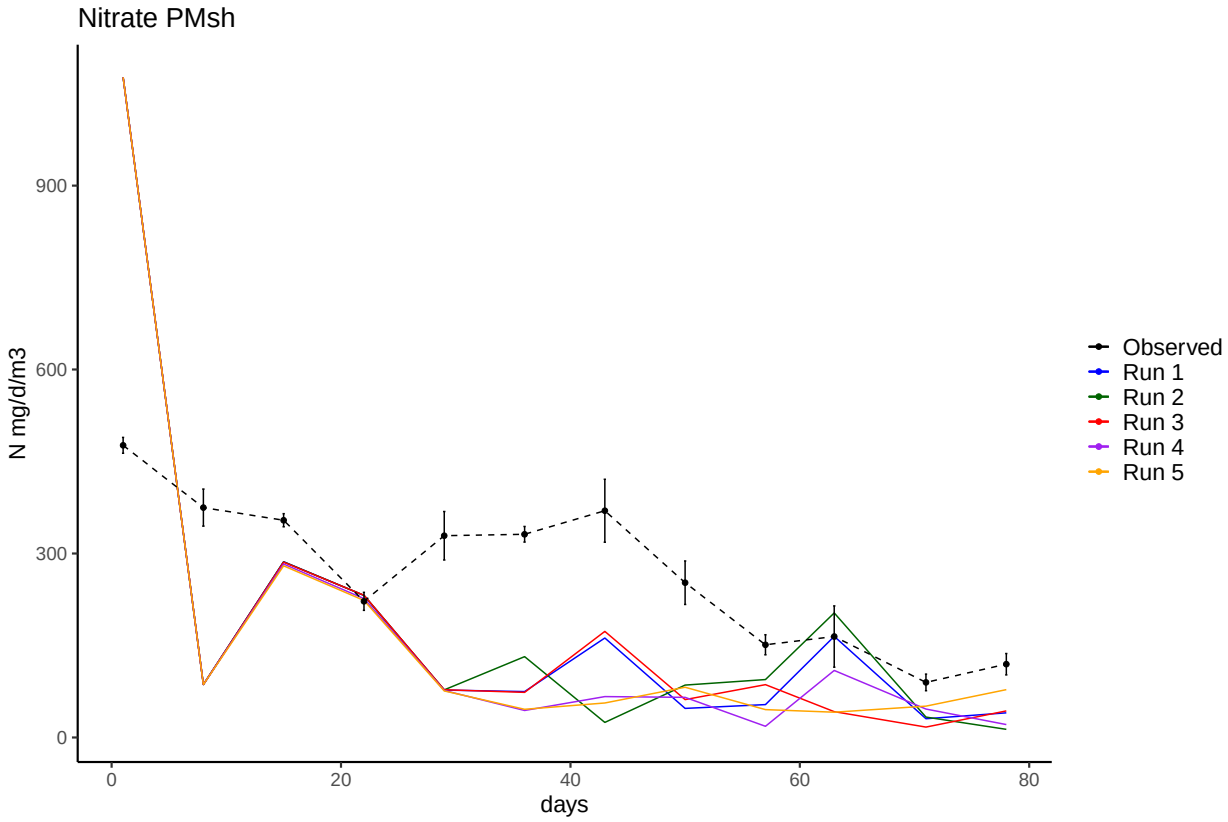
Nitrate PMsh
N mg/d/m3
900
600
300
0
0
20
40
60
80
days
Observed
Run 1
Run 2
Run 3
Run 4
Run 5

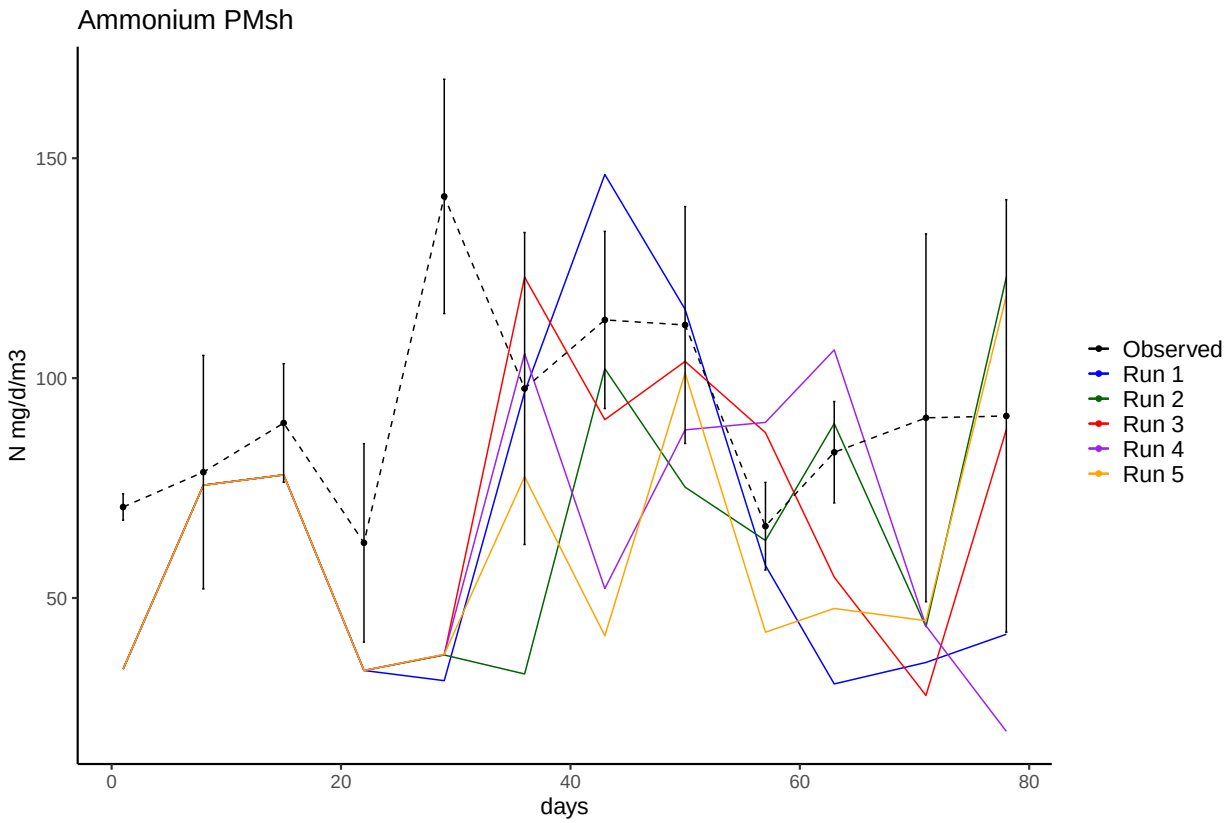
Ammonium PMsh
N mg/d/m3
150
100
50
0
20
40
60
80
days
Observed
Run 1
Run 2
Run 3
Run 4
Run 5

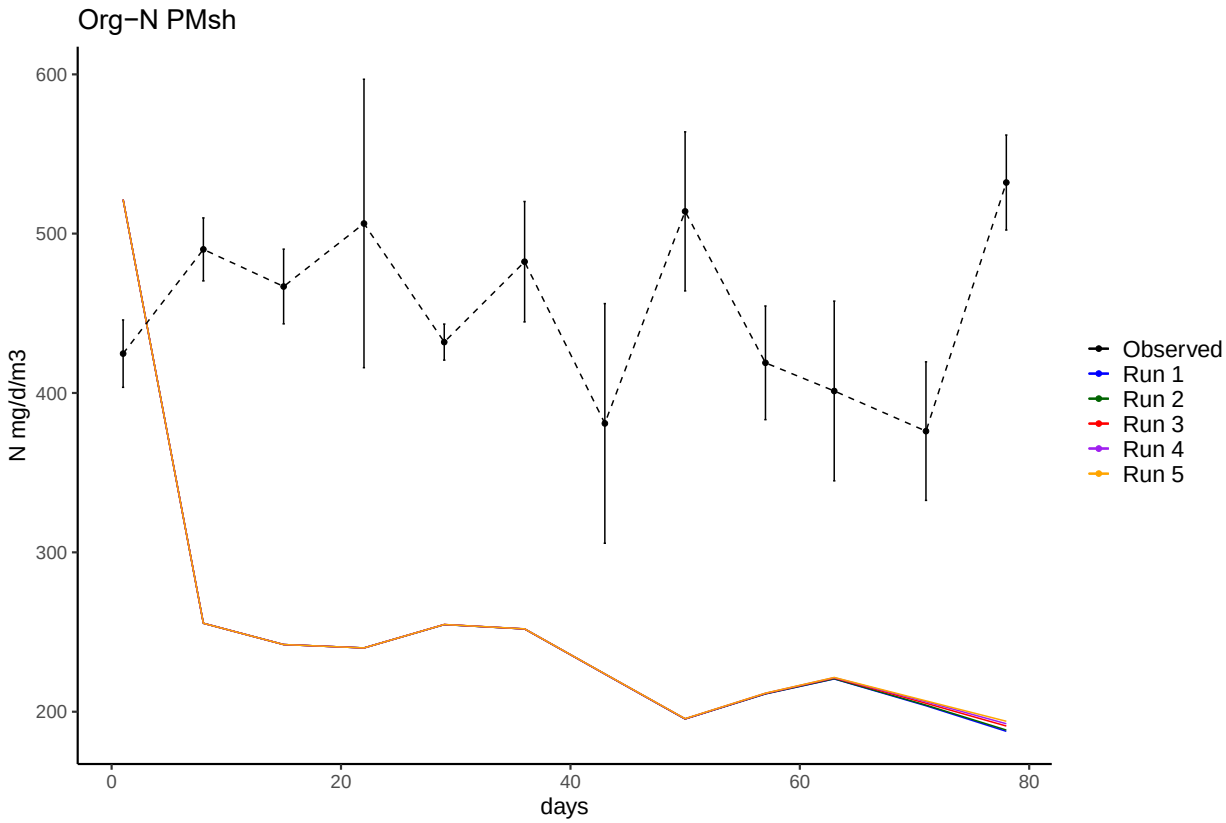

Figure S12. Sensitivity plot for PMsh on nitrogen outflows

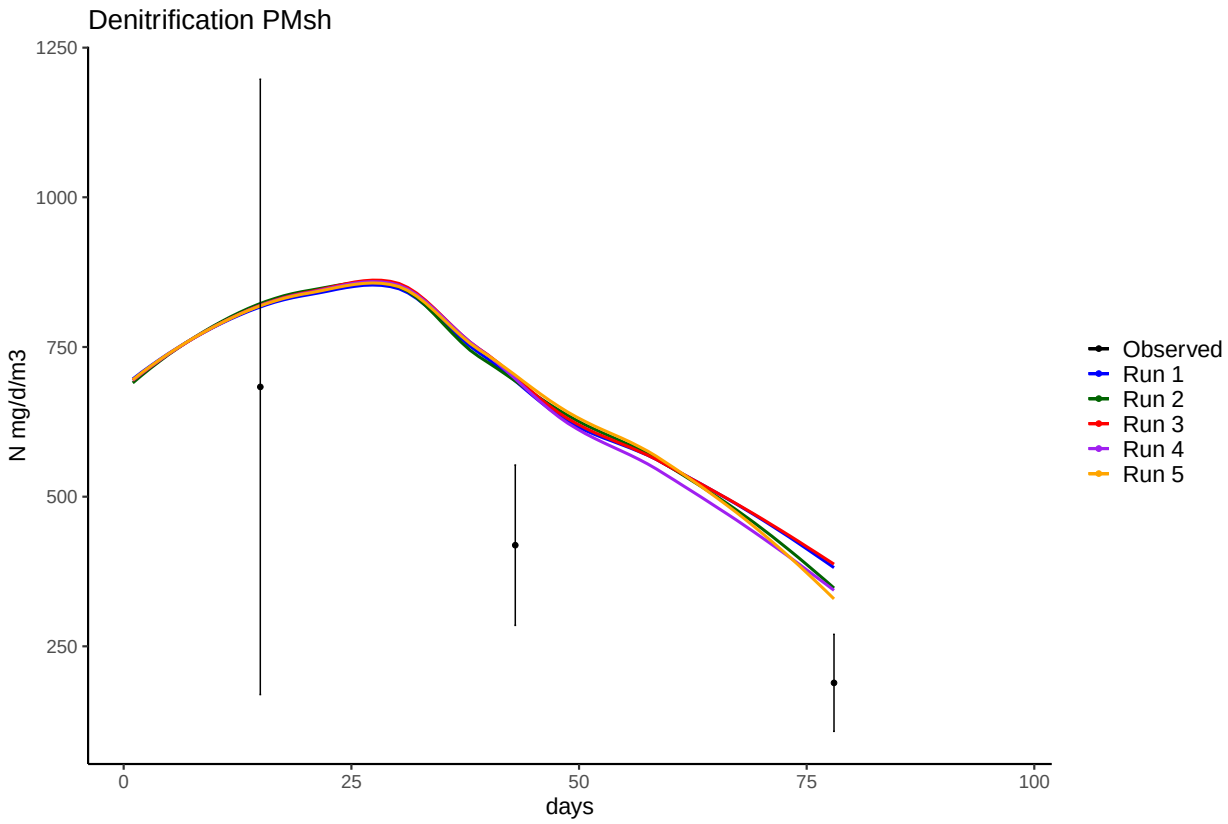

Figure S13. Sensitivity plot for PMsh on denitrification. Lines represent the average modeled value the grey area represent the deviation from the mean for each of the sensitivities tested.

References

Alam SK, Ager LA, Rosegger TM, Lange TR. 1996. The effects of mechanical harvesting of floating plant tussock communities on water quality in lake Istokpoga, Florida. Lake Reserv Manag. 12(4):455–461. https://doi.org/10.1080/07438149609354285

Andersen HE, Blicher-Mathiesen G, Bechmann M, Povilaitis A, Iital A, Lagzdins A, Kyllmar K. 2014. Mitigating diffuse nitrogen losses in the Nordic-Baltic countries. Agric Ecosyst Environ. 195:53–60. https://doi.org/10.1016/j.agee.2014.05.009

Anderson IC, Tobias CR, Neikirk BB, Wetzel RL. 1997. Development of a process-based nitrogen mass balance model for a Virginia (USA) Spartina alterniflora salt marsh: implications for net DIN flux. MARINE ECOLOGY PROGRESS SERIES Mar Ecol Prog Ser. 159:13–27.

Barco A, Borin M. 2020. Treatment performances of floating wetlands: A decade of studies in North Italy. Ecol Eng. 158. https://doi.org/10.1016/j.ecoleng.2020.106016

Booth D, Hartley D, Jackson R. 2002. Forest cover, impervious-surface area, and the mitigation of stormwater impacts. JOURNAL OF THE AMERICAN WATER RESOURES ASSOCIATION. 38(3):835–947.

Borne KE, Tanner CC, Fassman-Beck EA. 2013. Stormwater nitrogen removal performance of a floating treatment wetland. Water Science and Technology. 68(7):1657–1664. https://doi.org/10.2166/wst.2013.410

Boynton WR, Bailey EM. 2008. Sediment Oxygen and Nutrient Exchange Measurements from Chesapeake Bay, Tributary Rivers and Maryland Coastal Bays: Development of a Comprehensive Database & Analysis of Factors Controlling Patterns and Magnitude of Sediment-Water Exchanges. [place unknown].

Boynton WR, Hagy JD, Cornwell JC, Kemp WM, Greene SM, Owens MS, Baker JE, Larsen RK. 2008. Nutrient budgets and management actions in the Patuxent River estuary, Maryland. Estuaries and Coasts. 31(4):623–651. https://doi.org/10.1007/s12237-008-9052-9

Boynton WR, Hodgkins CLS, O'Leary CA, Bailey EM, Bayard AR, Wainger LA. 2014. Multi-decade Responses of a Tidal Creek System to Nutrient Load Reductions: Mattawoman Creek, Maryland USA. Estuaries and Coasts. 37(S1):111–127. https://doi.org/10.1007/s12237-013-9690-4

Boynton WR, Nixon SW. 2013. Budget analyses of estuarine ecosystems - BOOK - Estuarine Ecology 2nd Edition. In: Day JWJr, Crump BC, Kemp MW, Yáñez-Arancibia A, editors. Estuarine Ecology. 2nd ed. [place unknown]: John Wiley & Sons, Inc.; p. 443–464.

Brisson J, Carvalho P, Stein O, Weber K, Brix H, Zhao Y, Zurita F. 2024. Small-scale experiments: Using mesocosms and microcosms for testing hypotheses in treatment wetland research. Ecol Eng. 208. https://doi.org/10.1016/j.ecoleng.2024.107378

Butler Viruet IC, Testa JM, Harris LA. 2025. Understanding floating wetlands beyond retentions ponds: estimating nitrogen cycling and removal in tidal waters. Journal of Ecological Engineering Design.

Caffrey JM, Hollibaugh JT, Mortazavi B. 2016. Living oysters and their shells as sites of nitrification and denitrification. Mar Pollut Bull. 112(1–2):86–90. https://doi.org/10.1016/j.marpolbul.2016.08.038

Chapra SC. 2008. Surface Water-Quality Modeling [Internet]. [place unknown]: Waveland press. https://www.researchgate.net/publication/48447645

Chen C-C, Petersen JE, Kemp MW. 2000. Nutrient-uptake in experimental estuarine ecosystems: scaling and partitioning rates. MARINE ECOLOGY PROGRESS SERIES Mar Ecol Prog Ser. 200:103–116. https://doi.org/10.3354/meps155001

Chen C-C, Petersen JE, Kemp WM. 1997. Spatial and temporal scaling of periphyton growth on walls of estuarine mesocosms. Mar Ecol Prog Ser. 155:1–15. https://doi.org/10.3354/meps155001

Choi DS, Ready RC, Shortle JS. 2020. Valuing water quality benefits from adopting best management practices: A spatial approach. J Environ Qual. 49:582–592. https://doi.org/10.1002/JEQ2.20005

Cornwell JC, Owens MS, Boynton WR, Harris LA. 2016. Sediment-Water Nitrogen Exchange along the Potomac River Estuarine Salinity Gradient. J Coast Res. 32(4):776–787. https://doi.org/10.2112/JCOASTRES-D-15-00159.1

Deegan LA, Johnson DS, Warren RS, Peterson BJ, Fleeger JW, Fagherazzi S, Wollheim WM. 2012. Coastal eutrophication as a driver of salt marsh loss. Nature. 490:388–392. https://doi.org/10.1038/nature11533

Defo C, Kaur R, Bharadwaj A, Lal K, Kumar P. 2017. Modelling approaches for simulating wetland pollutant dynamics. Crit Rev Environ Sci Technol. 47(15):1371–1408. https://doi.org/10.1080/10643389.2017.1350126

Diaz RJ, Rosenberg R. 2008. Supplemental Materials - Spreading dead zones and consequences for marine ecosystems. Science (1979). 321(5891):926–929. https://doi.org/10.1126/science.1156401

Emerson CH, Wadzuk BM, Traver RG. 2010. Hydraulic evolution and total suspended solids capture of an infiltration trench. Hydrol Process. 24(8):1008–1014. https://doi.org/10.1002/HYP.7539

Faulwetter JL, Burr MD, Cunningham AB, Stewart FM, Camper AK, Stein OR. 2011. Floating treatment wetlands for domestic wastewater treatment. Water Science and Technology [Internet]. [accessed 2022 Nov 1] 64(10):2089–2095. https://doi.org/10.2166/wst.2011.576

Fennessey LAJ, Hamlett JM, Aron G, Lasota D. 2001. CHANGES IN RUNOFF DUE TO STORMWATER MANAGEMENT POND REGULATIONS. J Hydrol Eng.:317–327.

Filoso S, Palmer MA. 2011. Assessing stream restoration effectiveness at reducing nitrogen export to downstream waters. [place unknown].

Fulweiler RW, Nixon SW, Buckley BA, Granger SL. 2007. Reversal of the net dinitrogen gas flux in coastal marine sediments. Nature. 448(7150):180–182. https://doi.org/10.1038/nature05963

Gao L, Zhou W, Wu S, He S, Huang J, Zhang X. 2018. Nitrogen removal by thiosulfate-driven denitrification and plant uptake in enhanced floating treatment wetland. Science of the Total Environment. 621:1550–1558. https://doi.org/10.1016/j.scitotenv.2017.10.073

Gao X, Wang Y, Sun B, Li N. 2019. Nitrogen and phosphorus removal comparison between periphyton on artificial substrates and plant-periphyton complex in floating treatment wetlands. Environmental Science and Pollution Research. 26:21161–21171. https://doi.org/10.1007/S11356-019-05455-W/TABLES/4

Garcia Chance LM, Van Brunt SC, Majsztrik JC, White SA. 2019. Short- and long-term dynamics of nutrient removal in floating treatment wetlands. Water Res. 159:153–163. https://doi.org/10.1016/j.watres.2019.05.012

Garcia Chance LM, White SA. 2018. Aeration and plant coverage influence floating treatment wetland remediation efficacy. Ecol Eng. 122:62–68. https://doi.org/10.1016/j.ecoleng.2018.07.011

Gupta V, Courtemanche J, Gunn J, Mykytczuk N. 2020. Shallow floating treatment wetland capable of sulfate reduction in acid mine drainage impacted waters in a northern climate. J Environ Manage. 263. https://doi.org/10.1016/j.jenvman.2020.110351

Hancock GS, Holley JW, Chambers RM. 2010. A Field-Based Evaluation of Wet Retention Ponds: How Effective Are Ponds at Water Quantity Control?1. JAWRA Journal of the American Water Resources Association [Internet]. [accessed 2022 May 1] 46(6):1145–1158. https://doi.org/10.1111/J.1752-1688.2010.00481.X

Hassett B, Palmer M, Bernhardt E, Smith S, Carr J, Hart D. 2005. Restoring watersheds project by project: Trends in Chesapeake Bay tributary restoration. Front Ecol Environ. 3(5):259–267. https://doi.org/10.1890/1540-9295(2005)003[0259:RWPBPT]2.0.CO;2

Headley TR, Tanner CC. 2012. Constructed Wetlands With Floating Emergent Macrophytes: An Innovative Stormwater Treatment Technology. Crit Rev Environ Sci Technol [Internet]. [accessed 2022 Sep 25] 42(21):2261–2310. https://doi.org/10.1080/10643389.2011.574108

Howarth RW, Billen G, Swaney DP, Lajtha K. 1996. Legacy phosphorus in the Baltic Sea Catchment View project Living Coast-A full scale remediation project of a eutrophied bay of the

Baltic Sea View project. Biogeochemistry [Internet]. [accessed 2022 Nov 29] 35:75–139. https://www.researchgate.net/publication/230651077

Kadlec RH, Wallace SD. 2009. 6. Representing Treatment Performance. In: Treatment Wetlands. 2nd ed. Boca Raton, FL: CRC Press; p. 163–202.

Kana TM, Darkangelo C, Hunt DM, Oldham JB, Bennet GE, Conrwell JC. 1994. Membrane Inlet Mass Spectrometer for Rapid High-Precision Determination of N2, 02, and Ar in Environmental Water. Anal Chem. 66(23):4166–4170.

Karstens S, Langer M, Nyunoya H, Čaraitė I, Stybel N, Razinkovas-Baziukas A, Bochert R. 2021. Constructed floating wetlands made of natural materials as habitats in eutrophicated coastal lagoons in the Southern Baltic Sea. J Coast Conserv. 25(44):1–14. https://doi.org/10.1007/s11852-021-00826-3

Karstens S, Nazzari C, Bâlon C, Bielecka M, Grigaitis Ž, Schumacher J, Stybel N, Razinkovas-Baziukas A. 2018. Floating wetlands for nutrient removal in eutrophicated coastal lagoons: Decision support for site selection and permit process [Internet]. [accessed 2022 Nov 3]. https://doi.org/10.1016/j.marpol.2018.08.030

Kellogg ML, Cornwell JC, Owens MS, Paynter KT. 2013. Denitrification and nutrient assimilation on a restored oyster reef. Mar Ecol Prog Ser. 480:1–19. https://doi.org/10.3354/meps10331

Kemp MW, Smith EM, Marvin-DiPasquale M, Boynton WR. 1997. Organic carbon balance and net ecosystem metabolism in Chesapeake Bay. Mar Ecol Prog Ser. 150:229–248.

Kemp WM, Petersen ED, Houde C, Chen C, Cornwell JC, Porter ET. 2009. Spatial and temporal scaling. In: Petersen JE, Kennedy VS, Dennison WC, Kemp MW, editors. Enclosed Experimental Ecosystems and Scale: Tools for Understanding and Managing Coastal Ecosystems. [place unknown]: Springer ; p. 49–131.

Knight RL, Kadlec RH, Ohlendorf HM. 1999. The use of treatment wetlands for petroleum industry effluents. Environ Sci Technol. 33(7):973–980. https://doi.org/10.1021/es980740w

Kreeger D. 2014a. Determination of Belowground Biomass of Wetland Macrophytes. Partnership of the Delaware Estuary PDE Method . 39(4pp).

Kreeger D. 2014b. Determination of Aboveground Biomass of Wetland Macrophytes. Partnership of the Delaware Estuary PDE Method. 38(5pp).

Landaverde AC, Strosnider WHJ, White SA. 2024. Plant suitability for floating treatment wetland applications in brackish waters. Ecol Eng. 200. https://doi.org/10.1016/j.ecoleng.2024.107183

Lefcheck JS, Orth RJ, Dennison WC, Wilcox DJ, Murphy RR, Keisman J, Gurbisz C, Hannam M, Brooke Landry J, Moore KA, et al. 2018. Long-term nutrient reductions lead to the unprecedented recovery of a temperate coastal region. Proc Natl Acad Sci U S A. 115(14):3658–3662. https://doi.org/10.1073/pnas.1715798115

Lucke T, Walker C, Beecham S. 2019. Experimental designs of field-based constructed floating wetland studies: A review. Science of the Total Environment. 660:199–208. https://doi.org/10.1016/j.scitotenv.2019.01.018

Marimon ZA, Xuan Z, Chang N Bin. 2013. System dynamics modeling with sensitivity analysis for floating treatment wetlands in a stormwater wet pond. Ecol Modell. 267:66–79. https://doi.org/10.1016/J.ECOLMODEL.2013.07.017

Mazur CI, Al-Haj AN, Ray NE, Sanchez-Viruet I, Fulweiler RW. 2021. Low denitrification rates and variable benthic nutrient fluxes characterize Long Island Sound sediments. Biogeochemistry. 154(1):37–62. https://doi.org/10.1007/s10533-021-00795-7

McAndrew B, Ahn C. 2017a. Developing an ecosystem model of a floating wetland for water quality improvement on a stormwater pond. J Environ Manage. 202:198–207. https://doi.org/10.1016/J.JENVMAN.2017.07.035

McAndrew B, Ahn C. 2017b. Developing an ecosystem model of a floating wetland for water quality improvement on a stormwater pond. J Environ Manage. 202:198–207. https://doi.org/10.1016/j.jenvman.2017.07.035

McCuen RH. 1979. Downstream Effects of Stormwater Management Basins. Journal of the Hydraulics Division [Internet]. [accessed 2022 Nov 26] 105(11):1343–1356. https://doi.org/10.1061/JYCEAJ.0005300

Van De Moortel AMK, Meers E, De Pauw N, Tack FMG. 2010. Effects of vegetation, season and temperature on the removal of pollutants in experimental floating treatment wetlands. Water Air Soil Pollut [Internet]. [accessed 2022 Sep 7] 212(1–4):281–297. https://doi.org/10.1007/S11270-010-0342-Z/TABLES/7

Nixon SW. 1995. Coastal marine eutrophication: A definition, social causes, and future concerns. Ophelia [Internet]. 41(1):199–219. https://doi.org/10.1080/00785236.1995.10422044

Nixon SW, Fulweiler RW, Buckley BA, Granger SL, Nowicki BL, Henry KM. 2009. The impact of changing climate on phenology, productivity, and benthic-pelagic coupling in Narragansett Bay. Estuar Coast Shelf Sci. 82(1):1–18. https://doi.org/10.1016/j.ecss.2008.12.016

Passeport Elodie, Vidon Philippe, Forshay Kenneth J, Harris Lora, Sujay •, Kaushal S, Kellogg Dorothy Q, Lazar J, Mayer Paul, Stander Emilie K, et al. 2013. Ecological Engineering Practices for the Reduction of Excess Nitrogen in Human-Influenced Landscapes: A Guide for Watershed Managers. Environ Manage. 51:392–413. https://doi.org/10.1007/s00267-012-9970-y

Pennino MJ, Kaushal SS, Murthy SN, Blomquist JD, Cornwell JC, Harris LA. 2016. Sources and transformations of anthropogenic nitrogen along an urban river-estuarine continuum. Biogeosciences. 13(22):6211–6228. https://doi.org/10.5194/bg-13-6211-2016

Riemann B, Carstensen J, Dahl K, Fossing H, Hansen JW, Jakobsen HH, Josefson AB, Krause-Jensen D, Markager S, Staehr PA, et al. 2016. Recovery of Danish Coastal Ecosystems After Reductions in Nutrient Loading: A Holistic Ecosystem Approach. Estuarine and Coasts [Internet]. [accessed 2022 Nov 24] 39:82–97. https://doi.org/10.1007/s12237-015-9980-0

Sample DJ, Wre D. 2017. Floating wetlands for treatment of urban and agricultural runoff in Virginia.

Sanicola O, Lucke T, Stewart M, Tondera K, Walker C. 2019. Root and Shoot Biomass Growth of Constructed Floating Wetlands Plants in Saline Environments. International Journal of Environmental Research and Public Health 2019, Vol 16, Page 275 [Internet]. [accessed 2022 Nov 26] 16(2):275. https://doi.org/10.3390/IJERPH16020275

Scheffer M. 2004. Ecology of Shallow Lakes. Ecology of Shallow Lakes. https://doi.org/10.1007/978-1-4020-3154-0

Scheffer M, ndor Szabó S, Gragnani A, van Nes EH, Rinaldi S, Kautsky N, Norberg J, M Roijackers RM, M Franken RJ. 2003. Floating plant dominance as a stable state. PNAS April [Internet]. 1(7):4040–4045. www.pnas.orgcgidoi10.1073pnas.0737918100

Scientific and Technical Advisory Committee (STAC). 2023. Achieving Water Quality Goals in the Chesapeake Bay: A Comprehensive Evaluation of System Response [Internet]. Edgewater; [accessed 2025 Jan 22]. http://www.chesapeake.org/stac.

Sharma R, Vymazal J, Malaviya P. 2021. Application of floating treatment wetlands for stormwater runoff: A critical review of the recent developments with emphasis on heavy metals and nutrient removal. Science of the Total Environment. 777(146044). https://doi.org/10.1016/j.scitotenv.2021.146044

Shen J, Du J, Lucas L V. 2022. Simple relationships between residence time and annual nutrient retention, export, and loading for estuaries. Limnol Oceanogr. 67(4). https://doi.org/10.1002/lno.12045

Sherwood ET, Greening HS, Johansson JOR, Kaufman K, Raulerson GE. 2017. Tampa Bay (Florida, USA): Documenting Seagrass Recovery since the 1980's and Reviewing the Benefits. Southeast Geogr [Internet]. [accessed 2022 Nov 24] 57(3):16. https://doi.org/10.1353/sgo.2017.0026

Søndergaard M, Jensen JP, Jeppesen E. 2001. Retention and Internal Loading of Phosphorus in Shallow, Eutrophic Lakes. The Scientific World. 1:427–442. https://doi.org/10.1100/tsw.2001.72

Spangler JT, Sample DJ, Fox LJ, Owen JS, White SA. 2019. Floating treatment wetland aided nutrient removal from agricultural runoff using two wetland species. Ecol Eng. 127:468–479. https://doi.org/10.1016/j.ecoleng.2018.12.017

Stewart F. 2008. Control of Microbial Processes for Enhanced Water Treatment using Floating Island Treatment Systems. Bozeman.

Stewart FM, Mulholland T, Cunningham AB, Kania BG, Osterlund MT. 2008. Floating islands as an alternative to constructed wetlands for treatment of excess nutrients from agricultural and municipal wastes - Results of laboratory-scale tests. Land Contamination and Reclamation. 16(1):25–33. https://doi.org/10.2462/09670513.874

Strosnider WH, Schultz SE, Strosnider KAJ, Nairn RW. 2017. Effects on the Underlying Water Column by Extensive Floating Treatment Wetlands. J Environ Qual. 46(1):201–209. https://doi.org/10.2134/jeq2016.07.0257

Swarzenski CM, Swenson EM, Sasser CE, Gosselink JG. 1991. Marsh mat flotation in the Louisiana delta plain. Source: Journal of Ecology. 79(4):999–1011.

Tanner CC. 2006. Application of Floating Wetlands for Enhanced Stormwater Treatment: A Review [Internet]. [place unknown]. https://www.researchgate.net/publication/266409739

Tanner CC, Headley TR. 2011. Components of floating emergent macrophyte treatment wetlands influencing removal of stormwater pollutants. Ecol Eng. 37:474–486. https://doi.org/10.1016/j.ecoleng.2010.12.012

Testa JM, Boynton WR, Hodgkins CLS, Moore AL, Bailey EM, Rambo J. 2022. Biogeochemical states, rates, and exchanges exhibit linear responses to large nutrient load reductions in a shallow, eutrophic urban estuary. Limnol Oceanogr [Internet]. [accessed 2022 Nov 24] 67(4):739–752. https://doi.org/10.1002/lno.12037

Testa JM, Brady DC, Cornwell JC, Owens MS, Sanford LP, Newell CR, Suttles SE, Newell RIE. 2015. Modeling the impact of floating oyster (Crassostrea virginica) aquaculture on sediment-water nutrient and oxygen fluxes. Aquac Environ Interact. 7(3):205–222. https://doi.org/10.3354/aei00151

USEPA. 1999. Preliminary Data Summary of Urban Storm Water Best Management Practices. Washington, DC.

Vymazal J. 2007. Removal of nutrients in various types of constructed wetlands. Science of the Total Environment. 380(1–3):48–65. https://doi.org/10.1016/j.scitotenv.2006.09.014

Wang CY, Sample DJ. 2013. Assessing floating treatment wetlands nutrient removal performance through a first order kinetics model and statistical inference. Ecol Eng. 61:292–302. https://doi.org/10.1016/J.ECOLENG.2013.09.019

Wang CY, Sample DJ. 2014. Assessment of the nutrient removal effectiveness of floating treatment wetlands applied to urban retention ponds. J Environ Manage. 137:23–35. https://doi.org/10.1016/j.jenvman.2014.02.008

Wang CY, Sample DJ, Bell C. 2014. Vegetation effects on floating treatment wetland nutrient removal and harvesting strategies in urban stormwater ponds. Science of the Total Environment. 499:384–393. https://doi.org/10.1016/j.scitotenv.2014.08.063

Wang Y, Sun B, Gao X, Li N. 2019. Development and evaluation of a process-based model to assess nutrient removal in floating treatment wetlands. Science of the Total Environment. 694. https://doi.org/10.1016/j.scitotenv.2019.133633

Welsh AK, Burke DJ, Hamerlynck EP, Hahn D. 2010. Seasonal analyses of arbuscular mycorrhizae, nitrogen-fixing bacteria and growth performance of the salt marsh grass Spartina patens. Plant Soil. 330(1):251–266. https://doi.org/10.1007/s11104-009-0197-5

Yeh N, Yeh P, Chang YH. 2015. Artificial floating islands for environmental improvement. Renewable and Sustainable Energy Reviews. 47:616–622. https://doi.org/10.1016/J.RSER.2015.03.090

Zhao F, Aziz R, Rafiq MT, Li H, Zhenli H, Stoffella PJ, Yang X. 2013. Enhanced Purification of Eutrophic Water by Microbe-Inoculated Stereo Floating Beds Crop Safe Production and Biofortification in Nano-enabled Agriculture View project ecological View project. Polish Journal of Environmental Studies [Internet]. 22(3):957–964. https://www.researchgate.net/publication/286049858

Zimmermann CF, Keefe CW, Manager WA, Arar EJ. 1997. Method 440.0 - Determination of Carbon and Nitrogen in Sediments and Particulates of Estuarine/Coastal Waters Using Elemental Analysis. Washington DC.